

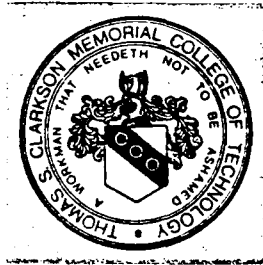
MICROCOPY RESOLUTION TEST CHART

1963-A

AD-A190 644

2

DTIC FILE COPY



Final Report AFOSR 84-0076

Nonlinear Analysis and Optimal Design of
Dynamic Mechanical Systems for Spacecraft
Application

Prepared by

K.D. Willmert and M. Sathyamoorthy
CLARKSON COLLEGE OF TECHNOLOGY / POTSDAM, NEW YORK 13676

DTIC
ELECTE
JAN 1 9 1988
S H D

DISTRIBUTION STATEMENT A

Approved for public release;
Distribution Unlimited

2

SECURITY CLASSIFICATION OF THIS PAGE (When Data Entered)

REPORT DOCUMENTATION PAGE		READ INSTRUCTIONS BEFORE COMPLETING FORM										
1. AFOSR NUMBER 87-2008	2. GOVT ACCESSION NO.	3. RECIPIENT'S CATALOG NUMBER										
4. TITLE (and Subtitle) Nonlinear Analysis and Optimal Design of Dynamic Mechanical Systems for Spacecraft Application	5. TYPE OF REPORT & PERIOD COVERED Final Technical Report Feb. 1, 1984 - July 31, 1987											
	6. PERFORMING ORG. REPORT NUMBER											
7. AUTHOR(s) K.D. Willmert and M. Sathyamoorthy	8. CONTRACT OR GRANT NUMBER(s) AFOSR 84-0076											
9. PERFORMING ORGANIZATION NAME AND ADDRESS Clarkson University Potsdam, New York 13676	10. PROGRAM ELEMENT, PROJECT, TASK AREA & WORK UNIT NUMBERS											
11. CONTROLLING OFFICE NAME AND ADDRESS Air Force Office of Scientific Research Washington D.C.	12. REPORT DATE September 1987											
	13. NUMBER OF PAGES Unclassified											
14. MONITORING AGENCY NAME & ADDRESS (if different from Controlling Office) SCIENCE CENTER	15. SECURITY CLASS. (of this report)											
	15a. DECLASSIFICATION/DOWNGRADING SCHEDULE											
16. DISTRIBUTION STATEMENT (of this Report) Approved for public release; distribution unlimited												
<table border="1"> <tr> <td colspan="2">Accession For</td> </tr> <tr> <td>NTIS</td> <td><input checked="" type="checkbox"/></td> </tr> <tr> <td>DTIC TAB</td> <td><input type="checkbox"/></td> </tr> <tr> <td>Unannounced</td> <td><input type="checkbox"/></td> </tr> <tr> <td>Justification</td> <td><input type="checkbox"/></td> </tr> </table>			Accession For		NTIS	<input checked="" type="checkbox"/>	DTIC TAB	<input type="checkbox"/>	Unannounced	<input type="checkbox"/>	Justification	<input type="checkbox"/>
Accession For												
NTIS	<input checked="" type="checkbox"/>											
DTIC TAB	<input type="checkbox"/>											
Unannounced	<input type="checkbox"/>											
Justification	<input type="checkbox"/>											
17. DISTRIBUTION STATEMENT (of the abstract entered in Block 20, if different from Report)												
18. SUPPLEMENTARY NOTES												
19. KEY WORDS (Continue on reverse side if necessary and identify by block number) Mechanism, vibrational analysis, optimization, geometric nonlinearity, material nonlinearity												
20. ABSTRACT (Continue on reverse side if necessary and identify by block number) See next page												

DTIC
SELECTED
JAN 19 1988
H

DTIC
COPY
PROTECTED

AFOSR-TK- 87-2008**ABSTRACT**

The goal of this research was to develop analysis and optimal design procedures for planar as well as spatial mechanisms that are frequently used in space structures. A nonlinear finite element procedure which was developed originally for planar mechanisms during the initial stages of this research, has been modified considerably to handle complex mechanisms with sliding masses and mechanisms operating at relatively high speeds. The analysis takes into account the effects of geometric and material nonlinearities, vibrational effects and coupling of deformations. Numerical results have been reported for certain mechanism examples. The effects of nonlinearities have been found to be significant on the dynamic behavior of mechanisms. Considerable progress has been made in developing a nonlinear finite element procedure for three-dimensional mechanisms. Numerical results obtained for some example problems indicate the validity of the current three-dimensional formulation. A new optimization algorithm has also been developed based on the Gauss method to handle various types of nonlinear constraints with the goal of reducing the number of analyses required to obtain an optimal design. Complete details of the nonlinear finite element procedures as well as the optimization technique are available in published papers, copies of which are included here in the Appendix. Because of the complex nature of the nonlinear analysis, which had to be repeated many times during the optimization process, considerable amount of computer time was needed for this research. To help overcome these computational difficulties, DoD and NSF provided funds through two separate grants to purchase a research computer and other associated equipment as well as access to a supercomputer.

FINAL TECHNICAL REPORT

AFOSR-TR- 87-2008

on

NONLINEAR ANALYSIS AND OPTIMAL DESIGN OF DYNAMIC

MECHANICAL SYSTEMS FOR SPACECRAFT APPLICATION

Air Force Office of Scientific Research

Grant No. AFOSR 84-0076

February 1, 1984 - July 31, 1987

Principal Investigators

K.D. Willmert

and

M. Sathyamoorthy

Department of Mechanical and Industrial Engineering

Clarkson University

Potsdam, New York 13676

September 1987

SUMMARY

A nonlinear finite element analysis procedure which was developed for planar mechanisms during the first phase of this research has undergone considerable modification to handle complex mechanisms with sliding masses and mechanisms operating at relatively high speeds. A suitable nonlinear finite element analysis procedure has also been developed for three-dimensional mechanisms. In both cases, the analysis takes into account the effects of geometric and material nonlinearities, vibrational effects, and coupling of deformations. Numerical results have been reported for certain mechanism examples. These results indicate significant influences of the geometric as well as the material nonlinearity effects on the dynamic behavior of mechanisms. In the optimal design area, a new algorithm has been developed for finding the minimum of a sum-of-squares objective function subject to general nonlinear constraints. The solution of some selected examples indicate good results in terms of the total number of objective function evaluations to obtain an optimal design. Complete details of these investigations as well as those of the nonlinear finite element analysis are included in the Appendix. To meet the extraordinary computational needs of this project, a separate VAX 11/785 computer and peripheral equipment were made available through a DoD research grant. The National Science Foundation also provided funds for some additional equipment as well as computational time on a supercomputer. The current research will continue with the help of a recently obtained National Science Foundation grant (Grant No. INT-8616036) which involves the development of a joint clearance model for mechanical mechanisms and its inclusion in the vibrational analysis of linkages undergoing large deformations due to high speeds and large loads.

RESEARCH OBJECTIVES

The objective of this research was to develop a nonlinear finite element dynamic analysis procedure for planar as well as spatial mechanisms that are frequently used in space structures. Included in the nonlinear analysis are the effects of curvature-displacement nonlinearity, nonlinearity due to extension or stretching (both caused by large deformations), material nonlinearity as well as combinations of these. In addition to the nonlinear analysis, an efficient optimal design method was to be developed to handle objective functions composed of combinations of

rigid body and deformation displacements involving geometric design variables as well as cross-sectional sizes of the members of the mechanism subject to limitations on stresses and deformations. Thus the proposed research involves the following.

- a) develop a nonlinear finite element procedure for dynamic planar mechanisms.
- b) develop an efficient optimization method involving a small number of analyses for mechanism design problems.
- c) extend the nonlinear analysis procedure developed for two-dimensional mechanisms to three-dimensional mechanisms.
- d) apply the optimization technique developed to simple mechanism problem.
- e) combine the nonlinear analysis procedure with the optimization technique to design complex three-dimensional mechanisms, robots and mechanical manipulators.

SIGNIFICANT ACCOMPLISHMENTS

A nonlinear finite element analysis procedure has been developed for planar mechanisms to handle geometric and material nonlinearities (see the publications list and Appendix for details). The results of several example mechanisms clearly indicate the need to include these types of nonlinearities in the dynamic analysis. The difficulties in extending this approach to complex planar mechanisms with sliding masses and mechanisms operating at relatively high speeds have been overcome by using a modified finite-element formulation to handle such complex cases. Some example problems using this new formulation have been considered in a paper entitled, "Vibrational Analysis of Mechanisms with Geometric and Material Nonlinearities" (with E. Kear, M. Sathyamoorthy and K.D. Willmert as authors) presented at the Joint AFOSR-SES Meeting held at the State University of New York at Buffalo in August 1986. Similar results have also been presented in a very recent paper entitled, "Effect of Geometric and Material Nonlinearities on Vibration of Planar Mechanisms" by E.B. Kear, M. Sathyamoorthy and K.D. Willmert, presented at the ARO/AFOSR Meeting on Nonlinear Vibrations, Stability and Dynamics of Structures and Mechanisms held at VPI & SU, Blacksburg, Virginia, March 1987. Considerable progress has also been made in developing a nonlinear finite element procedure for three-dimensional mechanisms. Some example problems have been solved and the results indicate

the validity of the three-dimensional formulation. The general three-dimensional formulation is given in a paper entitled, "Finite-Element Nonlinear Analysis of Three-Dimensional Mechanisms." by M. El-Sawy, K.D. Willmert and M. Sathyamoorthy included in the Appendix of this report.

In the optimization area, a very efficient optimality criterion technique called the Gauss Constrained Method has been developed to solve optimal design problems with objective functions which are the sum of squared quantities with general nonlinear constraints. The technique has the advantage of reducing the number of analyses required to obtain an optimal design, thereby significantly reducing the computational time. This method is described in a paper entitled, "The Development and Application of Gauss' Nonlinearly Constrained Optimization Method" (with D.R. Boston, K.D. Willmert and M. Sathyamoorthy as authors) published in the *Journal of Computer Methods in Applied Mechanics and Engineering*. In a paper entitled, "The Gauss Optimization Method for Problems with General Nonlinear Constraints" by T.E. Potter, K.D. Willmert and M. Sathyamoorthy (presented at the 22nd Annual Meeting of the Society of Engineering Science held at the Pennsylvania State University, University Park, Pennsylvania, October 1985), a new algorithm has been developed for finding the minimum of a sum-of-squares objective function subject to general nonlinear constraints. The solution of examples indicate good results in terms of the total number of objective function evaluations required by the algorithm to obtain an optimal design. The optimization techniques developed in this research as extensions of the Gauss method to handle various types of constraints, reduce the number of analyses required to obtain an optimal design. The method is now being used to solve additional example problems including various mechanisms.

Because of the very complex nonlinear analysis required, which must be repeated many times during the optimization process, a considerable amount of computer time was needed for this research. To meet these needs, a proposal entitled "Laboratory for Graphical Analysis of Nonlinear Deformations in Dynamic Structural-Mechanical Systems" was submitted to DoD under the DoD - University Instrumentation Program to purchase a separate research computer for this project. This resulted in a grant (No. AFOSR-85-0103) of \$101,567. Although the original proposal called for the purchase of a VAX 11/730, a very careful and thorough search for the best computer (with the available funds) resulted in the purchase of a much larger and faster VAX 11/785. Digital Equipment

Corporation offered a sizable reduction in cost of its VAX 11/785 computer under the DEC Educational Discount Program. Because of this reduction and because of additional cost sharing by Clarkson University's School of Engineering, it was possible to purchase the VAX 11/785 at no additional cost to DoD. The computer equipment purchased through DoD-URIP Grant and other sources includes

I. VAX 11/785 COMPUTER HARDWARE

1. VAX 11/780 Packaged System Including:	\$102,750
(A) VAX 11/780 CPU	
(B) 2-Mbytes ECC MOS (64-K chip) Memory	
(C) H9652 UNIBUS Expansion Cabinet with BA 11-K and DD11-DK	
(D) VAX/VMS License and Warranty	
2. TU80 9 Track Streaming Tape Drive with Cabinet	\$8,800
3. RUA81 456 Mbyte Fixed Disk	\$19,600
4. 2-Mbytes of Additional Memory	\$8,100
5. FP780 Floating Point Accelerator	\$8,960
6. Two DMF32-LP Communication Interfaces	\$5,250
7. 780 to 785 Upgrade Kit	\$80,000
8. 25 ft. RS 232 Sync Cable	\$95
9. Two 300/1200/2400 Baud Telephone Modems	\$1,060
10. Installation	N/C
11. Insurance and Transportation	\$1,817
12. Miscellaneous - Installation of Power, Phone Lines, Terminal Lines, etc.	<u>\$1,756</u>
Total Computer Hardware Cost	\$238,188

II. COMPUTER DISPLAY TERMINAL

1. Tektronix M4115B Computer Display Terminal	\$19,950
2. Option N1: Warranty-Plus	\$1,025
3. Option 2B: Additional 512 Kbytes RAM	\$4,600
4. Option 23: Additional Four Planes of Display Memory	\$6,000

5. Option 09: 4695 Color Copier Interface	\$500
6. Option 42: Single Flexible Disk	\$1,700
7. Display Stand	\$750
8. Software Package	\$1,000
9. 4695 Color Graphic Copier	\$1,595
10. Option 42: Warranty-Plus	\$430
11. 4926 10 Mbyte Hard Disk	\$4,200
12. Option N1: Warranty-Plus	\$210
13. Shipping	<u>\$371</u>
Total Display Terminal Cost	\$42,331

III. SOFTWARE FOR VAX 11/785 COMPUTER

1. VMS Operating System	N/C
2. FORTRAN License	\$5,170
3. DECNET Communication Software	\$2,950
4. IGL Graphics Software	\$2,677
5. PSI Access Software	<u>\$1,850</u>
Total Software Cost	\$12,647

IV. TOTAL HARDWARE & SOFTWARE COSTS \$293,166

The total value of the equipment and software is \$293,166. Discounts and contributions from Digital Equipment Corporation, Tektronix, Clarkson University's College of Engineering and the Department of Mechanical and Industrial Engineering total \$191,599. Thus, the total cost of the hardware and software to DoD remained at \$101,567 as originally proposed. It should be noted that the capabilities of the VAX 11/785 system, including the Tektronix 4115 graphic terminal, are enormous compared to the originally proposed VAX 11/730. The VAX 11/785 system is five times faster than the VAX 11/730, has 4 Mbytes of memory (compared to only 1 Mbyte of memory for VAX 11/730), 456 Mbyte of disk space (compared to 121 Mbyte of disk space) a total of 16 terminal lines, and a 9 track streaming tape drive (no tape drive was included in the original VAX 11/730 system).

Hardware and software were also purchased to tie the VAX 11/785 into Clarkson's campus-wide

computer network. The physical link is through the University's VAX 11/780, but this is tied to the other computers on campus, which is linked to other universities through BITNET. This tie in of the VAX 11/785 allows the users of this research computer access to many of the other facilities of the university, such as high speed printers, digital plotters, laser printers, etc. It also allows researchers with terminal connected to the other computers on campus to sign on to the VAX 11/785 as though they were directly connected.

The Tektronix 4115B computer display terminal, which is connected to the VAX 11/785 computer, has recently been expanded to improve its capabilities. Both a 3-dimensional wire frame and a shaded surface option have been added. These options allow the terminal to locally manipulate 3-dimensional objects, such as rotating them in 3-dimensional space, removing hidden lines, drawing shaded surfaces, etc. These expansions result in this terminal being equivalent to a Tektronix 4129 terminal, which is the most recent high-end terminal introduced by Tektronix. The total cost of these options was \$16,475, which was made possible through contributions from Gleason Foundation, Proctor and Gamble, Tektronix, Coming Glass Works as well as the University's School of Engineering.

A grant from the National Science Foundation (Grant No. DMC-8500627), with M. Sathyamoorthy and K.D. Willmert as principal investigator, included funds totaling \$10,715 for the further expansion of the graphic facilities. A Tektronix 4692 color graphics copier, a Tektronix 4107 low resolution graphic terminal and two Z-200 personal computers were purchased through this NSF grant. These purchases complement the high resolution Tektronix 4115B terminal obtained through the DoD-University Research Instrumentation Program. In addition to these equipment funds, this NSF grant provided, as part of its Cooperative Program on the Use of Supercomputers, twenty-five hours of CPU time on a Cray X-MP supercomputer. The program development and trial runs were done on the DoD funded in house VAX 11/785 research computer with final runs made at the supercomputer located at the University of Illinois.

A summary of funding sources including the 1984-85 DoD-URIP Grant to purchase the VAX 11/785 research computer and other associated equipment (including upgrades) is given below:

DoD - University Research Instrumentation Program	\$101,567
---	-----------

Digital Equipment Corporation Contribution	\$120,852
Tektronix Discount and Contribution	\$11,110
National Science Foundation	\$10,715
Clarkson University's College of Engineering Contribution	\$56,999
Department of Mechanical & Industrial Engineering	\$3,176
Clarkson's Educational Resource Center	\$3,300
Gleason Foundation	\$7,000
Proctor and Gamble	\$5,300
Corning Glass Works	<u>\$337</u>
TOTAL	\$320,356

As a result of contributions from all of these sources, the total value of the equipment within this laboratory exceeds \$300,000 for an investment of only slightly over \$100,000 from DoD.

A recent grant from the National Science Foundation (Grant No. INT-8616036), with K.D. Willmert and M. Sathyamoorthy as principal investigator, will help accomplish all the remaining goals of the current AFOSR research. The funded NSF research involves a cooperative effort between the principal investigators and a collaborator at the Korea Advanced Institute of Science and Technology in the Republic of Korea. The particular project will require the development of a joint clearance model for mechanical mechanisms and its inclusion in the vibrational analysis of linkages undergoing large deformations due to high speeds and large loads. Also included is the study of the optimal design of counter weights to reduce, as much as possible, the joint forces. The duration of the NSF research will be until December 1989.

PUBLICATIONS

a) Technical Reports

1. D.R. Boston, K.D. Willmert and M. Sathyamoorthy, "The Gauss Nonlinearly Constrained Method Applied to Mechanism Design," Department of Mechanical and Industrial Engineering, Clarkson University, Potsdam, NY, Report No. MIE-104, June 1984.
2. K.D. Willmert and M. Sathyamoorthy, "Research Progress and Forecast Report on Nonlinear Analysis

and Optimal Design of Dynamic Mechanical Systems for Spacecraft Application," Report to AFOSR in August 1984.

3. D.W. Tennant, K.D. Willmert and M. Sathyamoorthy, "Vibration of Mechanisms with Material and Geometric Nonlinearities Using Variable Length Finite Elements," Department of Mechanical and Industrial Engineering, Clarkson University, Potsdam, NY, Report No. MIE-106, October 1984.
4. K.D. Willmert and M. Sathyamoorthy, "Nonlinear Analysis and Optimal Design of Dynamic Mechanical Systems for Spacecraft Application," AFOSR Annual Technical Report No. 1, February 1985.
5. K.D. Willmert and M. Sathyamoorthy, "Research Progress and Forecast Report on Nonlinear Analysis and Optimal Design of Dynamic Mechanical Systems for Spacecraft Application," Report to AFOSR in August 1985.
6. K.D. Willmert, "Laboratory for Graphical Analysis of Nonlinear Deformations in Dynamic Structural-Mechanical Systems," DoD-University Research Instrumentation Program Final Report, April 1986.
7. K.D. Willmert and M. Sathyamoorthy, "Nonlinear Analysis and Optimal Design of Dynamic Mechanical Systems for Spacecraft Application" AFOSR Annual Technical Report No. 2, February 1986.
8. K.D. Willmert and M. Sathyamoorthy, "Research Progress and Forecast Report on Nonlinear Analysis and Optimal Design of Dynamic Mechanical Systems for Spacecraft Application," Report to AFOSR in August 1986.
9. M. Sathyamoorthy and K.D. Willmert, "Use of a Supercomputer for Nonlinear Analysis and Optimal Design of Dynamic Mechanical Systems," NSF Final Project Report, March 1987.

b) Technical Journals, Meetings and Conferences:

1. K.D. Willmert and M. Sathyamoorthy, "Optimal Design of Flexible Mechanisms," Presented at the Second Forum on Space Structures, McLean, Virginia, June 1984.
2. D.R. Boston, K.D. Willmert and M. Sathyamoorthy, "Gauss' Nonlinearly Constrained Optimization Method," Proceedings of the ASCE Engineering Mechanics Specialty Conference, University of Wyoming, Laramie, August 1984, pp. 82-85.
3. K.D. Willmert and M. Sathyamoorthy, "Optimal Design of Dynamic Mechanical Systems Undergoing

- Large Deformations," Presented at the Conference on Supercomputers in Mechanical Systems Research, Lawrence Livermore Laboratory, Livermore, California, September 1984.
4. M. Sathyamoorthy and K.D. Willmert, "Nonlinear Analysis and Design of Flexible Mechanisms"
Presented at the Third Forum on Large Space Structures, Texas A & M University, College Station, Texas, July 1985.
 5. T.E. Potter, K.D. Willmert and M. Sathyamoorthy, "The Gauss Optimization Method for Problems with General Nonlinear Constraints," Proceedings of the Society of Engineering Science Meeting, The Pennsylvania State University, University Park, Pennsylvania, October 1985, p. 10.
 6. D.W. Tennant, K.D. Willmert and M. Sathyamoorthy, "Finite Element Nonlinear Vibrational Analysis of Planar Mechanisms," Paper published in the Special Issue of Material Nonlinearity in Vibration Problems, AMD Vol. 71, ASME, November 1985, pp. 79-89.
 7. D.R. Boston, K.D. Willmert and M. Sathyamoorthy, "The Development and Application of Gauss' Nonlinearly Constrained Optimization Method," Computer Methods in Applied Mechanics and Engineering, Vol. 57, No. 1, 1986, pp. 17-24.
 8. Edward Kear III, M. Sathyamoorthy and K.D. Willmert, "Vibration Analysis of Mechanisms with Geometric and Material Nonlinearities," Paper presented at the Joint AFOSR-SES Meeting, State University of New York at Buffalo, August 1986.
 9. E.B. Kear III, M. Sathyamoorthy and K.D. Willmert, "Effect of Geometric and Material Nonlinearities on Vibration of Planar Mechanisms," Paper presented at the ARO/AFOSR Meeting on Nonlinear Vibrations, Stability and Dynamics of Structures and Mechanisms, VPI & SU, Blacksburg, Virginia, March 1987.
 10. M. El-Sawy, K.D. Willmert and M. Sathyamoorthy, "Finite Element Nonlinear Analysis of Three-Dimensional Mechanisms" In preparation for publication.

PROFESSIONAL PERSONNEL

1. K.D. Willmert, Professor and Chairman of Mechanical and Industrial Engineering, Project Supervisor.
2. M. Sathyamoorthy, Associate Professor of Mechanical and Industrial Engineering, Project

Supervisor.

3. T.E. Potter, Currently an off campus Ph.D. Student in Mechanical and Industrial Engineering working on optimization methods applicable to large mechanism design problems.
4. E.B. Kear III, Currently a Ph.D. student in Mechanical and Industrial Engineering working on nonlinear analysis techniques for deformation analysis of two and three-dimensional mechanisms.
5. M. El-Sawy, Currently a Ph.D. student (supported by Egyptian Government) in Mechanical and Industrial Engineering working on nonlinear analysis techniques for deformation of three-dimensional mechanisms.
6. B. Whispell, Currently an Ph.D. student (partially supported by Alcoa Foundation) in Mechanical and Industrial Engineering working on computer graphics for display of three-dimensional mechanisms undergoing deformations.

APPENDIX

PUBLICATIONS

SECOND FORUM ON SPACE STRUCTURES

PRECIS OF PROCEEDINGS
MEETING OF INVESTIGATORS OF
STRUCTURAL DYNAMICS AND CONTROLS
ISSUES IN LARGE SPACE STRUCTURES
TECHNOLOGY
11-13 JUNE 1984

SPONSORED BY

AF OFFICE OF SCIENTIFIC RESEARCH
BOLLING AFB DC 20332-6448

AIR FORCE FLIGHT DYNAMICS LABORATORY
WRIGHT-PATTERSON AFB OH 45433

NASA LANGLEY RESEARCH CENTER
HAMPTON VA 23665

Professor Ken Willmert
Mechanical and Industrial Engineering Department
Clarkson University
Potsdam, New York

Areas of Interest

- 1) Optimal Design of Mechanical and Structural Systems.
- 2) Nonlinear Deformation Analysis of Mechanical Devices Undergoing Dynamic Rigid Body Motion.

4. INTEGRATED DESIGN OF STRUCTURE AND CONTROL

by Vipperla B. Venkayya

Introduction

The panel identified several presentations relevant to the subject of integrated design. They included the following:

1. Ken Willmert of Clarkson University on the optimization of flexible mechanisms;
2. Mohan Aswani and G. T. Tseng of The Aerospace Corporation on continuum modeling of the plant as one means of simplifying structure-control optimization problems;
3. Manohar Kamat of VPI on the issues of plant nonlinearities (geometric and material), proposing that they be considered in control system design;
4. Moktar Salama of JPL on structure-control optimization with a single performance index consisting of the structural mass and the total control input;
5. Dale Berry of Purdue University on continuum modeling as a means of reducing plant dimensionality;
6. K. C. Park of Lockheed Palo Alto Research Lab on the use of transient energy density profiles to achieve optimum disturbance dissipation and control;
7. John Junkins of VPI on some recent results of eigenvalue placement via structural parameter optimization.

The material of these presentations was, to a certain extent, the basis for the panel discussions.

The panel proposed the following five topics for discussion:

Volume 1

ENGINEERING

MECHANICS

IN CIVIL ENGINEERING

Edited by

A. P. Boresi and K. P. Chong

Volume 1 ENGINEERING MECHANICS IN CIVIL ENGINEERING

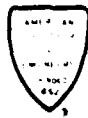
Proceedings of the
Fifth Engineering Mechanics Division
Specialty Conference

Sponsored by the
Engineering Mechanics Division
of the American Society of Civil Engineers

University of Wyoming
Laramie, Wyoming 82071
August 1-3, 1984

In cooperation with
The Department of Civil Engineering and
The Division of Conferences and Institutes
University of Wyoming

Edited by
A. P. Boresi and K. P. Chong



Published by the
American Society of Civil Engineers
145 East 47th Street
New York, New York 10017-2498

$$f(x) = \xi^T \xi$$

where ξ is assumed to be a column vector of order l , $\xi = \xi_1, \dots, \xi_l$ where ξ_i are l quadratic, $\xi_i = \xi_i^T x + \xi_i^0$ and ξ_i^T are $1 \times n$ row matrices and ξ_i^0 are scalars. The matrix A and the vector b are assumed to be constant and of the form:

$$g_i(x) = \frac{1}{2} x^T A_i x + b_i^T x + c_i \quad (1)$$

The gradient and matrix H of the quadratic objective function are $\nabla f(x) = 2 \xi^T A \xi$ and $H = 2 \xi^T A \xi$. In each iteration we assume there are r active constraints, $r \leq l$, where r is a function of x and ξ and ξ is (ξ_1, \dots, ξ_r) where $\xi_i = \xi_i^T x + \xi_i^0$ and ξ_i^T are

$$\begin{aligned} \nabla f(x) &= (A_1 \xi_1 + \dots + A_r \xi_r) + \xi^T A \xi \\ g_j(x) &= \frac{1}{2} x^T A_j x + b_j^T x + c_j \\ \lambda_j &> 0 \end{aligned} \quad (2)$$

Similar to the Gauss method, an iterative algorithm is used. A method is generated such that, in each iteration, the algorithm sign for a quadratic objective function is determined. The algorithm active at the optimal design are also active at the starting point. Solving equation (2) for (x_{j+1}, λ_j) and substituting the

$$\begin{aligned} \nabla f(x_{j+1}) &= \nabla f(x_j) + \sum_{i=1}^r \lambda_i \nabla g_i(x_j) \\ x_{j+1} &= (b + \frac{1}{2} \sum_{i=1}^r \lambda_i b_i + \frac{1}{2} \sum_{i=1}^r \lambda_i A_i x_j) / (A + \frac{1}{2} \sum_{i=1}^r \lambda_i A_i) \end{aligned} \quad (3)$$

We must now determine the method of choice of relative multipliers λ_i . The expression for x_{j+1} is substituted into the constraints of equation (2) resulting in a system of r nonlinear equations in r unknowns λ_i of the form:

$$\begin{aligned} g_i(x_j) &= \frac{1}{2} (G + \frac{1}{2} \sum_{k=1}^r \lambda_k A_k) x_j^T x_j + b_i^T x_j + c_i \\ (G x_j - \frac{1}{2} \sum_{k=1}^r \lambda_k A_k x_j) + b_i^T x_j + c_i &= 0 \\ (G x_j - \frac{1}{2} \sum_{k=1}^r \lambda_k A_k x_j) + b_i^T x_j + c_i &= 0 \end{aligned} \quad (4)$$

This system of equations is solved using the Gauss method. At each iteration, the method requires the solution of a system of r equations. If the method does not converge, which may be caused by the fact that the equations have no solution or that the method simply is not able to locate one, then a last approach is used. In this case, an objective function is formed which is the sum of the squares of the active constraints g_i . This method is called least squares method with respect to λ . In this work, the method was used only if the method is not able to locate one. It should be noted that the method is not able to

AN EFFICIENT NONLINEAR CONSTRAINED OPTIMIZATION METHOD

R. P. Boston*, K. D. Willmert* and M. Nathanaelsoorthy*

Abstract

Presented in this paper is a new optimization technique, called the Gauss Mechanism Constrained Technique which is applicable to design optimization with nonlinear objective functions and constraints. The method is an extension of a previously developed method for linear constrained optimization called the Gauss Constrained Technique. Both of these methods, based on Gauss' least squares method, have been demonstrated that the latter method conditions are automatically satisfied when the optimum is reached.

Introduction

The stress design of many structures and mechanical mechanisms has become a very complex and time consuming analyses at each iteration of the optimization. This is particularly critical if a large number of nonlinear analyses is required. In these cases especially, it is important that the optimization method require very few analyses, even at the expense of significantly increasing the amount of calculations in the optimization technique itself. For example in a recent effort, Lebes and Willmert [1] applied the relatively efficient Generalized Mechanism Gradient (GRG) Technique of Hasdon et al. [2] to mechanism design for path generation and rigid body guidance. The mechanism analyses were considered flexible, and thus a quasi-static (linear) finite element analysis was used to obtain deformations and stresses. The GRG element analysis was used to obtain deformations and stresses. The GRG method required as many as 10,000 mechanism analyses to obtain the optimal design. Optimization time approached twenty hours on an IBM 4341 mainframe computer. If a nonlinear analysis had been used, the corresponding times would have been considerably higher.

To reduce the number of analyses, Paradis and Willmert [3] developed a new direct method for efficient design of mechanisms. Gauss' method, which Willert [4] concluded to be very efficient for unconstrained mechanism design was modified to handle linear constraints. The resulting technique, referred to as the Gauss Constrained Technique, was more efficient and required very few objective function evaluations to obtain an optimal design. Their method has been extended, in this paper, to handle nonlinear constraints.

Review of the Method

The Gauss Constrained Technique is summarized as follows:

*Department of Industrial Engineering Department, Clarkson University, Pottsville, Pennsylvania.

is zero or not for these values of λ are then used in the iterative equation (7).

As in the original Gauss (constrained) Technique (as well as the gradient projection method) the criterion for dropping a constraint from the set of active constraints is the sign of λ_i . At any iteration the constraint corresponding to the most negative λ is dropped from the set of active constraints and a new vector of Lagrange Multipliers is determined. This procedure is repeated until all $\lambda_i > 0$. If this results in no active constraints, then the optimization technique continues by setting all $\lambda_i = 0$ in equation (7). In this case, the iterative expression, equation (7), can be shown to reduce to Gauss' method for unconstrained optimization

$$\mathbf{x}_{i+1} = \mathbf{x}_i - (\mathbf{H}_i)^{-1} \mathbf{g}_i$$

At each iteration a decision must be made as to whether or not a new constraint should be added to the set of active constraints. If the direction of minimization \mathbf{g}_i is defined as the direction from \mathbf{x}_i to \mathbf{x}_{i+1} , then a constraint is added only if a step in the \mathbf{g}_i direction will not violate the constraint.

These procedures can only be implemented if the constraint in question is active, i.e. $g_i(\mathbf{x}_{i+1}) = 0$. Therefore, during each iteration, no constraints may be violated. If a step is to be taken such that $g_i(\mathbf{x}_{i+1}) > 0$, a new design \mathbf{x}_{i+1} must be found along the line connecting \mathbf{x}_i and \mathbf{x}_{i+1} such that $g_i(\mathbf{x}_{i+1}) = 0$. This is accomplished by stepping back from a violated constraint until it is active.

Although the technique was developed assuming linear functions $\mathbf{f}(\mathbf{x})$, i.e. $\mathbf{F}(\mathbf{x})$ quadratic, the method is applicable to problems where the \mathbf{f} are general functions of \mathbf{x} . An especially important characteristic for mechanism design is that the technique requires a total of only one more objective function evaluation than iterations to obtain an optimal design, unlike the GRG technique of Lasdon et al [2], where a step length determination is required at each iteration.

Example Problem

In this example, a four-bar mechanism will be designed such that the coupler point (XX,YY) of the mechanism will closely generate the curve defined by the eight points as shown in Figure 1. The objective function to be minimized is the sum of the distances (squared) between the desired curve and the actual curve generated by the mechanism:

$$F(\mathbf{x}) = \sum_{i=1}^8 [(XX_i - X_{C_i})^2 + (YY_i - Y_{C_i})^2]$$

where (XC,YC) are the coordinates of the desired curve. The design variables x_1, \dots, x_{10} are link lengths, orientation of some of the links as well as the location of the crank pin. Note, the objective function is a highly nonlinear function of the design variables. This is the same problem that Paradis and Willmert [3] solved, however, a nonlinear constraint has been introduced here to constrain the location of the crank pin to a user defined circular region. Thus, our design problem contains ten variables, x_1, \dots, x_{10} , and thirteen inequality constraints $g_1, g_2, \dots, g_{13} = 1, \dots, 13$. The constraints are: (where XC=4, YC=6, R=3)

- $g_1 = 1 - x_2 \leq 0$
- $g_2 = 1 - x_5 \leq 0$
- $g_3 = x_2 - x_1 \leq 0$
- $g_4 = x_2 - x_3 \leq 0$
- $g_5 = x_2 - x_4 \leq 0$
- $g_6 = x_1 + x_2 - x_3 - x_4 = 0$
- $g_7 = x_2 + x_3 - x_1 - x_4 = 0$
- $g_8 = x_1 + x_4 - x_3 - x_5 = 0$
- $g_9 = x_1 - 30 \leq 0$
- $g_{10} = x_3 - 30 \leq 0$
- $g_{11} = x_4 - 30 \leq 0$
- $g_{12} = x_5 - 30 \leq 0$
- $g_{13} = (x_1 - X_C)^2 + (x_2 - Y_C)^2 - R^2 \leq 0$

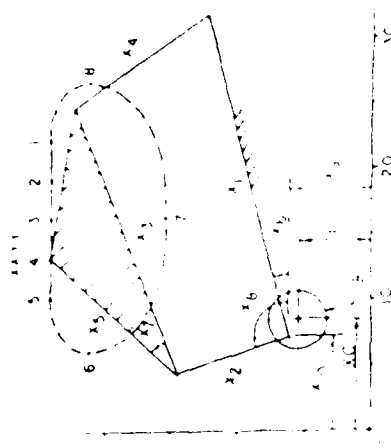


Figure 1. Four-Bar Mechanism Path Generation

For each of five different starting points, the final value of the objective function was $F = 0.0000$. At this point, the vector of design variables was (30.0, 8.177, 27.217, 12.322, 16.771, 31.027, 1.309, 1.309, 2.892, 6.790) with constraints g_9 and g_{13} active. The number of objective function evaluations required for each of the five starting points for the Gauss Nonlinearly Constrained Technique (GNLC) developed in this paper and the GRG method of Lasdon et al [2] are listed below.

Starting Point	1	2	3	4	5
GNLC	9	10	10	15	11
GRG	522	597	459	345	409

As expected the Gauss Nonlinearly Constrained method requires significantly fewer objective function evaluations.

Acknowledgements

Research sponsored by the Air Force Office of Scientific Research, Air Force Systems Command, AFOSR under Grant Number AFOSR 84-0076. The U.S. Government is authorized to reproduce and distribute reprints for government purposes not withstanding any copyright notation thereon.

References

1. DeKubec, M.J. and Willmert, K.D., "Optimal Design of Flexible Link Mechanisms," to be published in ASME Journal of Mechanisms, Transactions and Automatic in Design.
2. Lasdon, L.S., Waren, Adams and Ratner, M.W., "Global User's Guide," Cleveland State University, February 1982.
3. Paradis, M.J. and Willmert, K.D., "Optimal Mechanism Design Using the Gauss Constrained Method," ASME Paper No. 82-ET-91, 1982.
4. Wilde, D.F., "First Order Optimization in the Linear Squares Design Function Generating Mechanisms," Proceedings of the ASME Winter Meeting, ASME, New York, 1979, pp. 13-17.

OPTIMAL DESIGN
OF DYNAMIC MECHANICAL SYSTEMS
UNDERGOING LARGE DEFORMATIONS

K. D. Willmert
M. Sathyamoorthy

Mechanical and Industrial Engineering Department
Clarkson University
Potsdam, NY 13676

Introduction

The general purpose of most mechanical devices is to produce accurate two or three-dimensional movement of objects. However, for large external loads and/or high speed operation, sufficient forces, both inertial and externally applied, are produced to cause their members, joints, and support structure to deform. This results in a loss of accuracy of the device. To solve this problem, the current design procedure is to increase the stiffness of the members by modifying their cross-sectional sizes (commonly by increasing the areas) or changing the material used to reduce the deformations and stresses. The result is a more massive device which is difficult to control, requiring more power to drive and interacting with its structural support to an even greater extent.

Optimization methods have been applied to determine the member sizes by minimizing the weight subject to limitations on deformations and stresses. This can reduce the overall size of the device, but the result is still not the best design. The difficulty lies in the basic separation of variables in the design process. The device configuration (i.e., the number and type of members and joints) and the member lengths are designed first to produce the desired motion, assuming the members are rigid. Then, independently, the cross-sectional sizes are determined so that the actual motion deviates as little as possible from the rigid body motion. In this procedure, the deformations of the members are considered to have a detrimental effect on the overall motion. The goal, therefore, is to restrict or reduce them. However, these deformations can actually be used to improve the motion of the device if the geometric design variables (member lengths, etc.) and cross-sectional sizes of the members are combined and treated as a single set of design variables. Thus, the combined design problem is to select all of the design variables so that the actual motion of the device, which is a combination of the rigid body motion plus the deformations, is as close as possible to the desired motion. The usual rigid body constraints exist on this problem, such as limitations on the moveability of the device, locations of the support points, lengths of the members, etc. But also present are deformation and stress constraints, and natural frequency limitations associated with the flexibility of the members.

Depending on the type of motion desired, speed of operation of the device, and restrictions on the design, the solution of this design problem will be a

mechanism in which the deformations of the members serve to aid the mechanism in producing the desired motion. Thus a much wider range of motions is possible than could be obtained from a rigid link device. The optimal design, however, is likely to contain several members which are very flexible (any members that are required to be rigid can be designed using appropriate constraints). Because of these large deformations, a general nonlinear vibrational deformation and stress analysis is required. The types of nonlinearities include:

1. Nonlinear curvature-displacement relations
2. Extension or stretching of the neutral surface
3. Material nonlinearities (nonlinear stress-strain)
4. Effects of transverse shear and rotatory inertia due to realistically proportioned members
5. Joint clearances
6. Variable nature of the cross-section of the members
7. Interaction of the mechanical device with the support structure
8. Coupling of the degrees-of-freedom due to large deformations.

A typical analysis which takes into account all of these nonlinearities is iterative in nature requiring several iterations to obtain a solution.

Because of the complex nonlinear analysis required, which must be done many times during the optimization phase, considerable computational time is needed for this design procedure. Experience has shown that four to eight hours of computer time is common to perform just one analysis of a single planar four-bar or slider crank mechanism on an IBM 4341 computer. For more complex planar mechanical devices consisting of additional links, gears, cams and other elements, considerably longer times would be expected. For three-dimensional mechanisms, as exist in many applications of mechanical manipulators, automotive suspensions, etc., enormous computational times would be involved--again to perform just one analysis.

The mathematical optimization techniques currently available for solving optimal design

problems all require several iterations to obtain the best design. Some methods involve a large number of iterations, with each iteration requiring numerous analyses (obtaining numerical values for the objective function and constraints for particular values of the design variables). These methods are adequate if the design problem is small, since computational times are relatively insignificant. However for large design problems, or ones in which a complex analysis is required, it is extremely important that the optimization technique be efficient, particularly in terms of the number of analyses required. Even then, the solution of these problems is impossible on most computers currently at universities. The availability of a super computer to accomplish the optimal design of large mechanical systems is absolutely necessary.

Research Problems

The particular research problems in the area of optimal design of dynamic mechanical systems which require the use of super computers are:

1. Nonlinear Analysis of Mechanisms

Objective: Develop a large amplitude nonlinear deformation, stress and frequency analysis of two and three-dimensional mechanical systems undergoing high speed motion subjected to large external loads. Include:

- * Geometric and material nonlinearities
- * The effects of transverse shear and rotatory inertia
- * Joint clearances
- * Interaction of the mechanical devices with the support structure
- * Coupling of degrees-of-freedom due to large deformations

Supercomputer needs:

- * Complex nonlinear analysis requiring enormous amount of computer time due to the iterative nature of the problem.
- * Solutions to very complex mechanical devices consisting of many links, gears, cams and other mechanical elements.

Estimated reduction of computer time:

100 to 1

2. Efficient Optimization Methods for Nonlinear Mechanisms Design

Objective: Develop efficient optimization methods with the following characteristics to handle nonlinear mechanism design problems:

- * Minimize an objective function composed of a combination of rigid body and deformation displacements
- * Use geometric and cross-sectional size design

variables

- * Handle geometric, deformation, stress and frequency constraints
- * Requires a small number of function evaluations (iterations) to obtain the optimal design

Supercomputer needs:

- * Combining nonlinear analysis and optimization involves a considerable amount of computer time for each solution.
- * To handle objective functions which are highly nonlinear functions of the design variables.

Estimated reduction of computer time:

100 to 1

THIRD FORUM ON LARGE SPACE STRUCTURES

Rudder Conference Tower

Texas A&M University

July 8-10, 1985

SPONSORS

Dr. Tony Amos, AFOSR

Dr. V.B. Venkayya, AFFDL

FORUM CO-CHAIRMEN

David H. Allen

Walter E. Haisler

Texas A&M University

Nonlinear Analysis and Design of Flexible Mechanisms

K. D. Willmert, and
M. Sathyamoorthy
Clarkson University

A finite element approach is presented here for the nonlinear vibrational analysis of planar mechanisms. The analysis takes into account the effects of material and geometric nonlinearities on the dynamic behavior. The geometric nonlinearities included in this study are due to stretching of the neutral axis and the curvature-displacement nonlinearity, both caused by *large deformations*. The material nonlinearity is due to a nonlinear stress-strain relationship of hermite polynomials which ensure compatibility of curvative between elements. Using a variable correlation table, a global system of nonlinear equations is derived in terms of the global unknowns and the kinematics of the mechanism. A *harmonic series* technique is then used to obtain the steady state solutions to this system of nonlinear equations. Numerical results are presented for an example mechanism and the effects of the nonlinearities are discussed.

An optimization technique which is applicable to problems consisting of nonlinear objective functions and constraints, such as the one presented here, has also been developed and reported. The technique, called the Gauss Nonlinearly Constrained Technique, is illustrated with examples.

THE GAUSS OPTIMIZATION METHOD FOR
PROBLEMS WITH GENERAL NONLINEAR CONSTRAINTS

T. E. Potter, K. D. Willmert and M. Sathyamoorthy

Mechanical and Industrial Engineering Department
Clarkson University
Potsdam, NY 13676

ABSTRACT

A new algorithm is presented for finding the minimum of a nonnegative objective function subject to general nonlinear constraints. This algorithm, based of Gauss' method for unconstrained problems, is developed as an extension to the Gauss constrained technique for linear constraints. The derivation of the algorithm, using a Lagrange multiplier approach, is based on the Kuhn-Tucker conditions so that when the iteration process terminates these conditions are automatically satisfied. A feasible design is maintained throughout the iteration process. The solution of preliminary examples indicate excellent results in terms of the number of objective function evaluations required by the algorithm to obtain an optimal design.

INTRODUCTION

The optimal design of many complex structural and mechanical systems is hindered by the large computational times involved. Most currently available optimization techniques require a large number of analyses to obtain the optimal design. For small problems, or ones in which the analysis is simple, these methods are adequate; however, for large problems, or where a time consuming analysis is required, more efficient optimization methods are needed. The goal of this research was to develop such methods, particularly techniques applicable to mechanical mechanism design where the members are deforming because of high speed motion and large external forces. Computational times to perform a single analysis are enormous for problems of this type involving large deformations with nonlinear material characteristics. Thus the goal of the methods developed was to reduce the number of analyses, even at the expense of increased computational effort in the optimization technique itself, i.e. additional effort in finding new candidate design points to analyze.

The methods developed take advantage of the special characteristics of the optimization problem, similar to the optimality criterion techniques. This greatly improves their efficiency. For most mechanism design problems, the objective function can be formulated as a sum of squared quantities such as the difference between the desired performance and the actual performance of the mechanism at specified points during its motion. Thus the techniques were developed specifically to handle problems of this type, although the methods are applicable to objective functions which are general sums of nonnegative quantities, such as weight. Many mechanism problems have constraints which are only linear functions of the design variables. Thus a special method was developed for problems of this type. Other problems have constraints which are linear or quadratic, and another method was developed for this case. Some mechanism design problems have more general nonlinear constraints. Methods to handle these cases are currently being developed.

All of the techniques developed in this work have been based on Gauss' method [1] which is applicable to problems without constraints. Wilde [2] has shown this method to be particularly efficient on simple mechanism design problems. The research presented in this paper has extended this method to handle various types of constraints common to more complex mechanism design problems.

FORMULATION

For an unconstrained sum-of-squares objective function

$$f(\vec{x}) = \vec{\phi}^T \vec{\phi}, \quad (1)$$

where $\vec{\phi}$ is a vector of linear or nonlinear functions ϕ_i thru ϕ_p in x , the Gauss method for calculating the next iteration of the design variables, \vec{x}_{k+1} , given a current design, \vec{x}_k , is:

$$\vec{x}_{k+1} = \vec{x}_k - \left[J(\vec{x}_k) J^T(\vec{x}_k) \right]^{-1} J(\vec{x}_k) \vec{\phi}(\vec{x}_k), \quad (2)$$

where

$$J(\vec{x}) = \begin{bmatrix} \frac{\partial}{\partial x_1} \phi_1(\vec{x}) & \dots & \frac{\partial}{\partial x_p} \phi_p(\vec{x}) \end{bmatrix} = \nabla \vec{\phi}^T. \quad (3)$$

It is observed that only first derivatives of the ϕ functions are required and that the new design point is calculated directly from the current design without using a step length determination with associated one dimensional minimization. Himmelblau [1] has shown this method to be very efficient for unconstrained minimization problems.

This technique has been extended to handle linear inequality constraints of the form

$$g_i(\vec{x}) = \vec{b}_i^T \vec{x} - c_i \leq 0, \quad i = 1, \dots, M \quad (4)$$

as well as equality constraints

$$h_i(\vec{x}) = \vec{d}_i^T \vec{x} - e_i = 0, \quad i = 1, \dots, L. \quad (5)$$

In the derivation of the optimization method, the ϕ_i functions are assumed to be linear in \vec{x} of the form

$$\vec{\phi} = J^T \vec{x} + \vec{u}. \quad (6)$$

where J is a constant matrix. However the resulting technique is applicable to problems in which the ϕ_i 's are general nonlinear functions of \vec{x} .

At iteration k , the L equality constraints and any of the inequality constraints that are active can be combined and written in the form

$$B^T \vec{x} - \vec{C} = 0. \quad (7)$$

If at the next iteration, $k+1$, the variables \vec{x}_{k+1} are at the optimum design, then the Kuhn-Tucker conditions will be satisfied

$$\nabla f(\vec{x}_{k+1}) + B\vec{\lambda} = 0 \quad (8)$$

$$B^T \vec{x}_{k+1} - \vec{C} = 0 \quad (9)$$

and

$$\vec{\lambda} \geq 0 \quad (10)$$

where $\vec{\lambda}$ is the vector of Lagrange multipliers. The gradient of f is given by

$$\nabla f(\vec{x}) = 2J\vec{\phi}(\vec{x}). \quad (11)$$

Expanding $\vec{\phi}(\vec{x})$ in a Taylor series results in

$$\vec{\phi}(\vec{x}_{k+1}) = \vec{\phi}(\vec{x}_k) + J^T \left[\vec{x}_{k+1} - \vec{x}_k \right] + (\text{higher order terms}) \quad (12)$$

It is noted that the higher order terms are equal to zero if $\vec{\phi}$ is linear. If $\vec{\phi}$ is not linear then these terms will be neglected and the expansion is only approximate. If equation (12) is substituted into equation (11), evaluated at \vec{x}_{k+1} , the result is

$$\nabla f(\vec{x}_{k+1}) = 2J \left[\vec{\phi}(\vec{x}_k) + J^T \left[\vec{x}_{k+1} - \vec{x}_k \right] \right]. \quad (13)$$

This may be substituted into the first Kuhn-Tucker condition.

equation (8), and then solved for \vec{x}_{k+1} :

$$\vec{x}_{k+1} = \vec{x}_k - [2JJ^T]^{-1} [2J\vec{\phi}(\vec{x}_k) + B\vec{\lambda}]. \quad (14)$$

Plugging this equation for \vec{x}_{k+1} into the second Kuhn-Tucker condition, equation (9), yields

$$B^T \vec{x}_k - \vec{C} - B^T [2JJ^T]^{-1} [2J\vec{\phi}(\vec{x}_k) + B\vec{\lambda}] = 0. \quad (15)$$

If the same set of constraints that are active at \vec{x}_{k+1} were also active at \vec{x}_k , then $B^T \vec{x}_k - \vec{C} = 0$. Using this result, equation (15) can be solved for $\vec{\lambda}$ as

$$\vec{\lambda} = - \left[B [2JJ^T]^{-1} B \right]^{-1} B^T [2JJ^T]^{-1} 2J\vec{\phi}(\vec{x}_k). \quad (16)$$

Substituting this back into equation (14) and simplifying yields an iterative expression for \vec{x}_{k+1} which will give the optimum solution if the constraints that are active at the optimum point (iteration k+1) are active at iteration k:

$$\vec{x}_{k+1} = \vec{x}_k - \left[I - [JJ^T]^{-1} B \left[B^T [JJ^T]^{-1} B \right]^{-1} B^T \right] [JJ^T]^{-1} J\vec{\phi}(\vec{x}_k). \quad (17)$$

This expression is equivalent to that derived by Paradis and Willmert [3] using a Gradient Projection method as the foundation. The technique converges to the optimal design in one iteration if the objective function, f , is quadratic and the starting point is on the constraints which are active at the optimal design. If f is not quadratic, the technique can still be applied, but it will generally require several iterations to reach the optimal design. When the technique terminates, the Kuhn-Tucker conditions will be satisfied independent of the form of the objective function.

Paradis and Willmert demonstrated the efficiency of this method by solving several examples. One example presented was the optimal design of a four-bar mechanism to generate a desired coupler point path. The Gauss constrained technique was compared with the Davidon-Fletcher-Powell method using an interior penalty function approach to handle constraints. Using four different starting points, the Gauss constrained method required from 23 to 33 objective function evaluations whereas the Davidon-Fletcher-Powell method required from 209 to 622. While not all starting points yielded the same optimal design, both methods reached the same local minimum from each starting point. Other examples also showed considerable improvement over existing methods.

The Gauss method has also been extended to include quadratic inequality constraints or quadratic approximations to higher order nonlinear constraints. In this work the constraints are assumed to

have the form

$$g_1(\bar{x}) = \frac{1}{2} \bar{x}^T A_1 \bar{x} + \bar{B}_1^T \bar{x} - C_1 \leq 0, \quad i = 1, \dots, M. \quad (18)$$

If at iteration $k+1$ there are r active constraints ($r \leq M$), the Kuhn-Tucker conditions will be

$$\nabla f(\bar{x}_{k+1}) + \sum_{j=1}^r \left[A_j \bar{x}_{k+1} + \bar{B}_j \right] \lambda_j = 0 \quad (19)$$

$$\frac{1}{2} \bar{x}_{k+1}^T A_j \bar{x}_{k+1} + \bar{B}_j^T \bar{x}_{k+1} - C_j = 0, \quad j = 1, \dots, r \quad (20)$$

and

$$\bar{\lambda} \geq 0 \quad (21)$$

where the summation in equation (19) and the j subscript in equation (20) refer to the set of active constraints only.

Using a derivation similar to that for linear constraints, substituting the expression for the gradient of f , equation (13), into the first Kuhn-Tucker condition, equation (19), and solving for \bar{x}_{k+1} produces

$$\bar{x}_{k+1} = \left[2JJ^T + \sum_{j=1}^r A_j \lambda_j \right]^{-1} \left[2JJ^T \bar{x}_k - \nabla f(\bar{x}_k) - \sum_{j=1}^r \bar{B}_j \lambda_j \right]. \quad (22)$$

This expression for \bar{x}_{k+1} in terms of $\bar{\lambda}$ is now substituted into the second Kuhn-Tucker condition, equation (20), to obtain:

$$\begin{aligned} & \frac{1}{2} \left[\left[2JJ^T + \sum_{j=1}^r A_j \lambda_j \right]^{-1} \left[2JJ^T \bar{x}_k - \nabla f(\bar{x}_k) - \sum_{j=1}^r \bar{B}_j \lambda_j \right] \right]^T \\ & A_i \left[\left[2JJ^T + \sum_{j=1}^r A_j \lambda_j \right]^{-1} \left[2JJ^T \bar{x}_k - \nabla f(\bar{x}_k) - \sum_{j=1}^r \bar{B}_j \lambda_j \right] \right] \\ & + B_i \left[\left[2JJ^T + \sum_{j=1}^r A_j \lambda_j \right]^{-1} \left[2JJ^T \bar{x}_k - \nabla f(\bar{x}_k) - \sum_{j=1}^r \bar{B}_j \lambda_j \right] \right] \\ & - C_i = 0, \quad i = 1, \dots, r. \end{aligned} \quad (23)$$

These r nonlinear equations in terms of the new unknowns, λ_1 thru λ_r , and the old design variables, \bar{x}_k , are solved by an iterative process for the values of λ_1 thru λ_r . The lambda values are then substituted into equation (22) which will yield new values for the design

variables. It is observed that the matrix $2JJ^T$ is the matrix of second partial derivatives, G , of the objective function if it is quadratic. Thus, by replacing $2JJ^T$ in equation (22) and (23), this technique becomes a modification of the second order method rather than the Gauss method.

At the optimum design all constraints will either be satisfied (less than zero) or active (equal to zero) and each active constraint will have a corresponding lambda whose value is greater than or equal to zero. If, at some iteration the set of design variables yields a violated constraint, then obviously the optimum point has not been reached. In this case, the newly violated constraint will be added to the set of active constraints and the procedure allowed to continue. If at some iteration the set of design variables yields all active or satisfied constraints, but one or more of the active constraints has a corresponding negative lambda, then the optimum design has also not been reached. The negative lambda implies that the iteration process would like to move away from the corresponding constraint boundary toward the feasible region where the constraint is satisfied. Thus, the constraint is dropped from the set of active constraints and the process allowed to continue. If more than one negative lambda existed, then constraints are dropped one at a time starting with the constraint with the most negative lambda.

A constraint is added to the set of active constraints if it should become either active (equal to zero) or violated (greater than zero) when the step is taken from x_k to x_{k+1} . In the case where a constraint becomes violated, a line^k is "drawn" between x_k and x_{k+1} and the actual step is taken to the farthest point along^k the line^{k+1} so that no constraints are violated. In effect, this procedure is the same as stepping back from x_{k+1} toward x_k until the newly violated constraint is just active (equal to zero). The constraint is then added to the set of active constraints for the next iteration.

An example problem with quadratic constraints given by Boston, Willmert and Sathyamoorthy [4] shows this method to be very efficient when compared to the generalized reduced gradient method (GRG). The problem consisted of finding the optimal design of a four-bar mechanism (minimizing the coupler point path error with respect to a given path) subject to several linear constraints on link length and movability. Additionally, constraints were placed on the crank pin to limit its location to the intersection of two circular (quadratic) regions. The program was run for a four by four matrix of problems which included four different starting points and four different conditions of the quadratic constraints. For all sixteen runs, the number of objective function evaluations for this new method ranged from 8 to 32 (average was 15), while the GRG method required from 303 to 699 (average was 502) evaluations.

The interesting information here is that the solution to this quadratically constrained four-bar mechanism used no more objective function evaluations than the linearly constrained four-bar mechanism example by Paradis and Willmert. While these two examples are necessarily different, this tendency toward requiring similar numbers

of function evaluations for different classes of problems is very desirable. The net result is that we now have an optimization procedure for sum of squared quantities objective functions subject to linear and quadratic constraints that not only requires relatively few function evaluations, but seems to be constraint order independent. Now the need is to determine a method which will also work for higher order constraints.

Boston, et al. [4] attempted to apply this method to higher order problems, but met with mixed results. The problems encountered seemed to tie in with the higher order constraints rather than with the higher order objective functions. There are several limitations implicit in the algorithm which appear to be the source of the problems encountered. The first limitation has to do with the application of the constraints, equation (18), to the first Kuhn-Tucker condition, equation (19). When approximating a higher order function by a quadratic Taylor series expansion about some point \vec{x}_0 , not only is the A_i matrix a function of \vec{x}_0 , but so is the B_i vector and the C_i scalar. Thus the constraint approximation, equation (18), should be written as

$$g_1(\vec{x}) = \frac{1}{2} \vec{x}^T A_1(\vec{x}_0) \vec{x} + \left[\vec{B}_1(\vec{x}_0) \right]^T \vec{x} - C_1(\vec{x}_0) \leq 0, \quad i = 1, \dots, M \quad (24)$$

where

$$\vec{x} = \vec{x}_0 + \Delta \vec{x}. \quad (25)$$

As \vec{x} approaches \vec{x}_0 (or $\Delta \vec{x}$ approaches 0) then this approximation approaches the exact value of the constraint. Thus as the algorithm progresses along and constraints are added and dropped, the constraints must be reapproximated at the latest design to keep the step size small. This can be achieved by taking the new values of \vec{x} as generated by equation (22) and substituting them into the actual constraint equations to get improved values for the $A_i(\vec{x}_0)$, $B_i(\vec{x}_0)$, and $C_i(\vec{x}_0)$ terms in equation (24) with respect to the current design point.

The second limitation involves the second Kuhn-Tucker condition, equation (20), which is used to obtain the equation for the new values of λ , equation (23). This is simply the equation for the active constraints. In the original formulation, an attempt was made at obtaining a linear approximation in λ for this constraint equation. This would allow equation (23) to be solved explicitly for λ . However, failing this an iterative procedure was employed to find the values for λ . Now that an iterative process is required there is no advantage in keeping a quadratic approximation when the actual constraint will work just as well. Replacing equation (20) with the active nonlinear constraint equations will remove any errors due to the approximation process.

The stepping back procedure for violated constraints, described above, can also be a source of problems. With non-convex programming problems this procedure may lead to a situation where the algorithm cannot move away from a non-optimum design. Because the stepping

back procedure assumed a straight line path between the two design points, it is possible, when backing out of a newly violated constraint, to move into the violated region of the constraint that was active at the beginning of the step. The procedure would then step back still further until all constraints are satisfied. It is possible to end up with the same set of active constraints as at the start of the iteration. In this case the next iteration will produce the same design, which may be non-optimal.

Two alternatives are readily apparent which may solve this problem. The first one is that when a constraint becomes violated, repeat the step but include the newly violated constraint in the set of active constraints. The second alternative is to move to the point where the constraint is violated, and then iterate from there without stepping back. Of course, the violated constraint is added to the set of active constraints. Boston, et.al. [4] looked into this second alternative to some extent. They reported that it did not always work. However, it is not clear if it was the "no stepping back" that was the cause of the problems or if the second order approximations to the constraints contributed to the problems.

In summary, the Gauss nonlinearly constrained technique is very effective at solving quadratically constrained problems. No major difficulties appear to exist which would preclude it from solving problems with higher order constraints once the modifications discussed above are implemented. This method with the proposed modifications is currently the leading candidate as the best method for solving highly nonlinear mechanism design problems.

RESULTS

A verification of the effectiveness of the Gauss constrained method applied to problems with quadratic constraints is obtained by solving the Rosen-Suzuki test problem [5]:

$$\text{minimize } F(\vec{x}) = x_1^2 + x_2^2 + 2x_3^2 + x_4^2 - 5x_1 - 5x_2 - 21x_3 + 7x_4$$

subject to:

$$g_1(\vec{x}) = x_1^2 + x_2^2 + x_3^2 + x_4^2 + x_1 - x_2 + x_3 - x_4 - 8 \leq 0$$

$$g_2(\vec{x}) = x_1^2 + 2x_2^2 + x_3^2 + 2x_4^2 - x_1 - x_4 - 10 \leq 0$$

$$g_3(\vec{x}) = 2x_1^2 + x_2^2 + x_3^2 + 2x_4^2 - x_2 - x_4 - 5 \leq 0$$

The optimum design for this problem is at $\vec{x} = [0, 1, 2, -1]$

Two versions of the Gauss nonlinearly constrained technique and the generalized reduced gradient method, identified as GRG, were used

from four different starting points. One version of the Gauss nonlinearly constrained technique, identified as GNLC, uses the stepping back procedure and requires a feasible starting design and will always maintain a feasible design. The other version, identified as GNLC.NS, does not use the stepping back procedure and has no requirement on the feasibility of the design at any stage of the optimization. The results are summarized in Table I. It can easily be seen that the Gauss nonlinearly constrained technique is much more efficient with respect to number of function evaluations than the generalized reduced gradient method.

ALGORITHM	STARTING DESIGN, \vec{x}_0	NUMBER OF ITERATIONS	FUNCTION EVALUATIONS
GNLC.NS	[0,0,0,0]	2	3
GC.NS	[1,1,1,1]	2	3
GC.NS	[2,2,2,2]	2	3
GNLC.NS	[0,0, $\sqrt{5}$,0]	3	4
GNLC	[0,0, $\sqrt{5}$,0]	3	4
GNLC	[0,0,0,0]	5	6
GNLC	[1,1,1,1]	5	6
GRG	[0,0, $\sqrt{5}$,0]	9	83
GRG	[0,0,0,0]	11	106
GRG	[1,1,1,1]	11	133
GRG	[2,2,2,2]	11	144

Table I: Comparison of Algorithms

CONCLUSIONS

The optimization techniques developed in this research as extensions of the Gauss method to handle various types of constraints are effective approaches to reducing the number of analyses required to obtain an optimal design. As a result, the computational time for large problems should be reduced significantly.

ACKNOWLEDGEMENTS

This research is sponsored by the Air Force Office of Scientific Research, Air Force Systems Command, USAF, under Grant Numbers AFOSR-84-0076, and AFOSR-85-0103 and the National Science Foundation under Grant No. DMC-8500627. The U.S. Government is authorized to reproduce and distribute reprints for government purposes notwithstanding any copyright notation thereon.

REFERENCES

1. Himmelblau, D. M., "Applied Nonlinear Programming", McGraw-Hill, New York, 1972.
2. Wilde, D. J., "Error Linearization in the Least-Squares Design of Function Generating Mechanisms", *Progress in Engineering Optimization-1981*, ASME, 1981, pp. 33-37.
3. Paradis, M. J. and Willmert, K. D., "Optimal Mechanism Design Using the Gauss Constrained Method", *Trans. of ASME, Journal of Mechanisms, Transmissions and Automation in Design*, Vol. 105, 1983, pp. 187-196.
4. Boston, D. R., Willmert, K. D. and Sathyamoorthy, M., "Gauss Nonlinearly Constrained Optimization Method", *Proceedings of the 5th ASCE Engineering Mechanics Division Specialty Conference, Laramie, WY.*, 1984, pp. 82-85.
5. Rosen, J. B. and Suzuki, S., "Construction of Nonlinear Programming Test Problems", *Communications of the ACM*, Vol. 8, 1965, pp. 113.

FINITE ELEMENT NONLINEAR VIBRATIONAL ANALYSIS OF PLANAR MECHANISMS

D. W. Tennant, K. D. Willmert, and M. Sathyamoorthy
Department of Mechanical and Industrial Engineering
Clarkson University
Potsdam, New York

ABSTRACT

A finite element approach is presented in this paper for the nonlinear vibrational analysis of planar mechanisms. The analysis takes into account the effects of material and geometric nonlinearities on the dynamic behavior. The geometric nonlinearities included in this study are due to stretching of the neutral axis and the curvature-displacement nonlinearity, both caused by large deformations. The material nonlinearity is due to a nonlinear stress-strain relationship of the Ramberg-Osgood type. The analysis presented here makes use of hermite polynomials which ensure compatibility of curvature between elements. Using a variable correlation table, a global system of nonlinear equations are derived in terms of the global unknowns and the kinematics of the mechanism. A harmonic series technique is then used to obtain the steady state solutions to this system of nonlinear equations. Numerical results are presented for an example mechanism and the effects of the nonlinearities are discussed.

INTRODUCTION

The importance of flexibility of linkages on the performance of high speed minimum-mass mechanisms is well recognized. A considerable amount of research has been done in this area in the last two decades. While it is desirable to develop analytical and numerical procedures that enable the design of rigid link mechanisms and robots to perform a given function with specified reliability, it is also important to evaluate the effects of flexibility of elastic members on their performance. It is known that a mechanism designed for operation at low speeds may not perform satisfactorily at high speeds due to the effects of large inertia forces and resulting elastic deformations. Thus it becomes necessary to include in the dynamic analysis of mechanisms, not only the effect of the rigid body motion, but also the flexibility of the linkages.

Most of the previous investigations in the area of elastic analysis of mechanisms have been carried out within the framework of the linear theory [1-17]. However, Viscomi and Ayre [18] used a Galerkin-type nonlinear analysis procedure to study the vibrations of a slider-crank mechanism. A later work by Sadler and Sandor [19] used the lumped parameter approach to a nonlinear dynamic model of an elastic linkage. The mechanism analyzed in this paper was a general four-bar linkage and the analytical model included the response coupling associated with both the transmission of forces at the pin joints and the dependence of the undeformed motion of a link on the elastic motion of other links. A

finite element analysis, with the aid of the piecewise linear method of Martin, was used by Sevak and McLarnan [20] to carry out the nonlinear analysis of a mechanism. Further nonlinear work dealing with the vibrations of elastic mechanisms are reported in References [21-23]. In a recent investigation, Thompson and Sung [24] used a variational formulation for the nonlinear finite element analysis of planar mechanisms considering geometric nonlinearities. Some experimental results were also presented.

This paper is concerned with the nonlinear vibrational analysis of general planar mechanisms. A finite element method is used which includes the effects of both geometric and material nonlinearities. The geometric nonlinearities included in this study are due to stretching of the neutral axis with partially constrained ends and a general curvature-displacement relationship, both caused by large deformations. The material nonlinearity is of the Ramberg-Osgood type with three parameters to represent the nonlinear stress-strain relationship [25-27]. Additional effects considered are transverse shear and rotatory inertia and changes in cross-section due to realistically proportioned members. The governing nonlinear differential equations are derived for each element in terms of the axial and transverse deformations, rotations, curvatures, and shear deformation angles. These equations are then assembled with the aid of a variable correlation table and the resulting global system of equations is solved using an iterative technique based on a harmonic series solution procedure.

FINITE ELEMENT FORMULATION

A finite element method is presented below for the nonlinear analysis of a general closed looped mechanism. The mechanism can be composed of various combinations of simple four bar chains, frame elements, sliders moving on fixed references, or sliders moving on rotating links. Each link is divided into one or more elements with each element having the local coordinate system as shown in Figure 1. If a slider is present, the masses M_1 and M_2 are located at ends 1 and 2, as shown. The length of the element Δ is constant except for links with sliders moving along them.

The displacement vector of any point (a) on the element's neutral axis is given by:

$$S = (X_1 \cos \gamma + Y_1 \sin \gamma + x + u)i + (Y_1 \cos \gamma - X_1 \sin \gamma + w)j \quad (1)$$

where X_1 and Y_1 are the coordinates of end 1 of the element given by the rigid body motion. The coordinate x is measured along the element's neutral axis from 1 to 2 and γ is the angle between the rigid body position and the X-axis. The axial and transverse displacements of point (a) from the rigid body position are given by u and w , respectively. This equation takes into account both the rigid body motion and the elastic displacements and defines the position of any point along the neutral axis.

Differentiating Equation 1 with respect to time yields the velocity of any point (a). The unit vectors i and j move with coordinate system and vary with time. The angular velocity of any differential line segment on the neutral axis of the element is given by:

$$\dot{\gamma}_t + \dot{w}_{,xt} \quad (2)$$

where $\dot{\gamma}_t$ is the derivative of γ with respect to time and $\dot{w}_{,xt}$ is the derivative of the transverse displacement with respect to the local coordinate x and time t .

The kinetic energy due to rotation of the element is given by:

$$\begin{aligned} K.E.R = & \frac{1}{2} \int_{-\frac{h}{2}}^{\frac{h}{2}} \int_0^{\Delta} \rho A_x |S_{,t}|^2 + \rho I_z (\dot{\gamma}_t + \dot{w}_{,xt})^2 dx dy \\ & + \frac{1}{2} M_1 |S_{,t}|_{x=0}^2 + \frac{1}{2} M_2 |S_{,t}|_{x=\Delta}^2 \end{aligned} \quad (3)$$

where ρ is the mass density and A_x and I_z are the cross sectional area and moment of inertia of the element respectively. The term $\rho I_z (\dot{\gamma}_t + \dot{w}_{,xt})^2 / 2$ represents

the effect of rotatory inertia. The kinetic energy due to beam bending associated with transverse shear [28] is:

$$K.E.B = \frac{1}{2} \int_0^L \int_{-h/2}^{h/2} \rho \{I_{21} \dot{\gamma}_x^2\} dx dy \quad (4)$$

where γ is a measure of the transverse shear angle.

The strain energy for the element is given by:

$$U = \int_{vol} \int_0^{\epsilon} \sigma d\epsilon dvol + \int_{vol} \frac{1}{2} \tau_{xy} \gamma_{xy} dvol \quad (5)$$

where σ , ϵ , τ_{xy} , and γ_{xy} are the normal stress, normal strain, shear stress and shear strain, respectively. For a nonlinear material of the Ramberg-Osgood type [25-27], the relationship between stress and strain is:

$$\sigma = A \epsilon + B \epsilon^m \quad (6)$$

where A corresponds to Young's modulus E , and $B\epsilon^m$ represents the nonlinear term. A , B and m are constants for the particular material being considered. The above relationship, Equation 6, is valid only for positive strains. If the strain is negative, the following expression is used:

$$\sigma = A \epsilon + B (-\epsilon)^m \quad \text{if } \epsilon < 0 \quad (7)$$

The change in sign of the nonlinear term results in the same overall effect on the stress-strain relationship as for positive strain, i.e. either hardening or softening depending on the values of B and m .

Using the Ramberg-Osgood relationship, the following expression for the strain energy is obtained for positive strain $\epsilon \geq 0$:

$$U = \int_0^L \int_{-h/2}^{h/2} \left\{ \frac{1}{2} A \epsilon^2 + \frac{1}{m+1} B \epsilon^{m+1} \right\} dx dy + \int_0^L \int_{-h/2}^{h/2} \frac{1}{2} G_{xy} \gamma_{xy}^2 dx dy \quad (8)$$

where x is the axial coordinate, y is the transverse coordinate, and G_{xy} is the shear modulus. When $\epsilon < 0$ the equation is:

$$U = \int_0^L \int_{-h/2}^{h/2} \left\{ \frac{1}{2} A \epsilon^2 + \frac{1}{m+1} B (-\epsilon)^{m+1} \right\} dx dy + \int_0^L \int_{-h/2}^{h/2} \frac{1}{2} G_{xy} \gamma_{xy}^2 dx dy \quad (9)$$

The nonlinear expression for the curvature R of a planar static beam undergoing large deformations is:

$$\frac{1}{R} = \frac{w_{,xx}}{(1 + w_{,x}^2)^{3/2}} \quad (10)$$

Thus the strain is

$$\epsilon = -\frac{y}{R} = -\frac{y w_{,xx}}{(1 + w_{,x}^2)^{3/2}} \quad (11)$$

Combining the geometric nonlinearities due to stretching of the neutral axis and the curvature-displacement nonlinearity, results in the expressions for normal and shear strain:

$$\epsilon = u_{,x} + \frac{1}{2} D_s w_{,x}^2 + \frac{y^2_{,x}}{(1 + D_b w_{,x}^2)^{3/2}} \quad (12)$$

$$\gamma_{xy} = w_{,x} + \alpha \quad (13)$$

Substituting these expressions for strain into the strain energy Equations (8) and (9) produces, for $\epsilon \geq 0$ or $\epsilon < 0$:

$$\begin{aligned} \text{S.E.} = & \int_{-\frac{h}{2}}^{\frac{h}{2}} \int_0^{\Delta} b \left\{ \frac{1}{2} A \left(u_{,x} + \frac{1}{2} D_s w_{,x}^2 + \frac{y^2_{,x}}{(1 + D_b w_{,x}^2)^{3/2}} \right)^2 \right. \\ & - \frac{D_k}{m+1} B \left(\pm u_{,x} \pm \frac{1}{2} D_s w_{,x}^2 \pm \frac{y^2_{,x}}{(1 + D_b w_{,x}^2)^{3/2}} \right)^{m+1} \\ & \left. + \frac{1}{2} C_{xy} (w_{,x} + \alpha)^2 \right\} dx dy \quad (14,15) \end{aligned}$$

For equation (15) negative sign is applicable in all the terms containing \pm signs and is valid for $\epsilon < 0$. In Equations (12), (14) and (15), D_k , D_b and D_s are tracing constants representing the effects of material nonlinearity, geometric nonlinearity due to curvature, and geometric nonlinearity due to stretching of neutral axis, respectively. Each tracing constant is equated to unity when that particular nonlinearity is being considered and is equated to zero when it is not.

In order to represent realistically proportioned members, changes in cross section are included. Each element is divided into sections of varying lengths with constant area. The integrations involved in the element equations are carried out in a piecewise fashion with the area in each section taken as a constant. This procedure provides a reasonable approximation of variable cross sectional members without having to resort to large numbers of elements.

The Lagrangian function L is defined as

$$L = \sum_{k=1}^S \sum_{i=1}^{N_k} (K.E.R + K.E.B - S.E.)_{ik} \quad (16)$$

where N_k is the total number of elements in the k^{th} link and S is the number of links in the mechanism. Substituting Equations (3), (4) and (14) into Equation (16), the Lagrangian L can be expressed in terms of the displacements u and w , the shear angle α , and the rigid body motion.

Hermite polynomials are used to approximate u , w , and α in order to satisfy the boundary conditions of various types of mechanisms easily and to ensure interelement compatibility. The axial deformation u is approximated by a linear shape function given by

$$u(x,t) = U_1(t) N_1(x) + U_2(t) N_2(x) \quad (17)$$

Similarly, fifth degree polynomial shape functions are used to approximate the transverse deformation w :

$$\begin{aligned} w(x,t) = & W_1(t) H_{11}(x) + \bar{\theta}_1(t) H_{21}(x) + \bar{m}_1(t) H_{31}(x) \\ & + W_2(t) H_{12}(x) + \bar{\theta}_2(t) H_{22}(x) + \bar{m}_2(t) H_{32}(x) \quad (18) \end{aligned}$$

The shear angle α is also approximated by a fifth degree polynomial in order to make it compatible with the transverse displacement w . Therefore α is assumed to be:

$$\begin{aligned} \alpha(x,t) = & \bar{\alpha}_1(t) H_{11}(x) + \bar{\psi}_1(t) H_{21}(x) + \bar{\lambda}_1(t) H_{31}(x) \\ & + \bar{\alpha}_2(t) H_{12}(x) + \bar{\psi}_2(t) H_{22}(x) + \bar{\lambda}_2(t) H_{32}(x) \quad (19) \end{aligned}$$

where $\dot{\alpha}$ and $\ddot{\alpha}$ are the first and second derivatives of α , respectively. The Hermite polynomials are given by:

$$\begin{aligned} N_1(x) &= 1 - e & ; & & N_2(x) &= e & & & (20) \\ H_{11}(x) &= 1 - 10e^3 + 15e^4 - 6e^5 & ; & & H_{12}(x) &= 10e^3 - 15e^4 + 6e^5 \\ H_{21}(x) &= \Delta(e - 6e^3 + 8e^4 - 3e^5) & ; & & H_{22}(x) &= \Delta(-4e^3 + 7e^4 - 3e^5) \\ H_{31}(x) &= \Delta^2(e^2 - 3e^3 + 3e^4 - e^5)/2 & ; & & H_{32}(x) &= \Delta^2(e^3 - 2e^4 + e^5)/2 & & & (21) \end{aligned}$$

where, $e = x/\Delta$.

A transformation of coordinates is now introduced to change from the moving coordinate system associated with the elements to global coordinates. Only U_1 , W_1 , U_2 and W_2 need to be transformed. The other coordinates are angles or derivatives of angles which are not directional on the X, Y coordinate system used. The transformations are:

$$\begin{aligned} U_1 &= \bar{U}_1 \cos\phi_1 - \bar{W}_1 \sin\phi_1 & ; & & U_2 &= \bar{U}_2 \cos\phi_2 - \bar{W}_2 \sin\phi_2 \\ \bar{W}_1 &= \bar{U}_1 \sin\phi_1 + \bar{W}_1 \cos\phi_1 & ; & & \bar{W}_2 &= \bar{U}_2 \sin\phi_2 + \bar{W}_2 \cos\phi_2 & & & (22) \end{aligned}$$

For pin connections the transformation angles ϕ_1 and ϕ_2 are set equal to $-\gamma$ (the rigid body angle) which transforms the coordinates back to the global coordinates. For sliders moving on rotating links the transformation becomes more involved. In this case, the deformation of the driver link must be transformed to correspond to the axial and transverse deformation of the output link [14].

Substituting the expressions from Equation (22) into Equations (17) and (18), the global coordinates for the system are then:

$$\bar{q} = [\bar{U}_1 \bar{W}_1 \bar{\theta}_1 \bar{m}_1 \bar{\alpha}_1 \bar{\psi}_1 \bar{\lambda}_1 \bar{U}_2 \bar{W}_2 \bar{\theta}_2 \bar{m}_2 \bar{\alpha}_2 \bar{\psi}_2 \bar{\lambda}_2]^T \quad (23)$$

The Lagrangian function is then written in terms of the transformed element coordinates. Differentiating the Lagrangian with respect to the element coordinates, the following element equations are obtained:

$$\frac{d}{dt} \left(\frac{\partial L}{\partial \dot{q}_{i,t}} \right) - \frac{\partial L}{\partial q_i} = 0 \quad (24)$$

In differentiating the expressions for the kinetic and strain energies in Equations (3), (4) and (14), it must be remembered that Δ , which is the upper limit of integration, is a function of time. The operations carried out in Equation (24) results in a system of nonlinear element differential equations. Assembling the element matrices for the particular mechanism being solved results in the global system of equations:

$$M \bar{Q}_{,tt} + C \bar{Q}_{,t} + (K_e + K_n) \bar{Q} = \bar{F}(t) \quad (25)$$

The M , C , K_e and K_n matrices are all functions of time. The C matrix results from the kinetic energy of the system. No damping was included in the formulation of the problem. The $C \bar{Q}_{,t}$ term was found to be small and thus was ignored in the analysis. The matrix K_e is the linear portion of the total stiffness matrix. It is a function of rigid body motion, but is not a function of the deformations \bar{Q} . The matrix K_n , however, is the nonlinear portion of the stiffness matrix. It is a function of the deformations \bar{Q} . Equation (25) is thus a nonlinear system of differential equations.

The derivation of the finite element Equation (25) is based on the assumption of positive strains ϵ . If the strain is negative a similar derivation is possible, based on Equation (15) for the strain energy rather than Equation (14). The only difference in the resulting Equation (25) is in the stiffness matrix. Wherever an ϵ^{m-1} occurs in the original formulation, it becomes $(-\epsilon)^{m-1}$ for negative strains. All other negative signs resulting from the introduction of $-\epsilon$ cancels out in the differentiations required. Thus in order to handle both

positive and negative strains the terms involving ϵ^{m-1} in the stiffness matrix were replaced by ϵ^{m-1} .

In order to solve the nonlinear system of Equation (25), an iterative approach was used. First the equations were solved using the linear terms only, i.e. the K_n matrix was ignored. This was accomplished by setting all of the tracing constants D_b , D_s and D_k equal to zero. The solution \bar{Q} for the linear equations was then used to determine values for the nonlinear stiffness matrix K_n . Equation (25) was then solved again for new values of \bar{Q} , and the process repeated. Experience showed that this procedure converged in from 3 to 5 iterations. To solve Equation (25) for $\bar{Q}(t)$, for particular K_n , a harmonic series solution method was used similar to that of Bahgat and Willmert [14]. This approach overcomes problems with stability, due to the time varying nature of the matrices, that sometimes result from an eigenvalue technique. The steady state solution is obtained without adding artificial damping. The solution, without the $C \dot{\bar{Q}}_t$ term, is given by:

$$\bar{Q}(t) = \sum_{n=0}^N (K - n^2 \omega^2 M)^{-1} (\bar{A}_n \cos n\omega t + \bar{B}_n \sin n\omega t) \quad (26)$$

where ω is the input crank speed, and \bar{A}_n and \bar{B}_n are solutions to the linear equations:

$$\bar{F}(t_k) = \sum_{n=0}^N \bar{A}_n \cos n\omega t_k + \sum_{n=0}^{N-1} \bar{B}_n \sin n\omega t_k \quad ; \quad k = 0, 1, \dots, 2N-1 \quad (27)$$

where \bar{B}_0 is set equal to zero. The values of t_k are the times at $2N$ equal time increments per revolution of the input crank given by:

$$t_k = \frac{t_k}{N\omega} \quad \text{for } k = 0, 1, \dots, 2N-1 \quad (28)$$

Computational experience indicates that a fairly accurate solution is obtained using only a few terms in Equation (26). As the number of terms increases the components of the matrix $(K - n^2 \omega^2 M)$ grow and thus the inverse $(K - n^2 \omega^2 M)^{-1}$ becomes small. The summation can therefore be truncated to reduce computational time.

The stress in the links is calculated by evaluating the strains from Equation (12). The stress can then be determined at any point in an element using Equations (6) and (7). To find the maximum stress in an element the maximum strain must be found. Setting the first derivative of Equation (12) to zero and solving the resulting expression, the position of the maximum strain is determined. Once the location is known, the maximum strain and stress can be evaluated.

The above formulation is based on the use of the shear angle α , which is appropriate particularly for short members. For long slender links this quantity is not required. The elimination of α reduces the size of the problem considerably since the nodal deformations α_1 , α_2 , λ_1 , λ_2 and λ_3 would no longer be present. For long slender members:

$$\alpha = -w_{,x} \quad (29)$$

Using this expression, the equation for strain energy (14) for positive shear ϵ reduces to:

$$\begin{aligned} \text{S.E.} = & \int_0^h \int_0^{\Delta} b \left(\frac{1}{2} A (u_{,x} + \frac{1}{2} D_b w_{,x}^2 - \frac{y w_{,xx}}{(1 + D_b w_{,x}^2)^{3/2}}) \right)^2 \\ & - \frac{D_k}{m+1} B (u_{,x} + \frac{1}{2} D_s w_{,x}^2 - \frac{y w_{,xx}}{(1 + D_b w_{,x}^2)^{3/2}})^{m+1} dx dy \quad (30) \end{aligned}$$

A similar expression exists for negative strain. The kinetic energy also changes if α is not present. The energy associated with transverse shear, Equation (4), is eliminated and thus Equation (3) represents the total kinetic energy of the

element. Using a procedure similar to the method outlined above, vibrational equations of the same form as Equation (25) can be obtained, but they will be smaller in size. However, nonlinear terms still exist in the stiffness matrix due to the material and geometric nonlinearities. The method of solution is thus identical to that outlined earlier.

EXAMPLE PROBLEMS

The following example is presented to illustrate the method of solution. The nonlinearities due to neutral axis stretching, and complex curvature-displacement and stress-strain relationships are all considered. A four-bar linkage, as shown in Figure 2, is used as the example with all of the members flexible and made of the same material. The data for the mechanism is: Length of input crank (AB) = 5.0 in, Length of coupler (BC) = 11.0 in, Length of rocker (CD) = 10.5 in, Fixed distance (AD) = 10.0 in, Cross section of links a rectangular, Height of rectangle = 1.0 in, and Width of rectangle = 0.25 in. The position of the input crank is zero degrees at $t = 0$ and the direction of rotation is counterclockwise. The mechanism is divided into three elements with each link in the mechanism taken as an element. The boundary conditions are that only moment and shear terms exist for the input crank's driven end (A). For the pin connections between links, there are deformations, rotations and shear terms, and for the rocker's fixed point there are only rotation and shear terms.

First, the deformations in the mechanism were determined with the shear angle α present. In this case the crank link was rotated at 100 rad/sec. The material properties, approximating aluminum, were as follows: $A = 10.87 \times 10^6$ lb/in², $B = 0.8387 \times 10^{11}$ lb/in², $m = 3.0$, and Mass density = 0.0002536 lb-sec²/in⁴. Three separate procedures were used to obtain numerical results. First the problem was solved using the linear analysis method of Bahgat and Willmert [14], with $E = A$. Next the method of this paper was used with the tracing constants equal to zero. Thus a linear analysis was obtained. Finally the method was applied with all tracing constants equal to one, i.e. a full nonlinear analysis. A representative deformation \bar{U}_1 as a function of crank position is shown in Figure 3. This is the horizontal deformation of the free end of the crank link. As can be seen, the three curves are very similar. The effect of the shear angle α is to increase the deformation slightly. For this slow speed the linear and nonlinear analyses were almost identical.

The same problem was solved again at a higher speed of 200 rad/sec. The resulting deformation \bar{U}_1 is shown in Figure 4. As can be seen, high frequency oscillations started to appear, with greater separation between the three analyses. At even higher speed these oscillations became more predominant to the point of instabilities in the motion at very high speeds.

The revised form of the analysis equations was considered next, i.e. the form without the shear angle α . Here a crank speed of 150 rad/sec was used. A comparison was made of the effects of the various nonlinearities on the deformations and stresses as compared to the linear analysis. Figures 5 and 6 show a comparison of the linear and nonlinear deformations \bar{U}_2 (the horizontal deformation of the free end of the output link) caused separately by geometric and material nonlinearities. Figures 7 and 8 show the maximum stresses in the connecting link of the mechanism. As expected, the material nonlinearity of the Ramberg-Osgood type results in deformations which are greater in magnitude than those obtained using a linear elastic model. The maximum stress decreased due to the presence of the term $B\epsilon^m$ subtracted from the linear stress expression.

The geometric nonlinearities considered, namely curvature displacement and stretching of the neutral axis, both due to large deformations produced mixed results with deformations reduced at some points and increased at other points. The effect of the geometric nonlinearities would be expected to produce a stiffening of the members [28] of the mechanism and thus produce smaller deformations. The increased deformations in this case might be due to the fact that the deformations are in relationship to the entire mechanism and not just to an individual beam element.

CONCLUSIONS

The nonlinear analysis procedure, using a finite element technique, is an

effective method of calculating the steady state deformations and stresses in a mechanism. Significant differences can occur between the linear and nonlinear approaches. This was particularly true for the stresses in the example considered in this work. Research is still needed on the overall effect of the shear angle α , and a more complete picture of the nonlinear terms in the analysis would be of value. Additional nonlinear effect should also be investigated, such as the effect on the translations of one link due to large deformations of the other links.

ACKNOWLEDGEMENTS

This research is sponsored by the Air Force Office of Scientific Research, Air Force Systems Command, USAF, under Grant Number AFOSR 84-0076. The U.S. Government is authorized to reproduce and distribute reprints for government purposes notwithstanding any copyright notation thereon.

REFERENCES

1. Jasinski, P.W., Lee, H.C. and Sandor, G.N., "Stability and Steady-State Vibrations in a High-Speed Slider-Crank Mechanism," Journal of Applied Mechanics, Trans. ASME, Vol. 37, 1970, pp. 1069-1076.
2. Winfrey, R.C., "Elastic Link Mechanism Dynamics," Journal of Engineering for Industry, Trans. ASME, Vol. 93, 1971, pp. 268-272.
3. Winfrey, R.C., "Dynamic Analysis of Elastic Link Mechanisms by Reduction of Coordinates," Journal of Engineering for Industry, Trans. ASME, Vol. 94, 1972, pp. 577-582.
4. Erdman, A.G., Sandor, G.N. and Oakberg, R.G., "A General Method of Kineto-Elastodynamic Analysis and Synthesis of Mechanisms," Journal of Engineering for Industry, Trans. ASME, Vol. 94, 1972, pp. 1193-1205.
5. Iman, I., Sandor, G.N. and Kramer, S.N., "Deflection and Stress Analysis in High Speed Planar Mechanisms with Elastic Links," Journal of Engineering for Industry, Trans. ASME, Vol. 95, 1973, pp. 541-548.
6. Sadler, J.P. and Sandor, G.N., "A Lumped Parameter Approach to Vibration and Stress Analysis of Elastic Linkages," Journal of Engineering for Industry, Trans. ASME, Vol. 95, 1973, pp. 549-557.
7. Winfrey, R.C., Anderson, R.V. and Gnilka, C.W., "Analysis of Elastic Machinery with Clearances," Journal of Engineering for Industry, Trans. ASME, Vol. 95, 1973, pp. 695-703.
8. Chu, S.C. and Pan, K.C., "Dynamic Response of a High-Speed Slider-Crank Mechanism with an Elastic Connecting Rod," Journal of Engineering for Industry, Trans. ASME, Vol. 97, 1975, pp. 542-550.
9. Bagci, D., "Dynamic Motion Analysis of Plane Mechanisms with Coulomb and Viscous Damping Via the Joint Force Analysis," Journal of Engineering for Industry, Trans. ASME, Vol. 97, 1975, pp. 551-560.
10. Sadler, J.P., "On the Analytical Lumped-Mass Model of an Elastic Four-Bar Mechanism," Journal of Engineering for Industry, Trans. ASME, Vol. 97, 1975, pp. 561-565.
11. Koster, M.P., "Effect of Flexibility of Driving Shaft on the Dynamic Behavior of a Cam Mechanism," Journal of Engineering for Industry, Trans. ASME, Vol. 97, 1975, pp. 595-602.
12. Dubowsky, S. and Gardner, T.N., "Dynamic Interactions of Link Elasticity and Clearance Connections in Planar Mechanical Systems," Journal of Engineering for Industry, Trans. ASME, Vol. 97, 1975, pp. 652-661.
13. Bahgat, B.M., "General Finite Element Vibrational Analysis of Planar Mechanisms," Ph.D. Dissertation, Clarkson College of Technology, Potsdam, N.Y., Nov. 1973.

14. Bahgat, B.M. and Willmert, K.D., "Finite Element Vibrational Analysis of Planar Mechanisms," Mechanism and Machine Theory, Vol. 11, 1976, pp. 47-71.
15. Khan, M.R. and Willmert, K.D., "Vibrational Analysis of Mechanisms Using Constant Length Finite Elements," ASME Paper No. 76-WA/DE-21, 1976.
16. Naganathan, G. and Willmert, K.D., "New Finite Elements For Quasi-Static Deformations and Stresses in Mechanisms," ASME Paper No. 80-WA/DSC-35, 1980.
17. Song, J.O. and Haug, E.J., "Dynamic Analysis of Planar Flexible Mechanisms," Computer Methods in Applied Mechanics and Engineering, Vol. 24, 1980, pp. 359-381.
18. Viscomi, B.V. and Ayre, R.S., "Nonlinear Dynamic Response of Elastic Slider-Crank Mechanism," Journal of Engineering for Industry, Trans. ASME, Vol. 93, 1971, pp. 251-262.
19. Sadler, J.P. and Sandor, G.N., "Nonlinear Vibration Analysis of Elastic Four-Bar Linkages," Journal of Engineering for Industry, Trans. ASME, Vol. 96, 1974, pp. 411-419.
20. Sevak, N.M. and McLarnan, C.W., "Optimal Synthesis of Flexible Link Mechanisms with Large Static Deflections," Journal of Engineering for Industry, Trans. ASME, Vol. 97, 1975, pp. 520-526.
21. Badlani, M. and Midha, A., "Member Initial Curvature Effects on the Elastic Slider-Crank Mechanism Response," Journal of Mechanical Design, Trans. ASME, Vol. 104, 1982, pp. 159-167.
22. Davidson, I., "Non-linear Effects in the Support Motion of an Elastically Mounted Slider Crank Mechanism," Journal of Sound and Vibration, Vol. 86, 1983, pp. 71-83.
23. Sivertsen, O.I. and Waloen, A.O., "Non-linear Finite Element Formulations for Dynamic Analysis of Mechanisms with Elastic Components," ASME Paper No. 82-DET-102, 1982.
24. Thompson, B.S. and Sung, C.K., "A Variational Formulation for the Nonlinear Finite Element Analysis of Flexible Linkages; Theory, Implementation and Experimental Results," ASME Paper No. 84-DET-15, 1984.
25. Ramberg, W. and Osgood, W.R., "Description of Stress-Strain Curves by Three Parameters," National Advisory Committee for Aeronautics, Technical Note No. 902, 1943.
26. Venkateswara Rao, G. and Krishna Murty, A.V., "An Alternate Form of the Ramberg-Osgood Formula for Matrix Displacement Analysis," Nuclear Engineering and Design, Vol. 17, 1971, pp. 297-308.
27. Papirno, R., "Goodness-of-Fit of the Ramberg-Osgood Analytic Stress-Strain Curve to Tensile Test Data," Journal of Testing and Evaluation, Vol. 10, 1982, pp. 263-268.
28. Sathyamoorthy, M., "Large Amplitude Vibrations of Moderately Thick Beams," Proceedings of the First International Modal Analysis Conference, Orlando, Florida, 1982, pp. 136-140.
29. Huang, T.C., "The Effects of Rotatory Inertia and of Shear Deformation on the Frequency and Normal Mode Equations of Uniform Beams with Simple End Conditions," Journal of Applied Mechanics, Trans. ASME, Vol. 28, 1961, pp. 579-584.

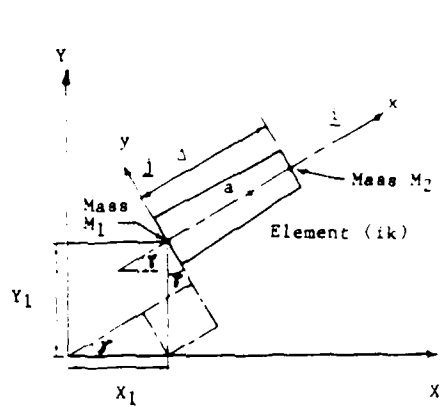


Fig. 1 General Element

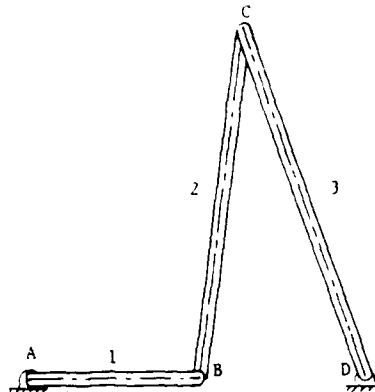


Fig. 2 Four Bar Mechanism

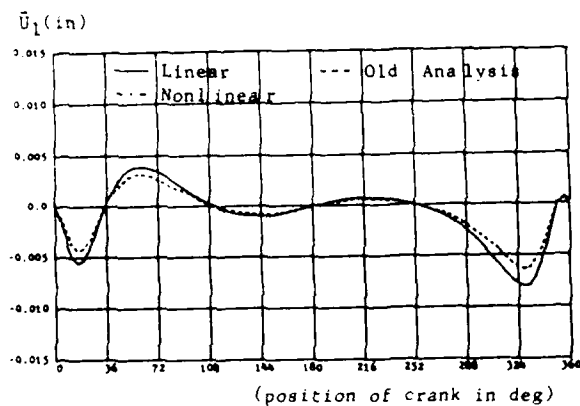


Fig. 3 Deformations \bar{U}_1 for Aluminum at 100 rad/sec

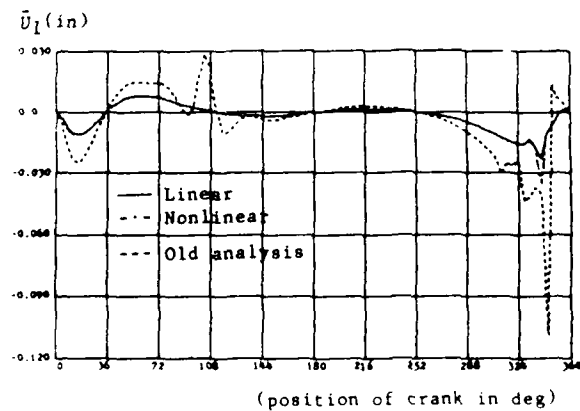


Fig. 4 Comparison of Deformations \bar{U}_1 at 200 rad/sec

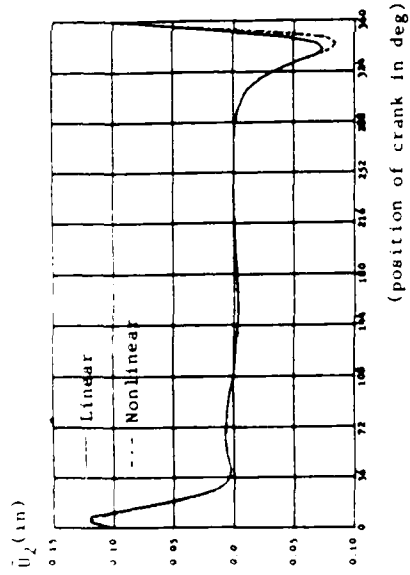


Fig. 5 Comparison of Deformations \bar{U}_2 at 150 rad/sec for Geometric Nonlinearities

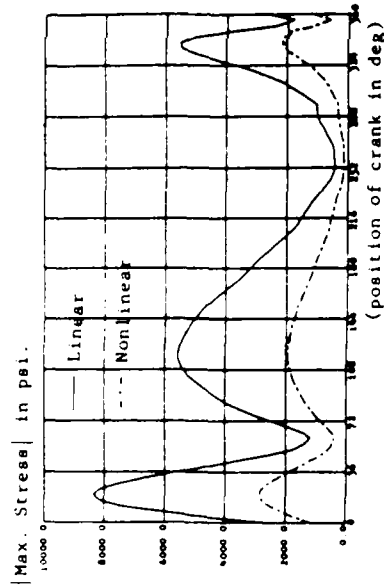


Fig. 7 Maximum Stresses in Element 2 at 150 rad/sec for Geometric Nonlinearities

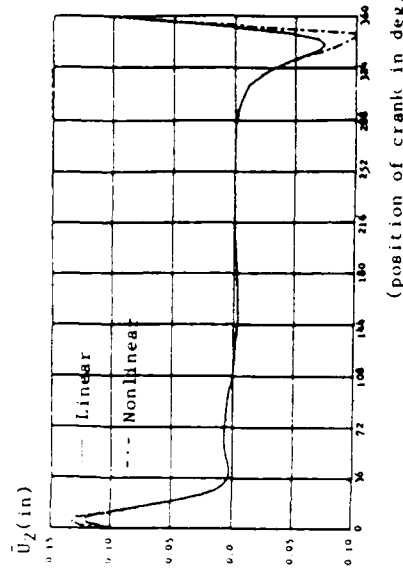


Fig. 6 Comparison of Deformations \bar{U}_2 at 150 rad/sec for Material Nonlinearity

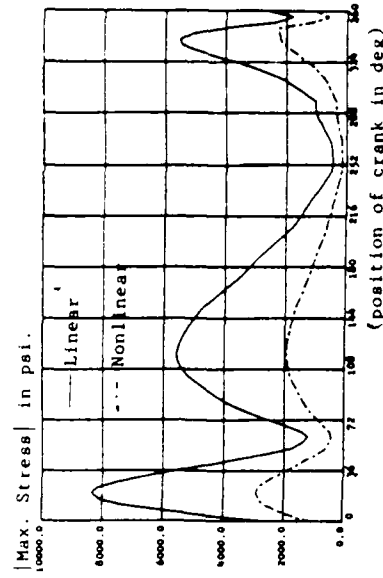


Fig. 8 Maximum Stresses in element 2 at 150 rad/sec for Material Nonlinearity

7

REPRINTED FROM:

COMPUTER METHODS

in

MECHANICS AND ENGINEERING

Volume 57, No. 1, August 1986

**DEVELOPMENT AND APPLICATION OF THE CAUSAL
LINEARLY CONSTRAINED OPTIMIZATION SCHEME**

W. J. BOSTON, K.D. WILLMERT and M. SATHYAMOORTHY

Engineering Department, Clarkson University, Potsdam, NY 13677

pp. 17-24

NORTH-HOLLAND · AMSTERDAM

THE DEVELOPMENT AND APPLICATION OF THE GAUSS NONLINEARLY CONSTRAINED OPTIMIZATION METHOD*

D.R. BOSTON, K.D. WILLMERT and M. SATHYAMOORTHY

Mechanical and Industrial Engineering Department, Clarkson University, Potsdam, NY 13676, U.S.A.

Received February 1985

Presented in this paper is a new optimization technique, called the Gauss nonlinearly constrained technique, which is applicable to design problems with nonlinear objective functions and constraints. The technique is an extension of a previously developed method for linear constraints, referred to as the Gauss constrained technique. Both of these techniques, based on the Gauss unconstrained method, have been developed so that the Kuhn-Tucker conditions are automatically satisfied when the procedure terminates.

1. Introduction

The optimal design of many structures and mechanical mechanisms involves one or more complex and time-consuming analyses at each iteration of the optimization. This is particularly critical if a large-deformation nonlinear analysis is required. In these cases especially, it is important that the optimization method requires very few analyses, even at the expense of significantly increasing the amount of calculations by the optimization technique itself. For example, in a recent work, DeRubes and Willmert [1] applied the relatively efficient generalized reduced gradient (GRG) technique of Lasdon et al. [2] to mechanism design for path generation and rigid-body guidance. The mechanism links were considered flexible, and thus a quasi-static (linear) finite element analysis was used to obtain deformations and stresses. The GRG required as many as 14,000 mechanism analyses to obtain the optimal design. Computation time approached twenty hours on an IBM 4341 mainframe computer. If a nonlinear analysis had been used, the corresponding times would have been considerably higher.

To reduce the number of analyses, Paradis and Willmert [3] developed a new direct method for efficient design of mechanisms. Gauss' method, which Wilde [4] concluded to be very efficient for unconstrained mechanism design, was modified to handle linear constraints. The resulting technique, referred to as the Gauss constrained technique, was highly efficient and required very few objective function evaluations to obtain an optimal design. Their method has been extended, in this paper, to handle nonlinear constraints.

*This research is sponsored by the Air Force Office of Scientific Research, Air Force Systems Command, USAF, under Grant Number AFOSR 84-0076. The U.S. Government is authorized to reproduce and distribute reprints for government purposes notwithstanding any copyright notation thereon.

2. Development of the method

The optimization problem consists of minimizing:

$$F(x) = \varphi^t \varphi, \quad (1)$$

where φ is a vector of general functions of the variables x . Many optimal design problems have objective functions of this form. For the derivation of the optimization technique, the φ are approximated by linear functions of x (which makes F quadratic) of the form:

$$\varphi \approx J^t x + c, \quad (2)$$

where J and c are a constant matrix and vector, respectively. However, the technique, once derived, will be applied to more general cases, where the φ are highly nonlinear functions of x . The constraints are approximated by a general quadratic of the form:

$$g(x) \approx \frac{1}{2} x^t A x + b^t x - d \leq 0, \quad i = 1, \dots, k, \quad (3)$$

The gradient of the objective function (1) is given by

$$\nabla F(x) = 2J\varphi, \quad (4)$$

which is exact, whether φ is linear or not, as long as J is the matrix of first partial derivatives of φ . The matrix of second partial derivatives of the objective function is

$$G = 2JJ^t, \quad (5)$$

which is exact only when φ is linear. At any given iteration we assume there are l active constraints (ordered such that $j = 1, 2, \dots, l$), where $l \leq k$. Thus, the Kuhn-Tucker conditions are

$$\nabla F(x) + (A_1 x + b_1) \lambda_1 + \dots + (A_l x + b_l) \lambda_l = 0, \quad (6)$$

$$g(x) = \frac{1}{2} x^t A x + b^t x - d = 0, \quad j = 1, \dots, l, \quad (7)$$

$$\lambda_j \geq 0, \quad j = 1, \dots, l. \quad (8)$$

Similar to the development of Paradis and Willmert [3], the new method is generated such that a single iteration yields the optimal design for a quadratic objective function, assuming that the constraints active at the optimal design are also active at the starting point. If $F(x)$ is quadratic, then the following equation is valid for any two points $x_{(j)}$ and x^* :

$$\nabla F(x_{(j)}) - \nabla F(x^*) = G(x_{(j)} - x^*) \quad (9)$$

Solving (6) for $\nabla F(x_{(j)})$, assuming $x_{(j)}$ is the optimal design, and substituting into (9) results in

the iterative expression (after solving for x_{i+1}):

$$x_{i+1} = \left(G + \sum_{j=1}^l A_j \lambda_j \right)^{-1} \left[Gx_i - \sum_{j=1}^l b_j \lambda_j - \nabla F(x_i) \right]. \quad (10)$$

If the objective function has the special form of (1), then the matrix G in the iterative equation would be replaced by (5), i.e. $G = 2JJ^T$. Otherwise, the method could still be applied as long as the matrix of second partial derivatives G , or an approximation to it, were known.

In order to use the iterative equation (10), the unknown vector of Lagrange multipliers λ must be determined. This is accomplished by substituting the expression for x_{i+1} , (10), into each of the active constraints of (7) resulting in a system of l nonlinear equations in l unknowns λ of the form:

$$\begin{aligned} g_i(\lambda) = & \frac{1}{2} \left\{ \left(G + \sum_{j=1}^l A_j \lambda_j \right)^{-1} \left[Gx_i - \sum_{j=1}^l b_j \lambda_j - \nabla F(x_i) \right] \right\} A_i \\ & \times \left\{ \left(G + \sum_{j=1}^l A_j \lambda_j \right)^{-1} \left[Gx_i - \sum_{j=1}^l b_j \lambda_j - \nabla F(x_i) \right] \right\} \\ & - b_i \left(G + \sum_{j=1}^l A_j \lambda_j \right)^{-1} \left[Gx_i - \sum_{j=1}^l b_j \lambda_j - \nabla F(x_i) \right] - d_i = 0, \quad i = 1, \dots, l. \end{aligned} \quad (11)$$

This system of equations in λ could be solved using several different methods. The approach used in this research was as follows. At each iteration, initially the Newton-Raphson technique was applied. If the method did not converge, which may be caused by the fact that the equations had no solution or that the method simply was not able to locate one, then another approach was used. In this case, an objective function H was formed which was the sum of the squares of the active constraints g_i . This unconstrained function was minimized with respect to λ . In this work Powell's method was used, but any available technique could be applied. The optimal values of λ (whether H is zero or not for these values of λ) were then used in the iterative equation (10).

As in the original Gauss constrained technique (as well as the gradient projection method), the criterion for dropping a constraint from the set of active constraints is the sign of λ_i . At any iteration the constraint corresponding to the most negative λ is dropped from the set of active constraints and a new vector of Lagrange multipliers is determined. This procedure is repeated until all $\lambda_i \geq 0$. If this results in no active constraints, then the optimization technique continues by setting all $\lambda_i = 0$ in (10). In this case, the iterative expression can be shown to reduce to Gauss' method for unconstrained optimization:

$$x_{i+1} = x_i - (JJ^T)^{-1} J\phi. \quad (12)$$

At each iteration a decision must be made as to whether or not a new constraint should be added to the set of active constraints. If the direction of minimization s_{i+1} is defined as the direction from x_i to x_{i+1} , then a constraint is added only if a step in the s_{i+1} direction will not satisfy the constraint.

Two different methods were used to handle violated constraints. The first approach was to do nothing special if a constraint became violated as a result of an iteration based on (10). Thus, whether a constraint is only active, i.e. $g_i = 0$, or violated, i.e. $g_i > 0$, it is treated the same in the optimization technique. The basis behind this approach was the assumption that eventually the method will satisfy all constraints, since these are equations (11) which the method attempts to satisfy at each iteration. This approach allows the optimization to start at any design whether it satisfies the constraints or not.

The other method of handling violated constraints was to start at a point which satisfied all constraints. Then, if a step is taken using (10) such that $g_i(\mathbf{x}_{j+1}) > 0$, a new design \mathbf{x}'_{j+1} was found along the line connecting \mathbf{x}_j and \mathbf{x}_{j+1} such that $g_i(\mathbf{x}'_{j+1}) = 0$. This was accomplished by stepping back from a violated constraint using the approximate equation

$$\mathbf{x}'_{j+1} = \mathbf{x}_j + \frac{(\mathbf{x}_{j+1} - \mathbf{x}_j)g_i(\mathbf{x}_j)}{g_i(\mathbf{x}_{j+1}) - g_i(\mathbf{x}_j)} \quad (13)$$

The design \mathbf{x}'_{j+1} was then used in the next iteration.

Although the technique was developed assuming linear functions $\varphi(\mathbf{x})$, i.e. $F(\mathbf{x})$ quadratic, the method is applicable to problems where the φ are general functions of \mathbf{x} . An especially important characteristic for mechanism design is that the technique requires a total of only one more objective function evaluation than iterations to obtain an optimal design, unlike the GRG technique of Lasdon et al. [2], where a step-length determination is required at each iteration.

3. Example problems

Several examples were considered in this work, two of which are presented here.

The first problem, which is a modified Rosen-Suzuki test problem, consists of a quadratic objective function in eight variables with seven quadratic inequality constraints as follows:

$$\begin{aligned} \text{Min } F(\mathbf{x}) = & x_1^2 + \frac{1}{2}x_2^2 + \frac{1}{2}x_3^2 + 3x_4^2 + 2x_5^2 + \frac{1}{2}x_6^2 + x_7^2 + \frac{1}{2}x_8^2 \\ & + 2x_1 - 3x_2 + 5x_3 + x_4 + 7x_5 + 2x_6 - x_7, \end{aligned}$$

$$\text{s.t. } g_1(\mathbf{x}) = \frac{1}{2}x_1^2 + \frac{1}{2}x_2^2 + 2x_3^2 - \frac{1}{2}x_4^2 + x_5^2 - 2x_6 - 4x_7 + 5x_8 - 10 \leq 0,$$

$$\begin{aligned} g_2(\mathbf{x}) = & x_1^2 + x_2^2 + x_3^2 + x_4^2 + x_5^2 + x_6^2 + x_7^2 + x_8^2 + x_1 + x_2 \\ & + x_3 - x_4 + x_5 - x_6 + x_7 - x_8 - 6 \leq 0, \end{aligned}$$

$$g_3(\mathbf{x}) = x_1^2 + 2x_2^2 + x_3^2 + 2x_4^2 + x_5^2 + 2x_6^2 + x_7 + 2x_8 - x_1 - x_2 - x_3 - x_4 - 13 \leq 0,$$

$$g_4(\mathbf{x}) = x_1 - 2x_2 + 3x_3 + 4x_4 + 5x_5 + 6x_6 + x_7 - x_8 - x_1 - x_2 - 5 \leq 0,$$

$$g_5(\mathbf{x}) = x_1 - x_2 - x_3 - x_4 - 11 \leq 0,$$

$$g_1(\mathbf{x}) = 2x_1^2 - 2x_2^2 - 2x_3^2 - 2x_4^2 + 3x_5^2 - 3x_6^2 + 3x_7^2 - 3x_8^2 \\ - 2x_9 - 2x_{10} - 2x_{11} - 2x_{12} + 2x_{13} - 2x_{14} - 10 \leq 0,$$

$$g_2(\mathbf{x}) = 4x_1^2 - 4x_2^2 + 2x_3^2 - 2x_4^2 - 5x_5 - 5x_6 + 5x_7 + 5x_8 - 20 \leq 0.$$

Tables 1 and 2 show the results of the optimization from two different starting points. Three different techniques were applied. The first two were variations of the Gauss nonlinearly

Table 1
Results of Rosen-Suzuki test problem

Starting point		Technique		
		GNLCNS	GNLC	GRG
Status	NI	2	3	14
feasible	NI	3	4	144
0.0	Y	0.8797	0.8797	-0.8797
1.0	Y	0.7030	0.7030	0.7030
0.0	Y	0.1092	0.1092	0.1092
1.0	Y ₁	0.8333	0.8333	0.8334
0.0	Y ₁	0.2015	0.2015	-0.2016
0.0	Y ₁	0.8570	0.8570	-0.8571
0.0	Y ₁	0.3993	0.3993	0.3993
0.0	Y ₁	0.3333	0.3333	0.3334
0.5	F	9.520	9.520	-9.520
0.25	G ₁	4	4	4

Table 2
Results of Rosen-Suzuki test problem

Starting point		Technique		
		GNLCNS	GNLC	GRG
Status	NI	3	—	24
infeasible	NI	4	—	276
0.0	Y	0.8797	—	0.8797
1.0	Y	0.7030	—	0.7030
0.0	Y	0.1092	—	0.1092
1.0	Y ₁	0.8333	—	0.8333
0.0	Y ₁	0.2015	—	0.2015
0.0	Y ₁	0.8570	—	0.8570
0.0	Y ₁	0.3993	—	0.3993
0.0	Y ₁	0.3333	—	0.3333
0.5	F	9.520	—	9.520
0.25	G ₁	4	—	4

constrained method. The first one, labeled GNLC.NS in the tables, ignored violated constraints, while the second, labeled GNLC, treated violated constraints using (13). Both of these methods were compared with the generalized reduced gradient technique, labeled GRG.

Table 1 shows the results from a starting point, where no constraints were active or violated. All three methods produced the same optimal design. The number of iterations NI and number of function evaluations NF for the GNLC methods were considerably less than for the GRG. Table 2 shows the results from a starting point in which three constraints were violated, while one was active. For this starting point only the GNLC.NS technique was applicable. Again, the number of iterations and function evaluations were less than for the GRG.

The second example consists of the design of a four-bar mechanism such that the coupler point (XX, YY) of the mechanism closely generated the curve defined by the eight points as shown in Fig. 1. The objective function to be minimized is the sum of the distances (squared) between the desired curve and the actual curve generated by the mechanism:

$$F(x) = \sum_{i=1}^8 (XX_i - XG_i)^2 + (YY_i - YG_i)^2,$$

where

$$XX_i = x_2 \cos \gamma_i + x_3 \cos \psi_i + x_{10}, \quad YY_i = x_2 \sin \gamma_i + x_3 \cos \psi_i + x_{10},$$

$$\psi_i = \gamma_i + \alpha_i + \eta_i - \epsilon_i,$$

$$\epsilon_i = \tan^{-1} \left[\frac{x_2 \sin(\gamma_i - \alpha_i)}{x_1 - x_2 \cos(\gamma_i - \alpha_i)} \right],$$

$$\eta_i = \cos^{-1} \left[\frac{x_1^2 + x_2^2 + x_3^2 - x_4^2 - 2x_1x_2 \cos(\gamma_i - \alpha_i)}{2x_1[x_1^2 + x_2^2 - 2x_1x_2 \cos(\gamma_i - \alpha_i)]^{1/2}} \right].$$

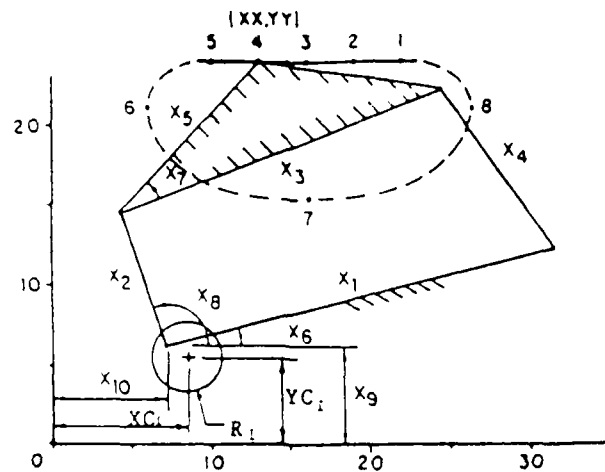


Fig. 1. Four-bar mechanism for path generation.

$$x_i = x_i + \Delta x_i$$

and (XG, YG) are the coordinates of the desired curve.

The design variables x_1, \dots, x_{10} are link lengths, orientation of some of the links as well as the location of the crank pin. Note, the objective function is a highly nonlinear function of the design variables. This is the same problem that Paradis and Willmert [3] solved, however, two nonlinear constraints, g_{13} and g_{14} , have been introduced here to constrain the location of the crank pin to two user-defined circular regions. Thus, our design problem contains ten variables, x_1, \dots, x_{10} , and fourteen inequality constraints $g_i(\mathbf{x}) \leq 0, i = 1, \dots, 14$. The constraints are:

$$g_1(\mathbf{x}) = 1 - x_2 \leq 0,$$

$$g_2(\mathbf{x}) = 1 - x_3 \leq 0,$$

$$g_3(\mathbf{x}) = x_2 - x_1 \leq 0,$$

$$g_4(\mathbf{x}) = x_2 - x_3 \leq 0,$$

$$g_5(\mathbf{x}) = x_2 - x_4 \leq 0,$$

$$g_6(\mathbf{x}) = x_1 + x_2 - x_3 - x_4 \leq 0,$$

$$g_7(\mathbf{x}) = x_2 + x_3 - x_1 - x_4 \leq 0,$$

$$g_8(\mathbf{x}) = x_2 + x_4 - x_1 - x_3 \leq 0,$$

$$g_9(\mathbf{x}) = x_1 - 30 \leq 0,$$

$$g_{10}(\mathbf{x}) = x_3 - 30 \leq 0,$$

$$g_{11}(\mathbf{x}) = x_2 - 30 \leq 0,$$

$$g_{12}(\mathbf{x}) = x_4 - 30 \leq 0,$$

$$g_{13}(\mathbf{x}) = (x_{10} - CX_1)^2 + (x_9 - CY_1)^2 - R_1^2 \leq 0,$$

$$g_{14}(\mathbf{x}) = (x_{10} - CX_2)^2 + (x_9 - CY_2)^2 - R_2^2 \leq 0,$$

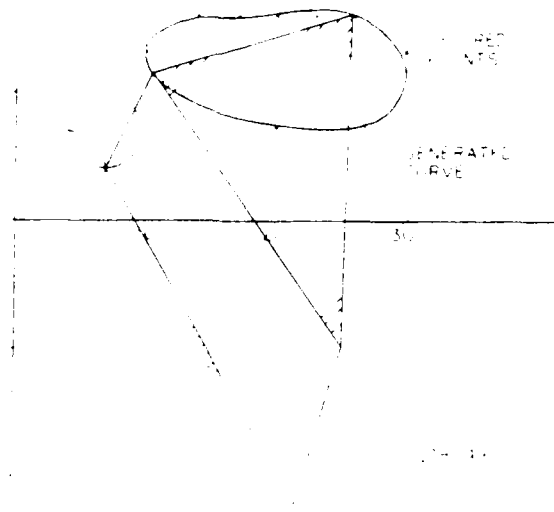


Fig. 2. Optimal mechanism

Table 3
Results of mechanism design problem

Starting point		GNLC	GRG
Status	NI	11	56
feasible	NF	12	389
15.0	X_1	30.0	30.0
5.0	X_2	8.345	8.345
15.0	X_3	25.821	25.821
5.0	X_4	12.817	12.817
15.0	X_5	16.026	16.026
-0.007	X_6^*	-1.063	-1.063
0.412	X_7^*	1.259	1.259
1.379	X_8^*	1.118	1.118
6.0	X_9	4.0	4.0
5.0	X_{10}	7.0	7.0
220.29	F	1.78349	1.78348
—	G_{ACT}	9.13.14	9.13.14

*Angle variables (radians)

where CX_1 , CY_1 , R_1 , CX_2 , CY_2 , and R_2 were 4, 4, 3, 7, 7, and 3, respectively.

The resulting optimal designs using the GNLC and GRG methods are shown in Table 3. The optimal mechanism is shown in Fig. 2. Again the Gauss nonlinearly constrained method required significantly fewer objective function evaluations.

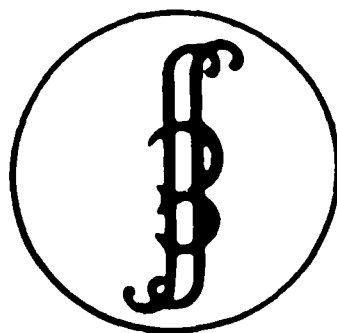
4. Conclusions

The Gauss nonlinearly constrained method is an effective technique of solving nonlinear design problems. It is particularly efficient for cases in which the evaluation of the objective function is very time-consuming. Although in some instances considerable calculations must be done per iteration, the amount required is still insignificant compared to that required to do just one analysis of a complex mechanical or structural system.

The method has been applied to a variety of problems consisting of objective functions of various complexities. In all cases it has worked well. However, it has received only limited application to problems involving constraints that are more than quadratically nonlinear. It appears that further research is required for such cases.

References

- [1] M.J. DeRubes and K.D. Willmert, Optimal design of flexible link mechanisms, in: C.F. Ruoff and T.E. Shoup, eds., *Computers in Engineering*, Vol. 2 (ASME, New York, 1983) 169-177.
- [2] L.S. Lasdon, A.D. Waren and M.W. Ratner, *GRG2 user's guide*, Cleveland State University, OH, February 1982.
- [3] M.J. Paradis and K.D. Willmert, Optimal mechanism design using the Gauss constrained method, ASME Paper No. 82-DET-91, 1982.
- [4] D.J. Wilde, Error linearization in the least-squares design of function generating mechanisms, in: R.W. Mayne and K.M. Ragsdell, eds., *Progress in Engineering Optimization* (ASME, New York, 1981) 33-37.



ABSTRACTS



23rd Annual Meeting
of the
Society of Engineering
Science

August 25, 26 and 27, 1986
at the
State University of New York
at Buffalo

VIBRATION ANALYSIS OF MECHANISMS
WITH GEOMETRIC AND MATERIAL NONLINEARITIES

Edward Kear III, M. Sathyamoorthy, and K. D. Willmert
Department of Mechanical and Industrial Engineering
Clarkson University
Potsdam, New York 13676

ABSTRACT

A nonlinear vibrational analysis for planar mechanisms with material and geometric nonlinearities is presented. The material nonlinearity of the Ramberg-Osgood type is employed for the nonlinear stress-strain behavior. The geometric nonlinearities that are included in this study are due to coupling of displacements, stretching and curvature-displacement. A finite element analysis, with high order hermite polynomials which ensure compatibility of curvature between elements, is used. The resulting nonlinear differential equations are solved by means of a harmonic series technique to obtain steady state solutions. The effects of the nonlinearities are discussed by means of an example problem.

Non-Linear Vibrations,
Stability, and Dynamics of
Structures and Mechanisms

23-25 March 1987

Abstracts

*Sponsored by
Army Research Office*

*Hosted by
Virginia Polytechnic Institute
and State University*

Effect of Geometric and Material Nonlinearities on Vibration of Planar Mechanisms*

E. B. Kear III M. Sathyamoorthy
K. D. Willmert

Department of Mechanical and Industrial Engineering
Clarkson University
Potsdam, New York 13676

Abstract

A nonlinear vibrational analysis for planar mechanisms with material and geometric nonlinearities, undergoing known rigid-body motions, is presented. Material nonlinearity of the Ramberg-Osgood type is employed for the nonlinear stress-strain behavior. The geometric nonlinearities, included in this study, are due to stretching and curvature. A finite element analysis, with high order hermite polynomials, which ensure compatibility of curvature between elements, is used. The resulting nonlinear differential equations are solved using an Adams fourth-order predictor-corrector algorithm (LSODE from ODEPACK) to obtain the transient vibrational response about the known, time dependent, rigid-body position. The effects of the nonlinearities are discussed by means of an example problem.

*This research is sponsored by the Air Force Office of Scientific Research, Air Force Systems Command, USAF, under Grant Number AFOSR 84-0076, and the National Science Foundation under Grant Number DMC-8500627. Supercomputing facilities of the National Center for Supercomputing Applications at the University of Illinois are being utilized for this research.

Effect of Geometric and Material Nonlinearities
on Vibration of Planar Mechanisms*

E. B. Kear III M. Sathyamoorthy

K. D. Willmert

Department of Mechanical and Industrial Engineering

Clarkson University

Potsdam, New York 13676

* This research is sponsored by the Air Force Office of Scientific Research, Air Force Systems Command, USAF, under Grant Number AFOSR 84-0076, and the National Science Foundation under Grant Number DMC-8500627. Supercomputing facilities of the National Center for Supercomputing Applications at the University of Illinois are being utilized for this research.

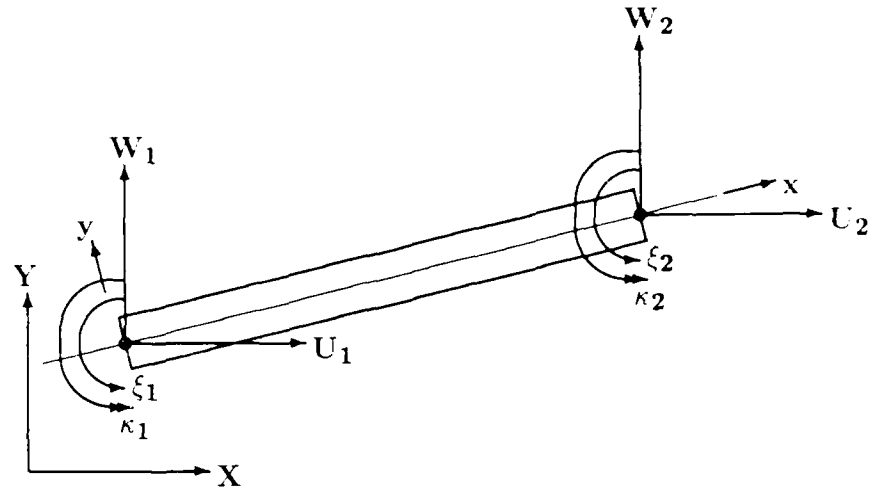


Figure 1: Global Displacements For Element i

$$\frac{d}{dt} \left(\frac{\partial KE}{\partial \dot{q}_j} \right) - \frac{\partial KE}{\partial q_j} + \frac{\partial SE}{\partial q_j} = 0 ; j = 1 \text{ to } n \quad (1)$$

$$\sum_{i=1}^k \left[\frac{d}{dt} \left(\frac{\partial KE}{\partial \dot{q}_j} \right) - \frac{\partial KE}{\partial q_j} + \frac{\partial SE}{\partial q_j} \right]_i = 0 ; j = 1 \text{ to } n \quad (2)$$

For Element i

$$KE = \frac{\rho}{2} \int_0^l (Av^2(x) + I\dot{\theta}^2(x)) dx \quad (3)$$

$$A = bt \quad ; \quad I = \frac{bt^3}{12} \quad (4)$$

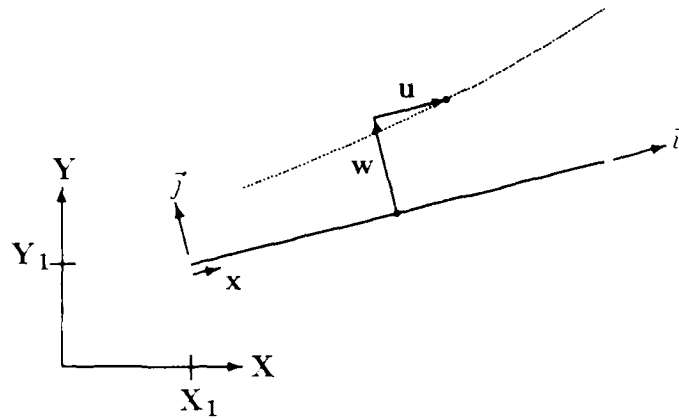


Figure 2: Deflected Element.

- X_1 is the X coordinate of end 1 of the reference.
- Y_1 is the Y coordinate of end 1 of the reference.
- ϕ is the angle between the reference and X axis.
- u is the axial displacement of a point from its reference position.
- w is the transverse displacement of a point from its reference position.
- \vec{i} is a unit vector in x direction.
- \vec{j} is a unit vector in y direction.

$$\begin{aligned} \vec{r} = & (X_1 \cos \phi + Y_1 \sin \phi + x + u) \vec{i} + \\ & (Y_1 \cos \phi - X_1 \sin \phi + w) \vec{j} \end{aligned} \quad (5)$$

$$\begin{aligned} \vec{v} = & (\dot{X}_1 \cos \phi + \dot{Y}_1 \sin \phi + \dot{u} - \dot{\phi}w) \vec{i} + \\ & (\dot{Y}_1 \cos \phi - \dot{X}_1 \sin \phi + \dot{w} + \dot{\phi}x + \dot{\phi}u) \vec{j} \end{aligned} \quad (6)$$

$$\begin{aligned} v^2(x) = & (\dot{X}_1 \cos \phi + \dot{Y}_1 \sin \phi + \dot{u} - \dot{\phi}w)^2 + \\ & (\dot{Y}_1 \cos \phi - \dot{X}_1 \sin \phi + \dot{w} + \dot{\phi}x + \dot{\phi}u)^2 \end{aligned} \quad (7)$$

$$\theta = \phi + \arctan \left(\frac{w_x}{u_x + 1} \right) \quad (8)$$

$$\dot{\theta} = \dot{\phi} + (\dot{w}_x(u_x + 1) - w_x \dot{u}_x) \quad (9)$$

$$\begin{aligned}
KE = & \frac{\rho}{2} \int_0^l \left(\right. \\
& A \left(\dot{X}_1 \cos \phi + \dot{Y}_1 \sin \phi + \dot{u} - \dot{\phi} w \right)^2 + \\
& A \left(\dot{Y}_1 \cos \phi - \dot{X}_1 \sin \phi + \dot{w} + \dot{\phi} x + \dot{\phi} u \right)^2 + \\
& \left. I \left(\dot{\phi} + \dot{w}_x (u_x + 1) - w_x \dot{u}_x \right)^2 \right) dx \quad (10)
\end{aligned}$$

$$\begin{aligned}
\frac{d}{dt} \left(\frac{\partial KE}{\partial \dot{q}_j} \right) - \frac{\partial KE}{\partial q_j} = & \rho \int_0^l \left(\right. \\
& A \left(\ddot{u} + \ddot{\phi} u + \ddot{\phi} x + 2\dot{\phi} \dot{u} - \dot{\phi}^2 w + \ddot{Y}_1 \cos \phi - \ddot{X}_1 \sin \phi \right) w_{q_j} + \\
& A \left(\ddot{u} - \ddot{\phi} w - 2\dot{\phi} \dot{w} - \dot{\phi}^2 u - \dot{\phi}^2 x + \ddot{Y}_1 \sin \phi + \ddot{X}_1 \cos \phi \right) u_{q_j} + \\
& \left. I \left(\ddot{\phi} + \ddot{w}_x (u_x + 1) - w_x \ddot{u}_x \right) \left(w_{xq_j} (u_x + 1) - w_x u_{xq_j} \right) \right) dx \quad (11)
\end{aligned}$$

$$\sigma = \begin{cases} E_1 \epsilon - E_2 \epsilon^m & \text{if } \epsilon > 0 \text{ or } m \text{ is an odd integer} \\ E_1 \epsilon + E_2 \epsilon^m & \text{otherwise} \end{cases} \quad (12)$$

$$\sigma = E_1 \epsilon - E_2 \epsilon |\epsilon|^{m-1} \quad (13)$$

$$\epsilon = \epsilon_n - y \kappa \quad (14)$$

$$m = 3 \quad (15)$$

$$SE = A \int_0^l \left(\frac{1}{2} E_1 \left(\epsilon_n^2 + \frac{1}{12} (t\kappa)^2 \right) - \frac{E_2}{20t\kappa} \left(\left(\epsilon_n + \frac{t\kappa}{2} \right)^5 - \left(\epsilon_n - \frac{t\kappa}{2} \right)^5 \right) \right) dx \quad (16)$$

$$\frac{\partial SE}{\partial q_j} = A \int_0^l \left(\left(E_1 \epsilon_n - E_2 \left(\epsilon_n^3 + \epsilon_n \left(\frac{t\kappa}{2} \right)^2 \right) \right) \epsilon_{n,q_j} + \left(E_1 \frac{t\kappa}{6} - E_2 \left(\epsilon_n^2 \left(\frac{t\kappa}{2} \right) + \frac{1}{5} \left(\frac{t\kappa}{2} \right)^3 \right) \right) \frac{t\kappa_{q_j}}{2} \right) dx \quad (17)$$

$$\epsilon_n = \frac{ds}{dx} - 1 \quad (18)$$

$$\epsilon_n = \left((u_x + 1)^2 + w_x^2 \right)^{1/2} - 1 \quad (19)$$

$$\epsilon_{nq_j} = (u_x + 1)u_{xq_j} + w_x w_{xq_j} \quad (20)$$

$$\kappa = \frac{d\xi}{ds} = \frac{d\xi}{dx} \frac{dx}{ds} \quad (21)$$

$$\xi = \arctan \frac{w_x}{u_x + 1} \quad (22)$$

$$\kappa = w_{xx}(u_x + 1) - w_x u_{xx} \quad (23)$$

$$\kappa_{q_j} = w_{xxq_j}(u_x + 1) + w_{xx}u_{xq_j} - w_{xq_j}u_{xx} - w_x u_{xxq_j} \quad (24)$$

$$\begin{aligned}
\sum_{j=1}^k \left[\frac{d}{dt} \left(\frac{\partial KE}{\partial \dot{q}_j} \right) - \frac{\partial KE}{\partial q_j} - \frac{\partial SE}{\partial q_j} = \int_0^t \left(\right. \\
\rho A (\ddot{u} + \ddot{\phi} u + \ddot{\phi} x + 2\dot{\phi} \dot{u} - \dot{\phi}^2 w + \ddot{Y}_1 \cos \phi - \ddot{X}_1 \sin \phi) w_{q_j} + \\
\rho A (\ddot{u} - \ddot{\phi} w - 2\dot{\phi} \dot{w} - \dot{\phi}^2 u - \dot{\phi}^2 x + \ddot{Y}_1 \sin \phi + \ddot{X}_1 \cos \phi) u_{q_j} + \\
\rho I (\ddot{\phi} + \ddot{u}_x (u_x + 1) - w_x \ddot{u}_x) (w_{xq_j} (u_x + 1) - w_x u_{xq_j}) - \\
A \left(E_1 \epsilon_n - E_2 \left(\epsilon_n^3 + \epsilon_n \left(\frac{t\kappa}{2} \right)^2 \right) \right) \epsilon_{nq_j} + \\
A \left(E_1 \frac{t\kappa}{6} - E_2 \left(\epsilon_n^2 \left(\frac{t\kappa}{2} \right) + \frac{1}{5} \left(\frac{t\kappa}{2} \right)^3 \right) \right) \frac{t\kappa_{q_j}}{2} dx \Big]_1
\end{aligned} \tag{25}$$

$$\begin{aligned}
u(x) &= n_1(U_1 \cos \phi + W_1 \sin \phi) + n_2(U_2 \cos \phi + W_2 \sin \phi) \\
w(x) &= h_1(W_1 \cos \phi - U_1 \sin \phi) + h_2\theta_1 + h_3m_1 + \\
&\quad h_4(W_2 \cos \phi - U_2 \sin \phi) + h_5\theta_2 + h_6m_2
\end{aligned} \tag{26}$$

$$\begin{aligned}
n_1 &= 1 - \frac{x}{\ell} \\
n_2 &= \frac{x}{\ell} \\
h_1 &= 1 - 10 \left(\frac{x}{\ell}\right)^3 + 15 \left(\frac{x}{\ell}\right)^4 - 6 \left(\frac{x}{\ell}\right)^5 \\
h_2 &= \ell \left(\frac{x}{\ell} - 6 \left(\frac{x}{\ell}\right)^3 + 8 \left(\frac{x}{\ell}\right)^4 - 3 \left(\frac{x}{\ell}\right)^5\right) \\
h_3 &= \frac{\ell^2}{2} \left(\left(\frac{x}{\ell}\right)^2 - 3 \left(\frac{x}{\ell}\right)^3 + 3 \left(\frac{x}{\ell}\right)^4 - \left(\frac{x}{\ell}\right)^5\right) \\
h_4 &= 10 \left(\frac{x}{\ell}\right)^3 - 15 \left(\frac{x}{\ell}\right)^4 + 6 \left(\frac{x}{\ell}\right)^5 \\
h_5 &= \ell \left(-4 \left(\frac{x}{\ell}\right)^3 + 7 \left(\frac{x}{\ell}\right)^4 - 3 \left(\frac{x}{\ell}\right)^5\right) \\
h_6 &= \frac{\ell^2}{2} \left(\left(\frac{x}{\ell}\right)^3 - 2 \left(\frac{x}{\ell}\right)^4 + \left(\frac{x}{\ell}\right)^5\right)
\end{aligned} \tag{27}$$

$$\begin{aligned}
u(x) &= h_1(U_1 \cos \phi + W_1 \sin \phi) + h_2(\cos \xi_1 - 1) - h_3 \kappa_1 \sin \xi_1 + \\
&\quad h_4(U_2 \cos \phi + W_2 \sin \phi) + h_5(\cos \xi_2 - 1) - h_6 \kappa_2 \sin \xi_2 \\
w(x) &= h_1(W_1 \cos \phi - U_1 \sin \phi) + h_2 \sin \xi_1 + h_3 \kappa_1 \cos \xi_1 + \\
&\quad h_4(W_2 \cos \phi - U_2 \sin \phi) + h_5 \sin \xi_2 + h_6 \kappa_2 \cos \xi_2
\end{aligned} \tag{28}$$

$$\begin{aligned}
h_1 &= 1 - 10 \left(\frac{x}{\ell}\right)^3 + 15 \left(\frac{x}{\ell}\right)^4 - 6 \left(\frac{x}{\ell}\right)^5 \\
h_2 &= \ell \left(\frac{x}{\ell} - 6 \left(\frac{x}{\ell}\right)^3 + 8 \left(\frac{x}{\ell}\right)^4 - 3 \left(\frac{x}{\ell}\right)^5\right) \\
h_3 &= \frac{\ell^2}{2} \left(\left(\frac{x}{\ell}\right)^2 - 3 \left(\frac{x}{\ell}\right)^3 + 3 \left(\frac{x}{\ell}\right)^4 - \left(\frac{x}{\ell}\right)^5\right) \\
h_4 &= 10 \left(\frac{x}{\ell}\right)^3 - 15 \left(\frac{x}{\ell}\right)^4 + 6 \left(\frac{x}{\ell}\right)^5 \\
h_5 &= \ell \left(-4 \left(\frac{x}{\ell}\right)^3 + 7 \left(\frac{x}{\ell}\right)^4 - 3 \left(\frac{x}{\ell}\right)^5\right) \\
h_6 &= \frac{\ell^2}{2} \left(\left(\frac{x}{\ell}\right)^3 - 2 \left(\frac{x}{\ell}\right)^4 + \left(\frac{x}{\ell}\right)^5\right)
\end{aligned} \tag{29}$$

$$[M] \{\ddot{q}\} = \{F(q, \dot{q})\} \quad (30)$$

$$\begin{aligned} q_1 &= q \\ q_2 &= \dot{q}_1 \\ \dot{q}_2 &= \ddot{q}_1 \end{aligned} \quad (31)$$

$$\begin{bmatrix} I & 0 \\ 0 & M \end{bmatrix} \begin{Bmatrix} \dot{q}_1 \\ \dot{q}_2 \end{Bmatrix} = \begin{Bmatrix} \dot{q} \\ F(q, \dot{q}) \end{Bmatrix} \quad (32)$$

$$\begin{Bmatrix} \dot{q}_1 \\ \dot{q}_2 \end{Bmatrix} = \begin{Bmatrix} q \\ [M]^{-1} \{F(q, \dot{q})\} \end{Bmatrix} \quad (33)$$

LSODE (Livermore Solver for Ordinary Differential Equations) can be used to solve a system of equations of the form

$$\{\dot{y}\} = \{F(t, y)\} \quad (34)$$

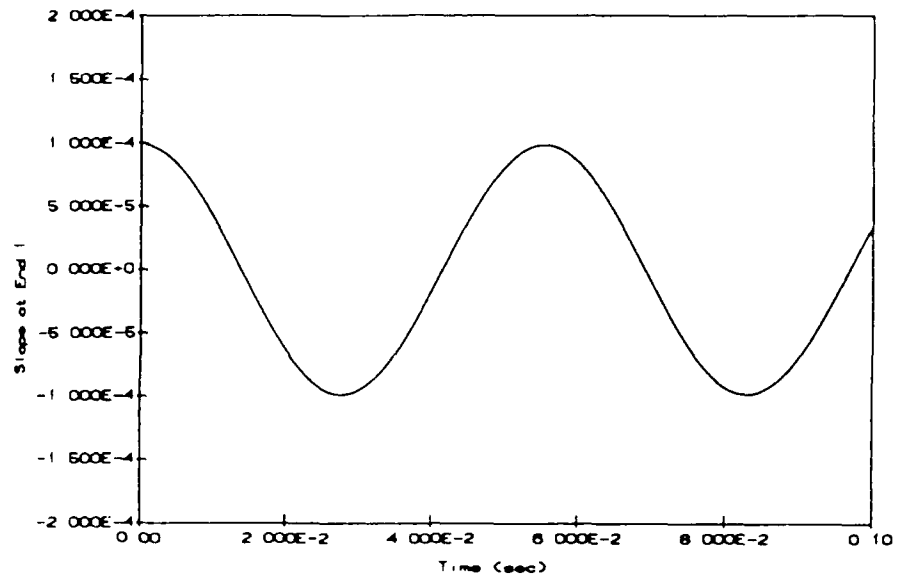


Figure 1. Response of a Pinned-Pinned Beam — 1st-Mode.

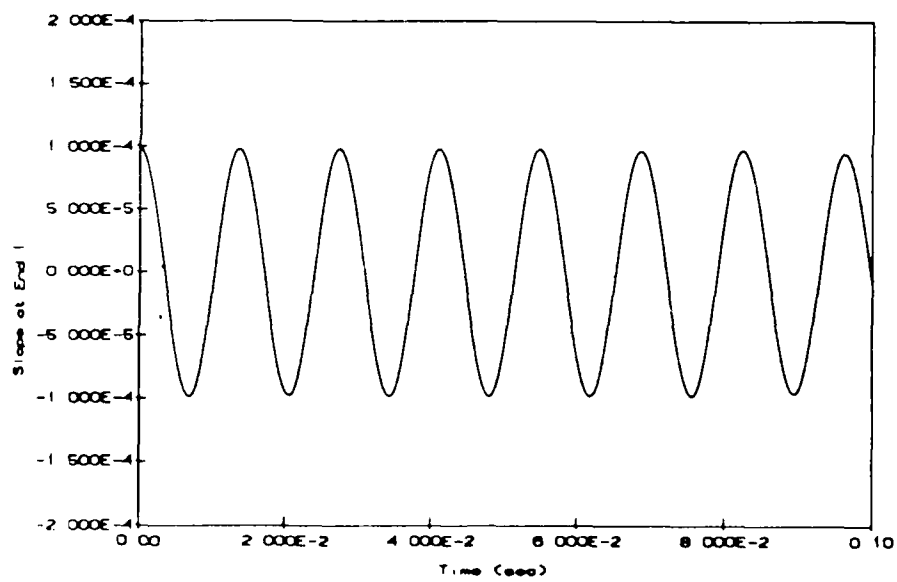


Figure 2. Response of a Pinned-Pinned Beam — 2nd-Mode.

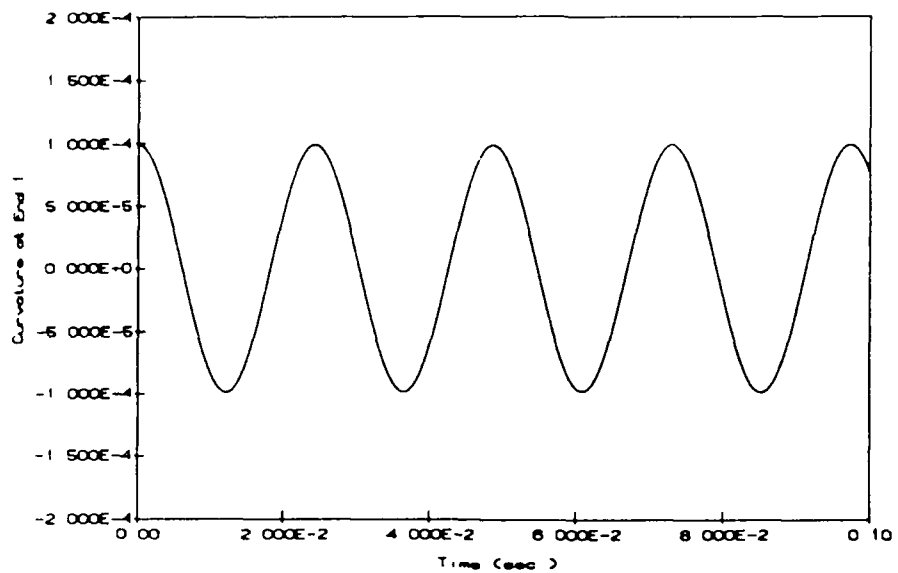


Figure 3. Response of a Clamped-Clamped Beam -- 1st-Mode.

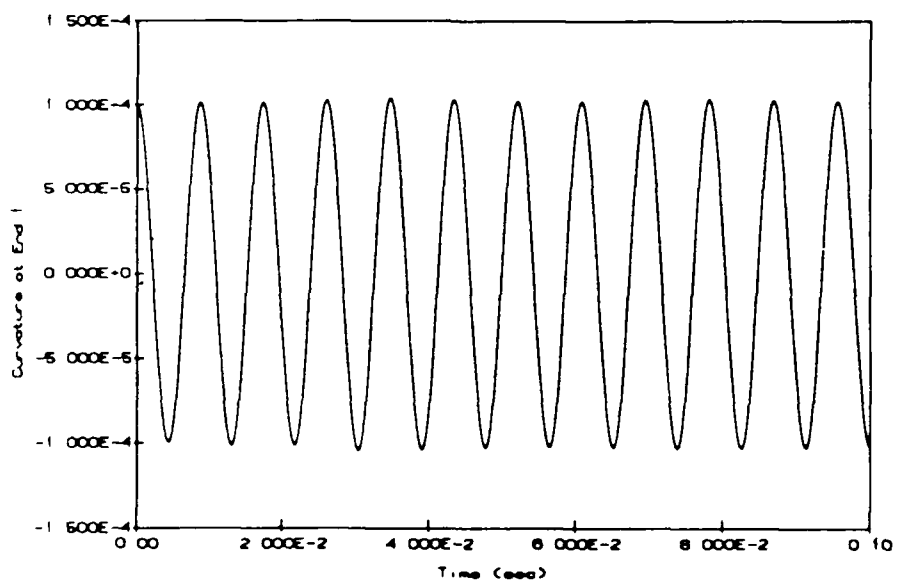


Figure 4. Response of a Clamped-Clamped Beam -- 2nd-Mode.

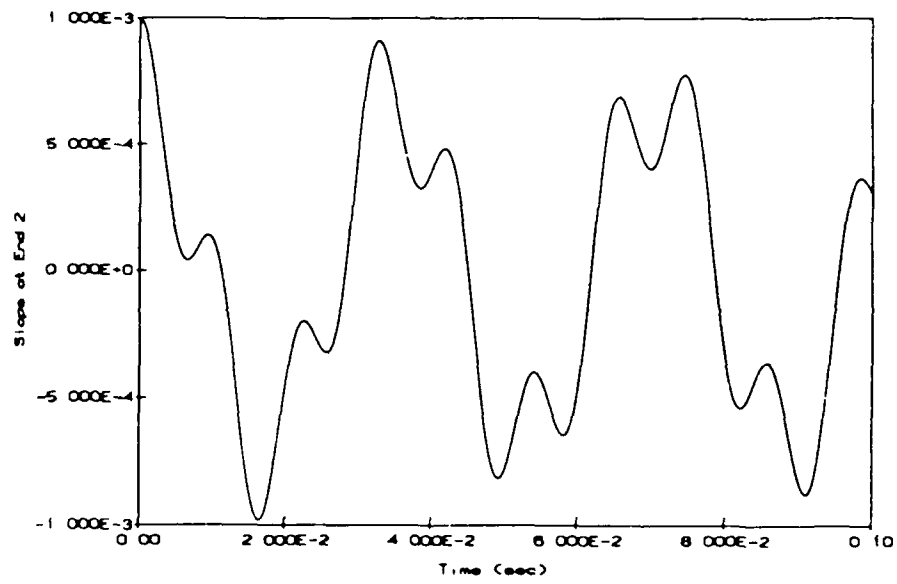


Figure 5. Response of a Clamped-Pinned Beam.

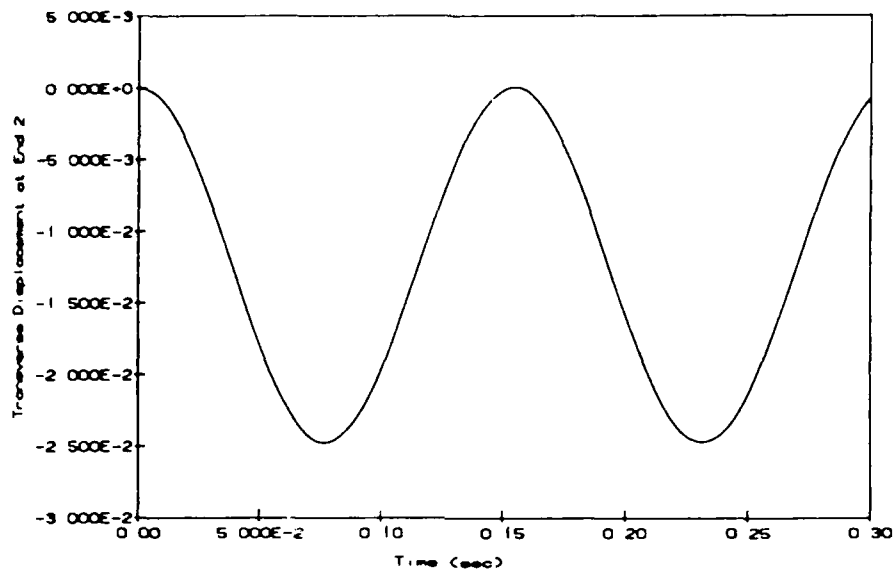


Figure 6. Response of a Rotating Cantilever Beam.

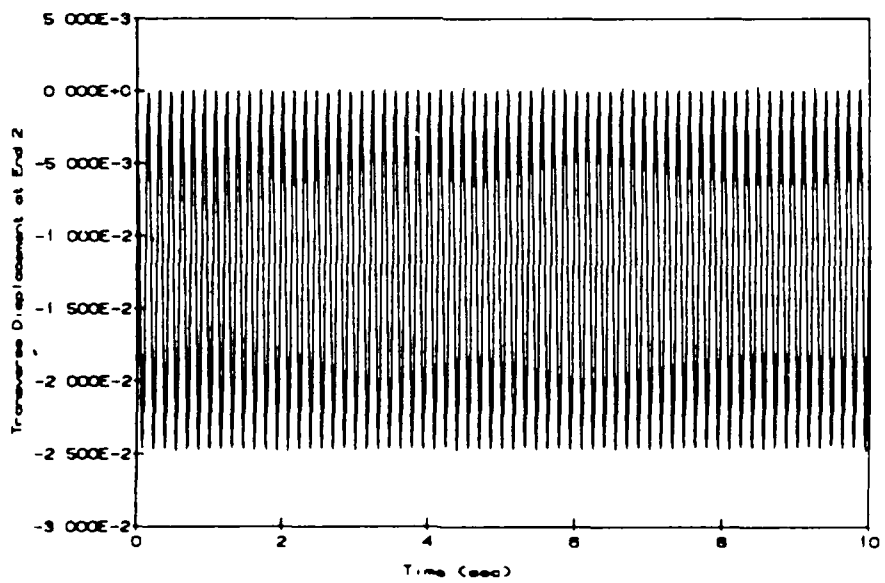


Figure 7. Transverse Response of a Rotating Cantilever Beam.

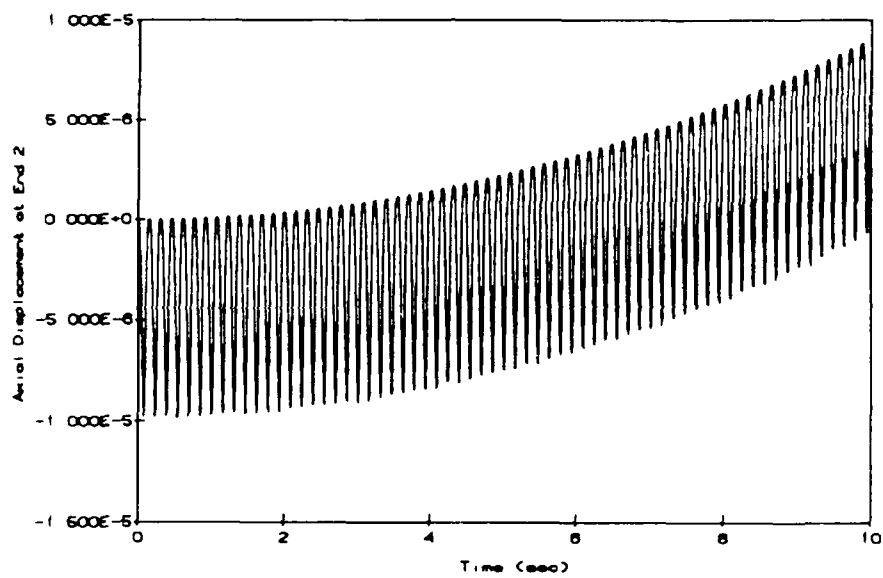


Figure 8. Axial Response of a Rotating Cantilever Beam.

FINITE ELEMENT NONLINEAR ANALYSIS OF

THREE-DIMENSIONAL MECHANISMS

M. El-Sawy

K.D. Willmert

and

M. Sathyamoorthy

Department of Mechanical and Industrial Engineering

Clarkson University

Potsdam, New York

Research Support by AFOSR

Under Grant No. AFOSR 84-0076

and

NSF Under Grant No. DMC-8500627

Consider a straight beam element with its elastic axis parallel to the x-axis of the fixed global system of coordinate G. Under the action of loads which are distributed along the beam element, it deforms. This deformation is described by the displacement of each point of the elastic axis. The components of these displacements u, v and w are in the direction of \hat{e}_{xG} , \hat{e}_{yG} and \hat{e}_{zG} , respectively (see Figure 1). In addition, each cross section is also rotated by angle θ about the elastic axis.

Due to this deformation, the triad \hat{e}_{xH} , \hat{e}_{yH} and \hat{e}_{zH} at the point B of the undeformed axis is transformed into a new rotated orthogonal triad of unite vectors \hat{e}_{xD} , \hat{e}_{yD} , \hat{e}_{zD} and the position vector of the point B, an elastic axis, after deformation becomes

$$\begin{aligned} \bar{R}_{BD} = & (X_G + Q_1)\hat{e}_{xG} + (Y_G + Q_2)\hat{e}_{yG} + (Z_G + Q_3)\hat{e}_{zG} \\ & + (x_p + u)\hat{e}_{xH} + v\hat{e}_{yH} + w\hat{e}_{zH} \end{aligned}$$

while the position vector \bar{R}_{PD} of the point P off the elastic axis after deformation reduces to

$$\begin{aligned} \bar{R}_p = & (X_G + Q_1)\hat{e}_{xG} + (Y_G + Q_2)\hat{e}_{yG} + (Z_G + Q_3)\hat{e}_{zG} \\ & + (x_p + u)\hat{e}_{xH} + v\hat{e}_{yH} + w\hat{e}_{zH} \\ & + y_p\hat{e}_{yD} + z_p\hat{e}_{zD} + \lambda\hat{e}_{xD} \end{aligned}$$

where λ is the warping displacement of the cross section which is considered an extension of the classical St. Venant torsion to a more general case.

To this point the elastic deformations of the element are defined for the general case where the deformations are due to the action of forces which are distributed along the beam element. In the case of mechanisms, the element is imposed to an additional angles of deformation γ_x , γ_y and γ_z , due to the elastic deformations of the other elements, in the directions x_H , y_H and z_H , respectively.

Finally, the position vector of the point P after deformation with respect to the undeformed system of coordinates will reduce to

$$\begin{aligned} R_p = & \mathbf{L}(\bar{X}^T + \bar{Q}_{dl}^T) + (x_H^T + \bar{U}^T)T_{rH} \\ & + (x_p^T T_{Dr} T_{rH})\hat{e}_H \end{aligned}$$

where

$$\bar{X}^T = \mathbf{L} \begin{bmatrix} X_G & Y_G & Z_G \end{bmatrix}$$

$$\bar{Q}_{al}^T = \begin{bmatrix} Q_1 & Q_2 & Q_3 \end{bmatrix}$$

$$\bar{X}_H^T = \begin{bmatrix} X_H & 0 & 0 \end{bmatrix}$$

$$\bar{U}^T = \begin{bmatrix} u & v & w \end{bmatrix}$$

$$\bar{x}_p^T = \begin{bmatrix} 0 & y_p & z_p \end{bmatrix}$$

T_{rH} is the elastic transformation matrix and is given by

$$T_{rH} = T_{rD} T_{DH} \text{ where}$$

T_{DH} is a transformation matrix of the body.

The velocity of the point P after deformation at any instant of time is given by

$$\begin{aligned} \dot{\bar{R}}_{pD} = & \begin{bmatrix} \dot{\bar{X}}^T + \dot{\bar{Q}}_{al} \end{bmatrix} T_{GH} + \begin{bmatrix} \dot{\bar{X}}^T + \dot{\bar{Q}}_{al} \end{bmatrix} \dot{T}_{GH} \\ & + \begin{bmatrix} \bar{x}_H^T + \bar{U}^T \end{bmatrix} \dot{T}_{rH} + \dot{\bar{U}}^T T_{rH} + \bar{x}_p^T \dot{T}_{rH} \hat{e}_H \\ & + \begin{bmatrix} \dot{\bar{X}}^T + \dot{\bar{Q}}_{al} \end{bmatrix} T_{GH} + \begin{bmatrix} \bar{X}_H + \bar{U}^T \end{bmatrix} T_{rH} + x_p^T T_{Dr} T_{rH} \hat{e}_H \end{aligned}$$

Using finite element expression to rewrite the previous equation and isolating the velocity terms, the expression can be written in the following form

$$\dot{\bar{R}}_p = \begin{bmatrix} a_x & a_\varphi & a_{qe} \end{bmatrix} \begin{Bmatrix} \dot{\bar{X}} \\ \dot{\bar{\psi}} \\ \dot{\bar{q}}_e \end{Bmatrix}$$

Also, if the axial deformations in the direction \hat{e}_{xH} , \hat{e}_{yH} and \hat{e}_{zH} are transformed to the global fixed coordinate, the final expression for the velocity reduces to

$$\dot{\bar{R}}_p = \begin{bmatrix} a_x & a_\varphi & a_q \end{bmatrix} \begin{Bmatrix} \dot{\bar{X}} \\ \dot{\bar{\psi}} \\ \dot{\bar{\theta}}_e \end{Bmatrix}$$

a) Kinetic Energy

If we consider the previous beam element with an additional two concentrated masses (m_{con1} , m_{con2}) at nodes 1 and nod2 respectively, then the kinetic energy of the element becomes:

$$KE = \int_{Vol} \frac{1}{2} \rho \dot{\bar{R}}_p^T \dot{\bar{R}}_p \, dvol + \frac{1}{2} m_{con1} \dot{\bar{R}}_1^T \dot{\bar{R}}_1 + \frac{1}{2} m_{con2} \dot{\bar{R}}_2^T \dot{\bar{R}}_2$$

where ρ is the mass density of the element, m_{con1} , m_{con2} are the concentrated masses of the nodes 1 and 2, respectively and $\dot{\bar{R}}_1$, $\dot{\bar{R}}_2$ are the velocities of the nodes 1 and 2.

The kinetic energy of the element can be rearranged in the following form

$$K = 1/2 \dot{\mathbf{X}}^T \dot{\mathbf{Q}} \dot{\mathbf{q}} \mathbf{M}_t \quad \left\{ \begin{array}{c} \dot{\mathbf{X}} \\ \dot{\mathbf{q}} \end{array} \right\}$$

b) Strain Energy

The strain energy of the element including material nonlinearity is

$$SE = \int_{Vol} \left[(1/2 E \epsilon_{xx})^2 - \frac{1}{m+1} B \epsilon_{xx}^{m+1} + 1/2 G (\epsilon_{xy}^2 + \epsilon_{xz}^2) \right] dvol$$

Lagrangian Expression is given by

$$L = KE - SE.$$

c) Examples:

1) Rotating cantilever beam (see Figures 2-7)

Length = 20.0 in

radius = 0.2 in

E = 10.87E6 lb/in²

$\rho = 2.536 \times 10^{-4}$ lb.s/in

operating speeds

$\omega = 100, 300, 500$ rad/s

Deformation using the formula given by 'Stephen.'

ω	100	300	500 rad/s
u_L	6.3799 E-4	5.7419E-3	1.5949E-2
v_L	1.3914E-4	1.2523E-3	3.4787E-3
w_L	-1.3905E-4	-1.2513E-3	-3.47648E-3

2) Four-Bar Linkage (see Figures 8-21)

Height of the beam = 1.0 in

Width of the beam = 0.25 in

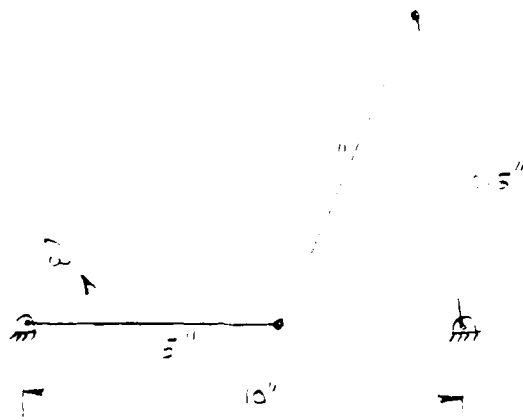
E = 10.87 E6 lb/in²

B = 8.387 E10 lb/in²

$$m = 3$$

$$\rho = 2.536E-4 \text{ lb sec}^2/\text{in}^4$$

working speed $\omega = 100 \text{ rad/s}, 150 \text{ rad/s}.$



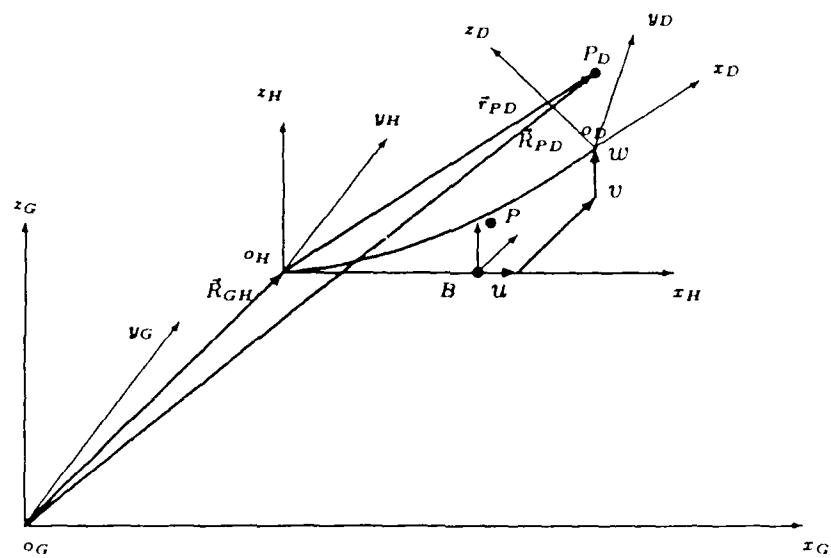


Figure 1 Position Vector of point P on the Deformed Element.

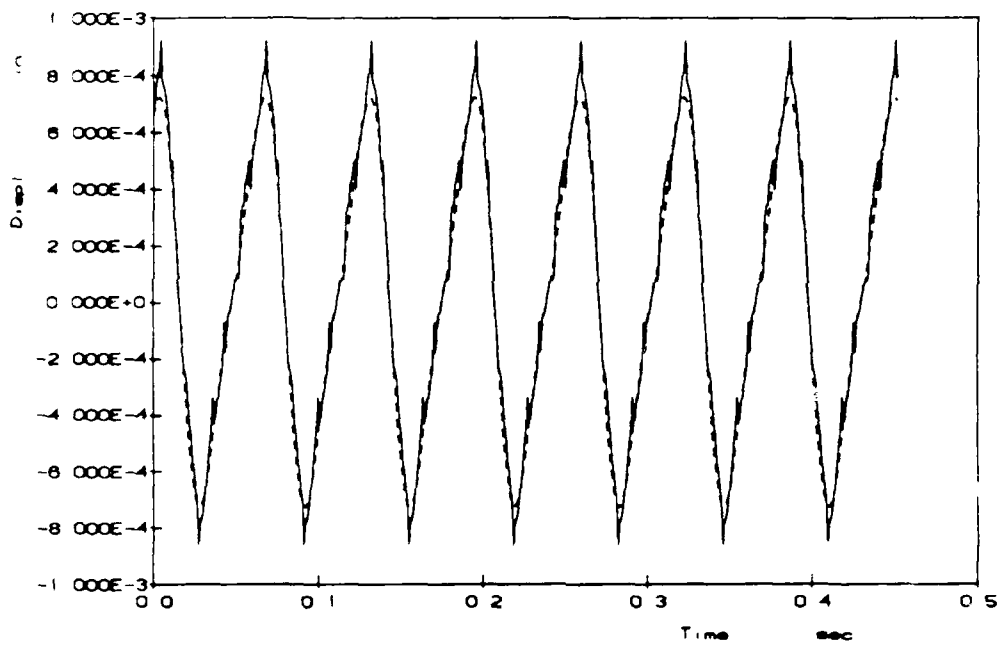


Figure 2 Axial Displacements in Global Coordinates. $\omega = 100$. rad/sec.

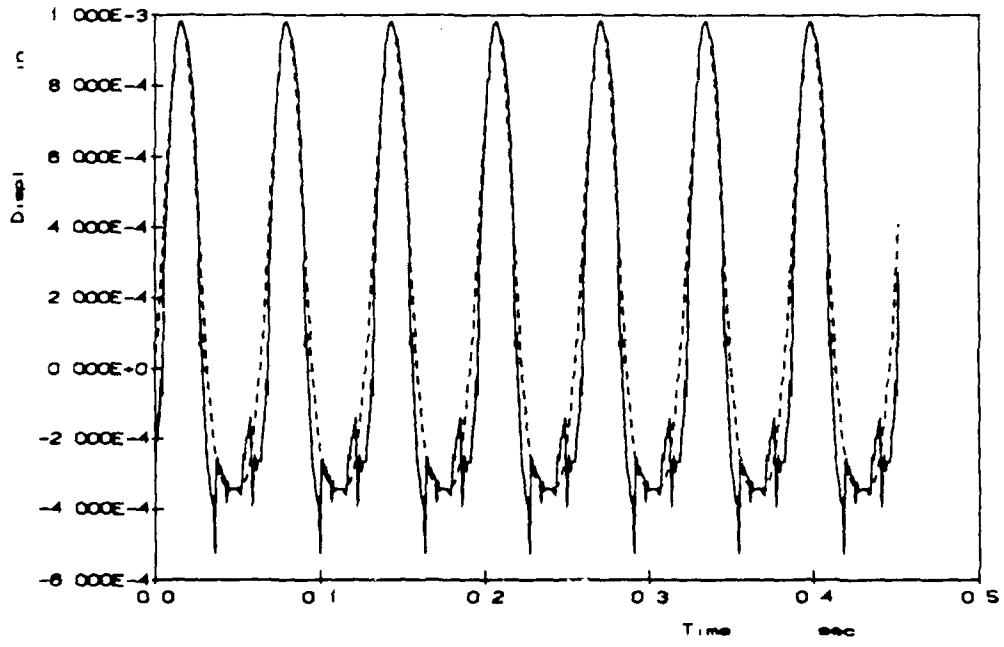


Figure 3 Lateral Displacements in Global Coordinates. $\omega = 100$. rad/sec.

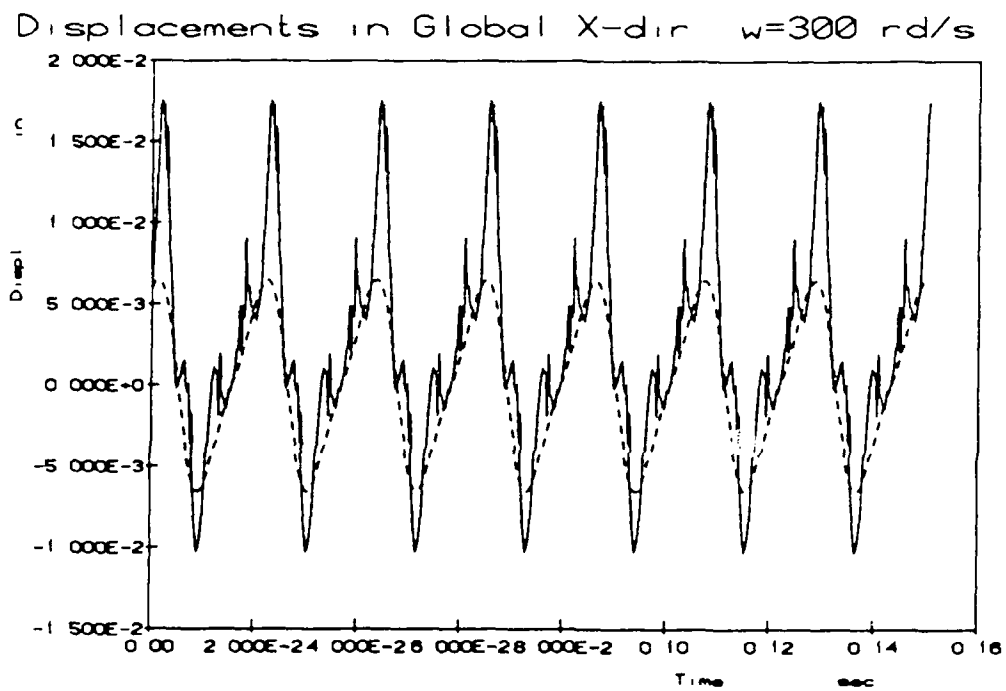


Figure 4 Axial Displacements in Global Coordinates. $\omega = 300$. rad/sec.

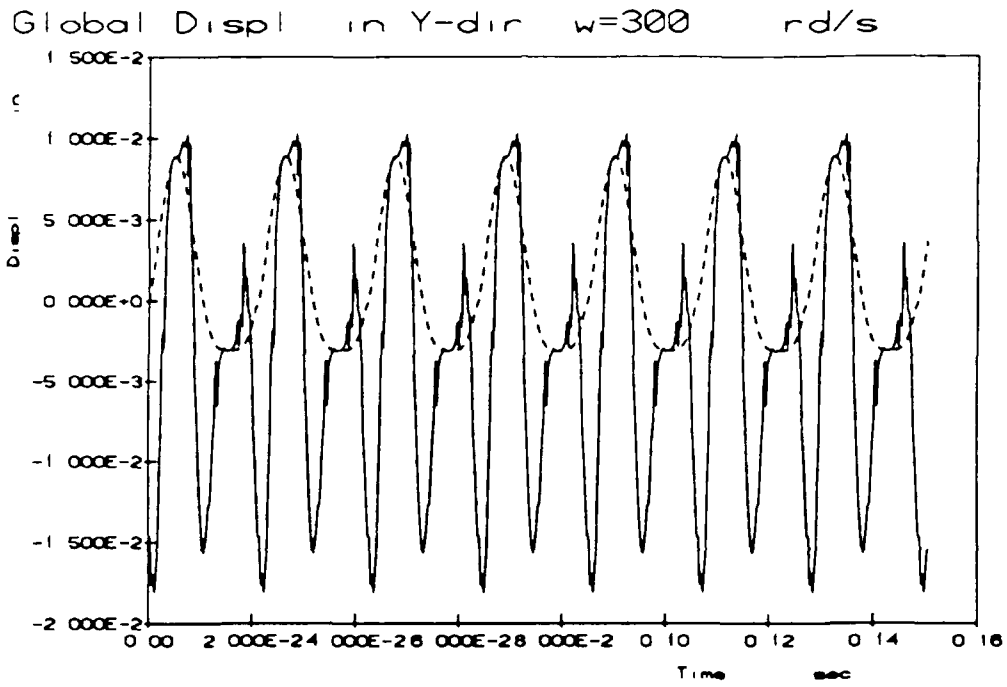


Figure 5 Lateral Displacements in Global Coordinates. $\omega = 300$. rad/sec.

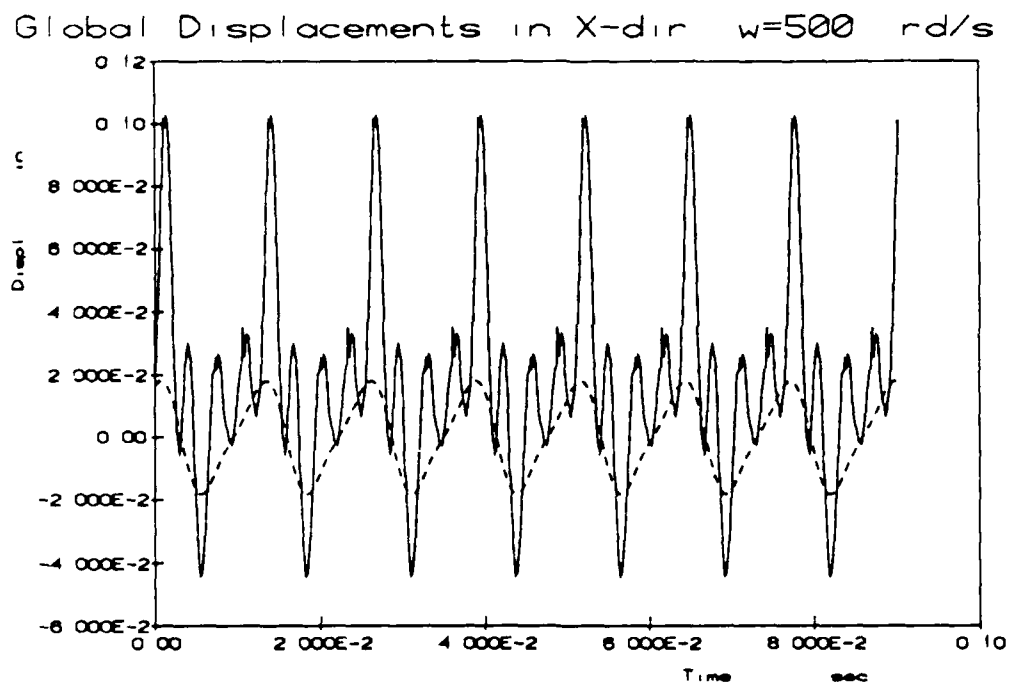


Figure 6 Axial Displacements in Global Coordinates. $\omega = 500$. rad/sec.

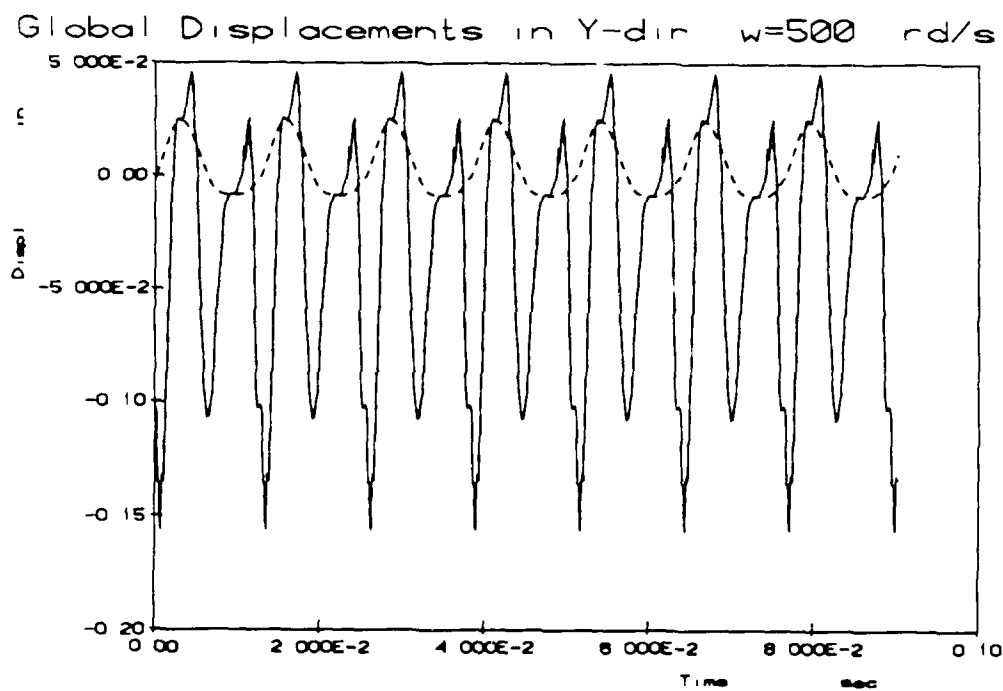


Figure 7 Lateral Displacements in Global Coordinates. $\omega = 500$. rad/sec.

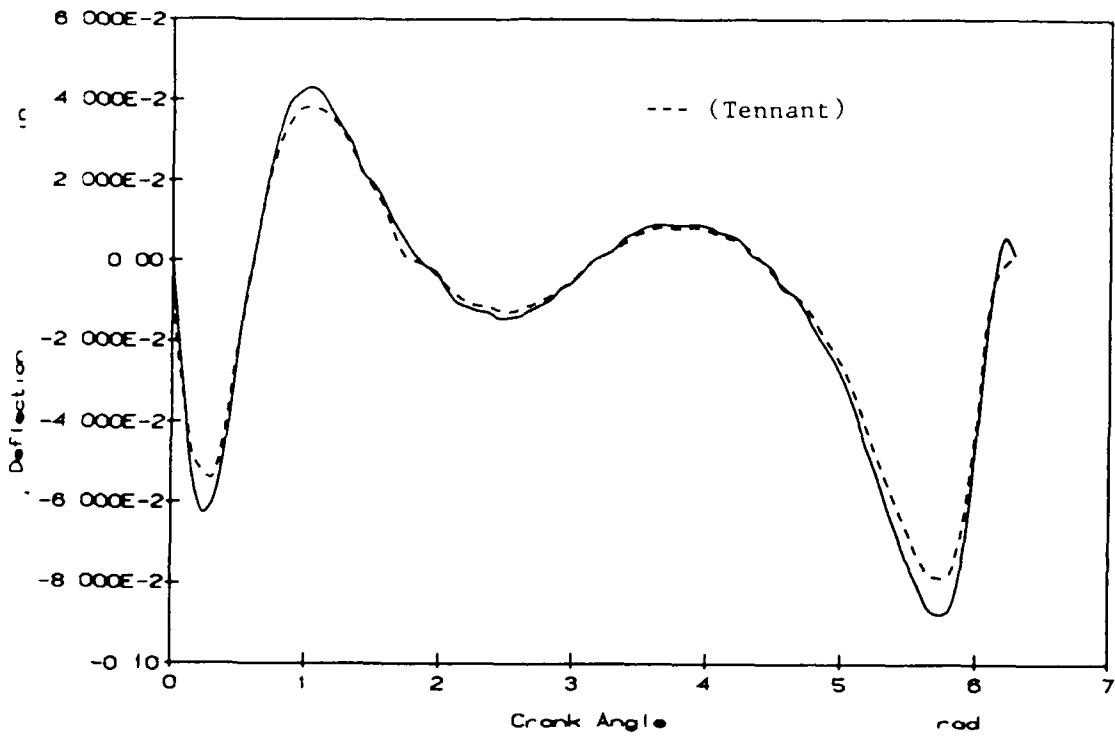


Figure 8 Axial Displacements of node 2 in Global Coordinates. $\omega = 100$. rad/sec.

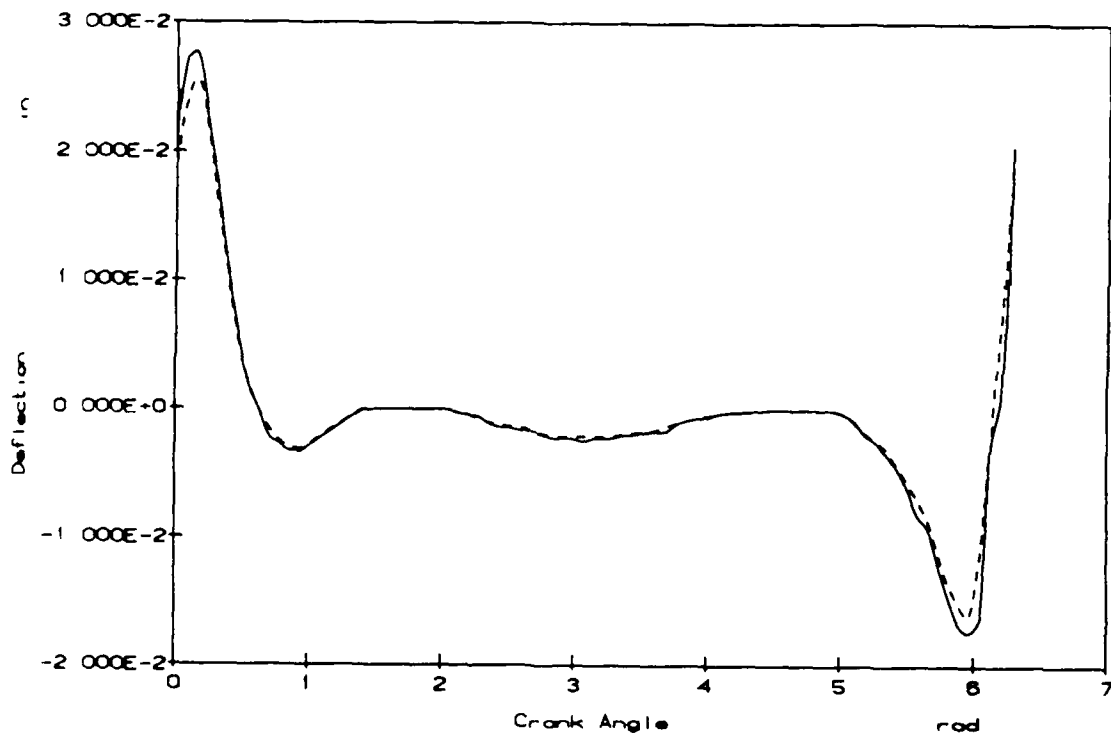


Figure 9 Vertical Displacements of node 2 in Global Coordinates. $\omega = 100$. rad/sec.

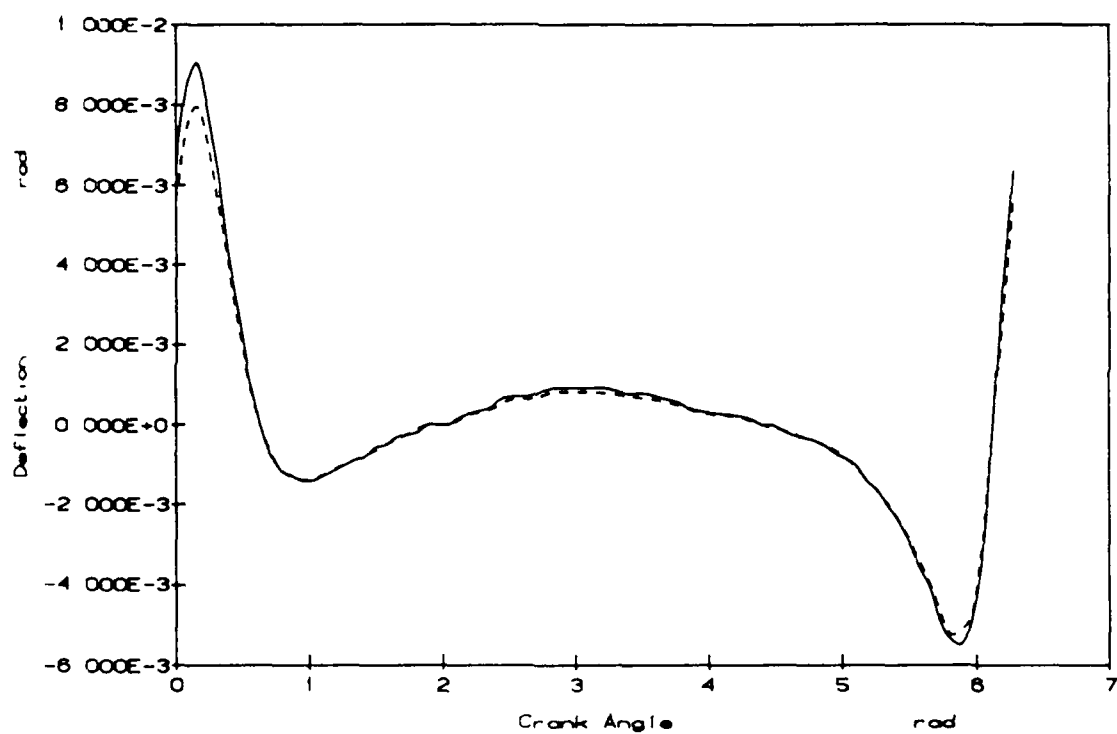


Figure 10 Angle of Rotation of node 2 in Global Coordinates. $\omega = 100$. rad/sec.

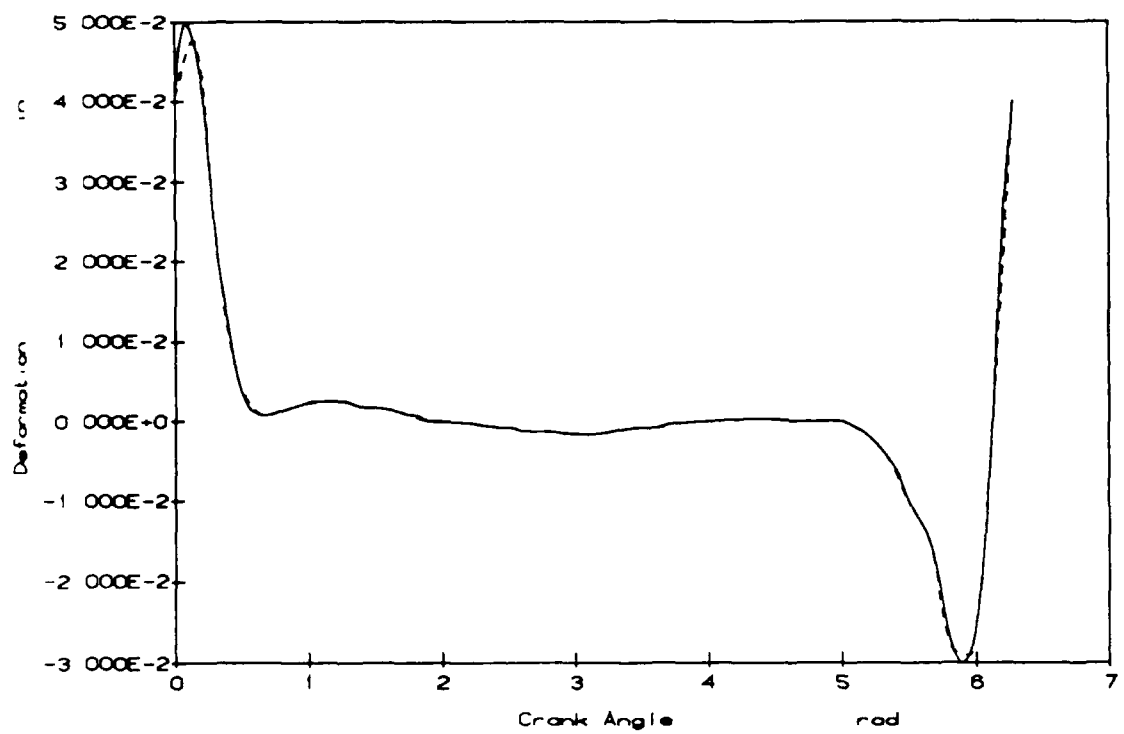


Figure 11 Axial Displacements of node 3 in Global Coordinates. $\omega = 100$. rad/sec.

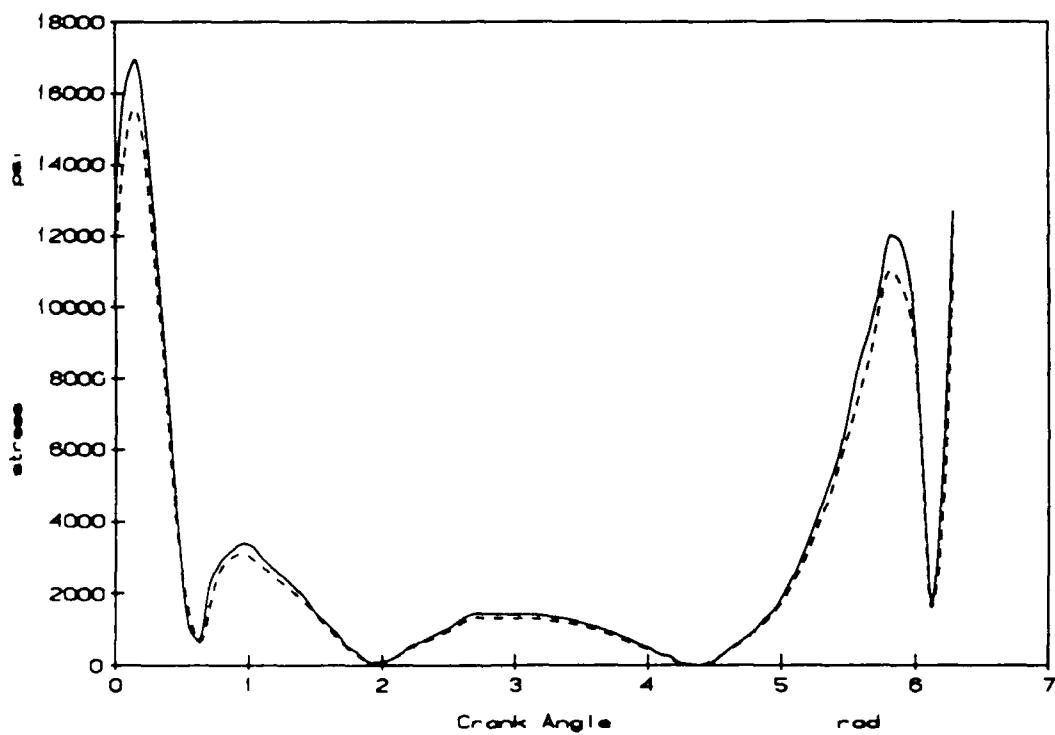


Figure 12 Maximum Absolute Stress of the element 1. $\omega = 100$. rad/sec.

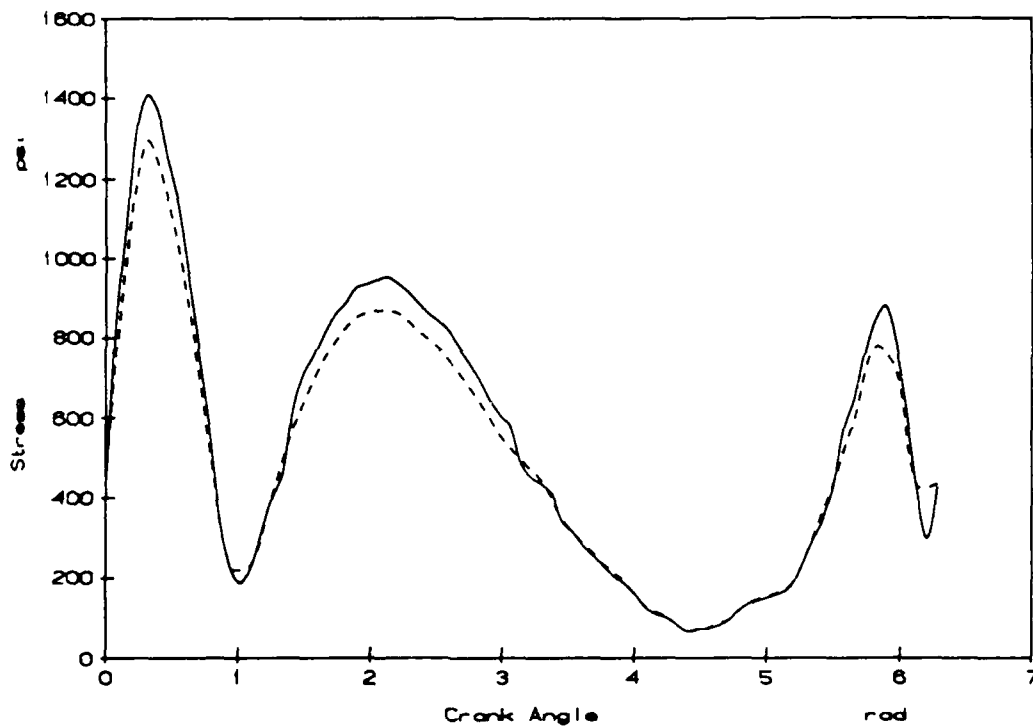


Figure 13 Maximum Absolute Stress of the element 2. $\omega = 100$. rad/sec.

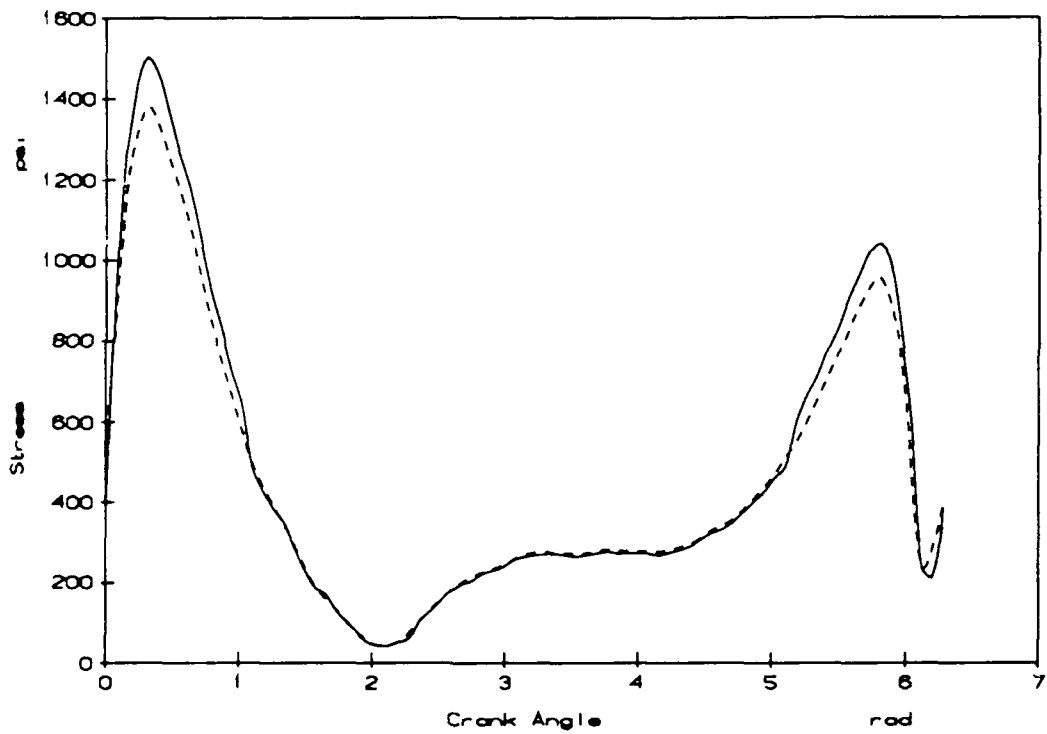


Figure 14 Maximum Absolute Stress of the element 3. $\omega = 100$. rad/sec.

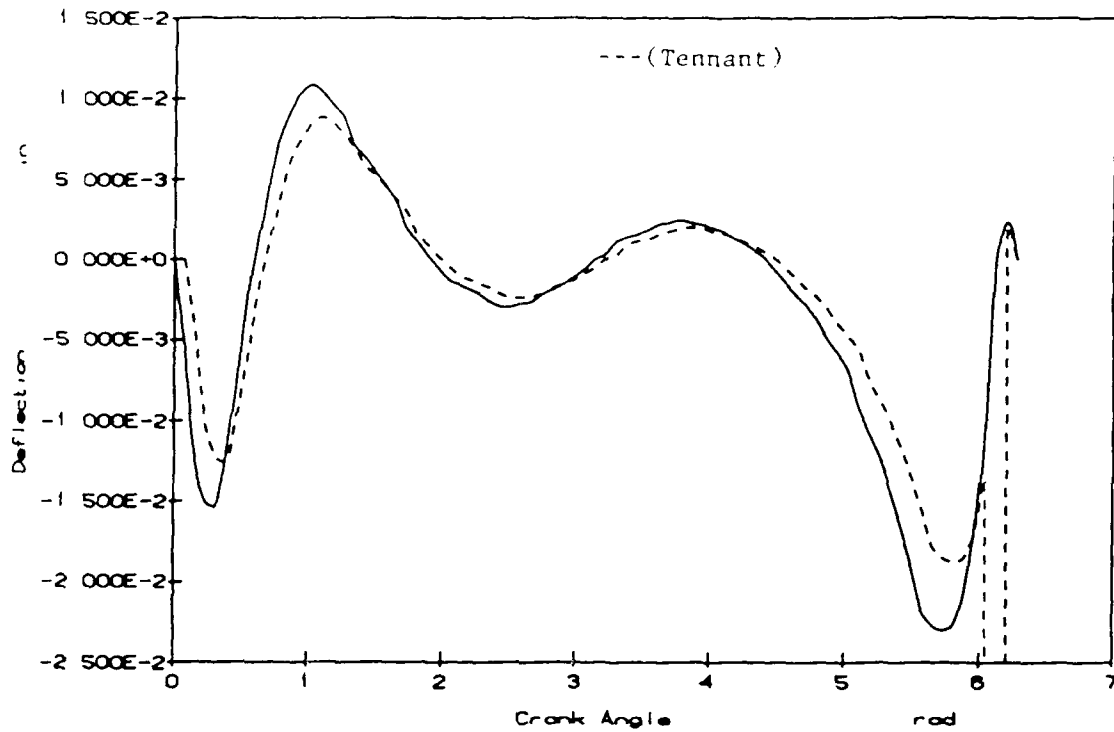


Figure 15 Axial Displacements of \bar{U}_1 in Global Coordinates. $\omega = 150$. rad/sec.

NO-A198 644

NONLINEAR ANALYSIS AND OPTIMAL DESIGN OF DYNAMIC
MECHANICAL SYSTEMS FOR SPACECRAFT APPLICATION(U)

2/2

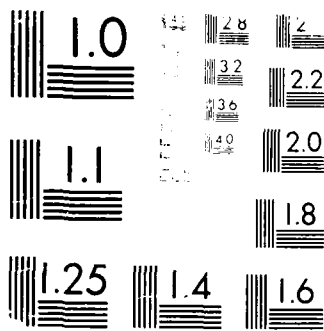
UNCLASSIFIED

CLARKSON UNIV POTSDAM NY K D WILLMERT ET AL SEP 87
AFOSR-TR-87-2008 AFOSR-84-0076

F/G 22/2

NL





MICROCOPY RESOLUTION TEST CHART
1010A - U.S. GOVERNMENT PRINTING OFFICE: 1963 O - 344-100

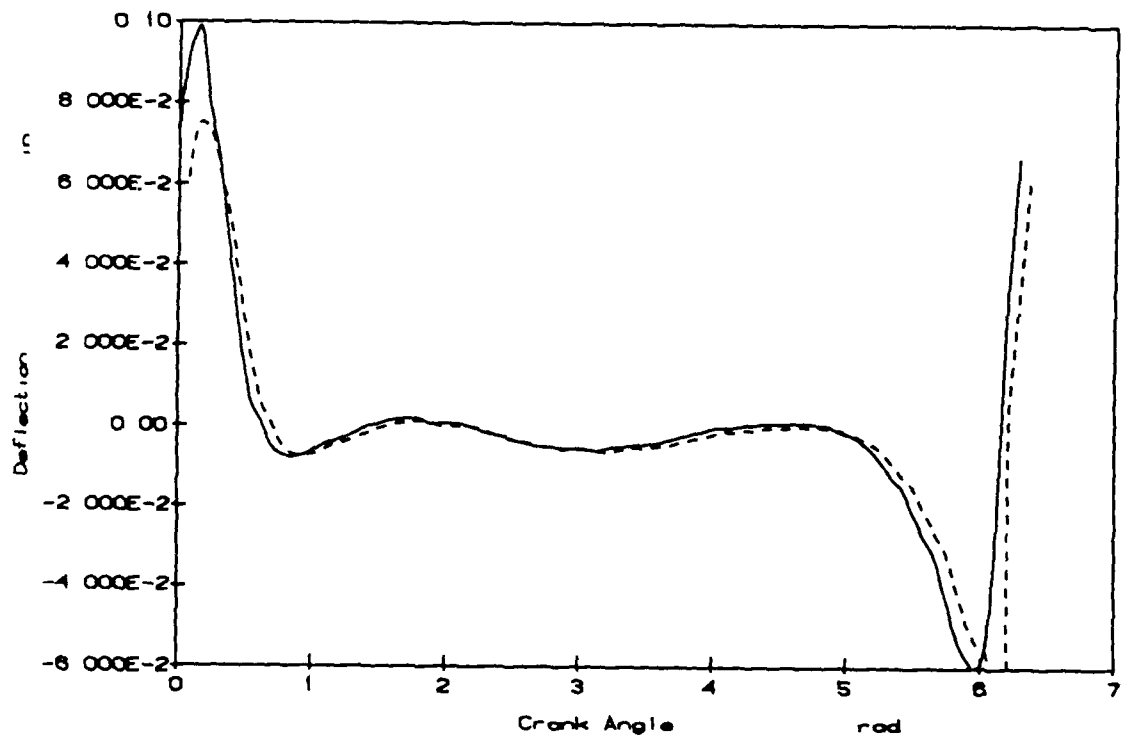


Figure 16 Vertical Displacements \bar{V}_1 in Global Coordinates. $\omega = 150$. rad/sec.

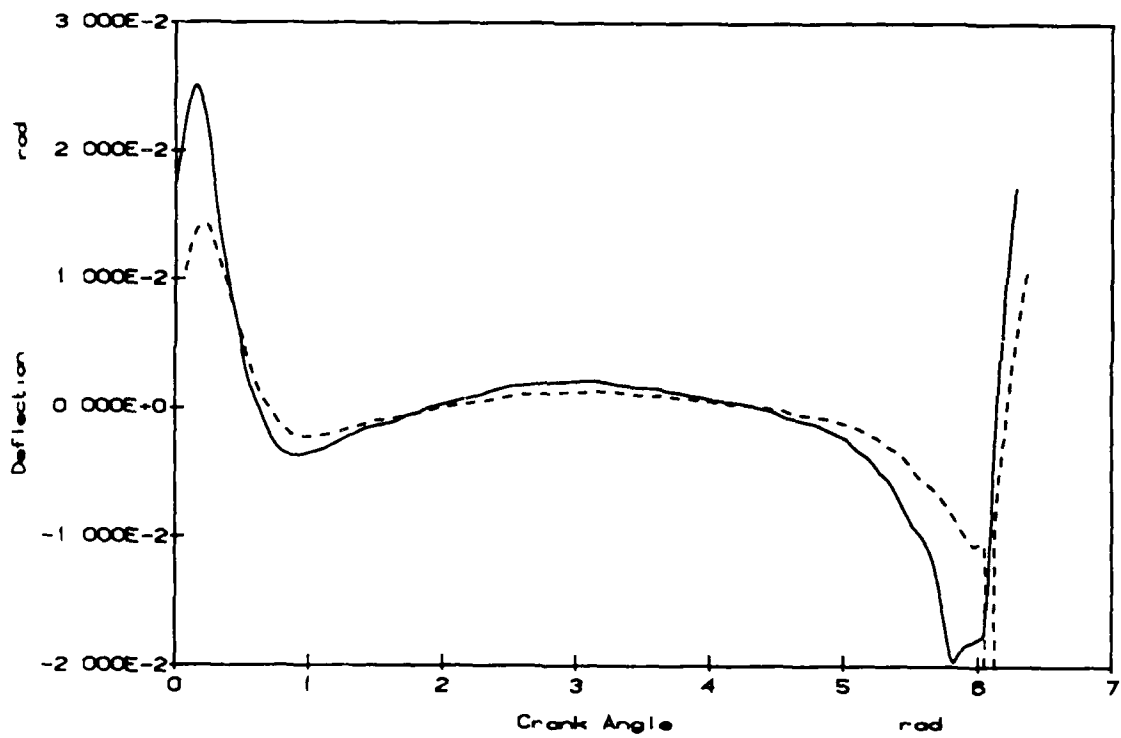


Figure 17 Angle of Rotation $\bar{\Theta}_1$ in Global Coordinates. $\omega = 150.$ rad/sec.

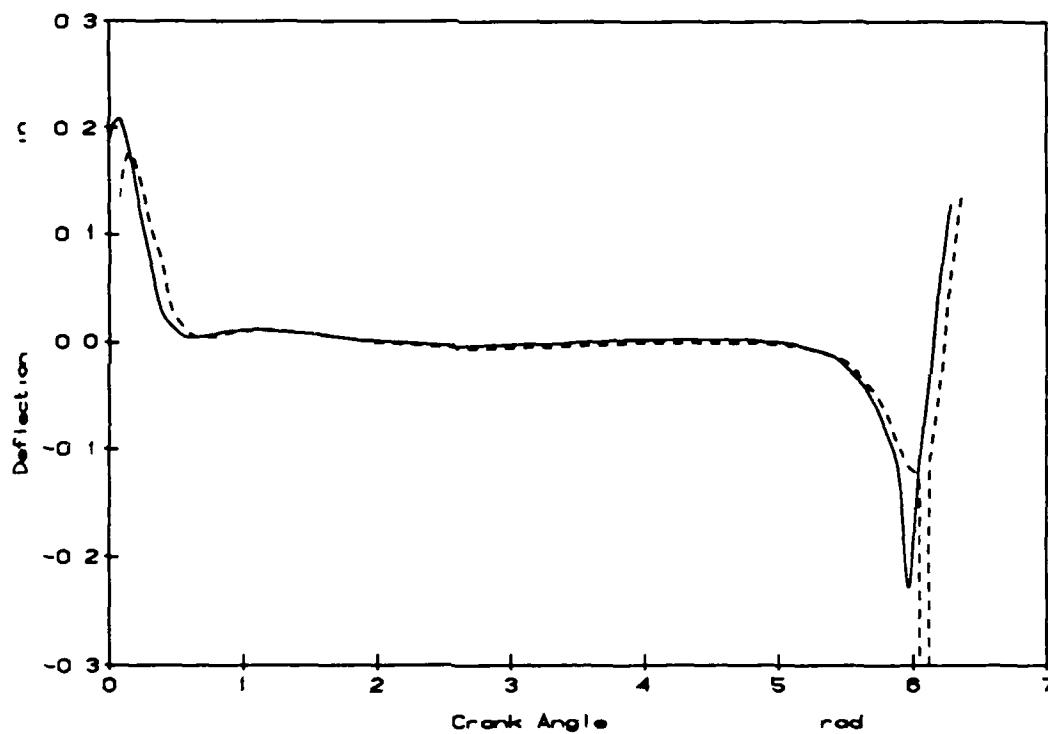


Figure 18 Axial Displacements \bar{U}_2 in Global Coordinates. $\omega = 150$.
rad/sec.

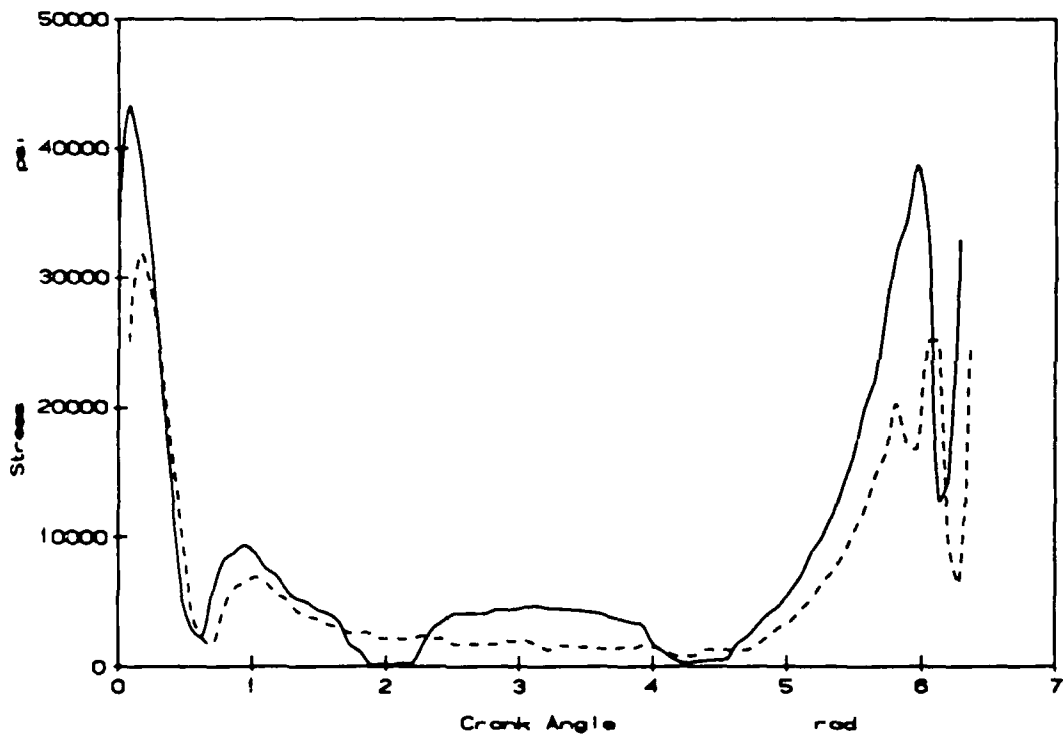


Figure 19 Maximum Stress of the element 1. $|\sigma_1|$ $\omega = 150$. rad/sec.

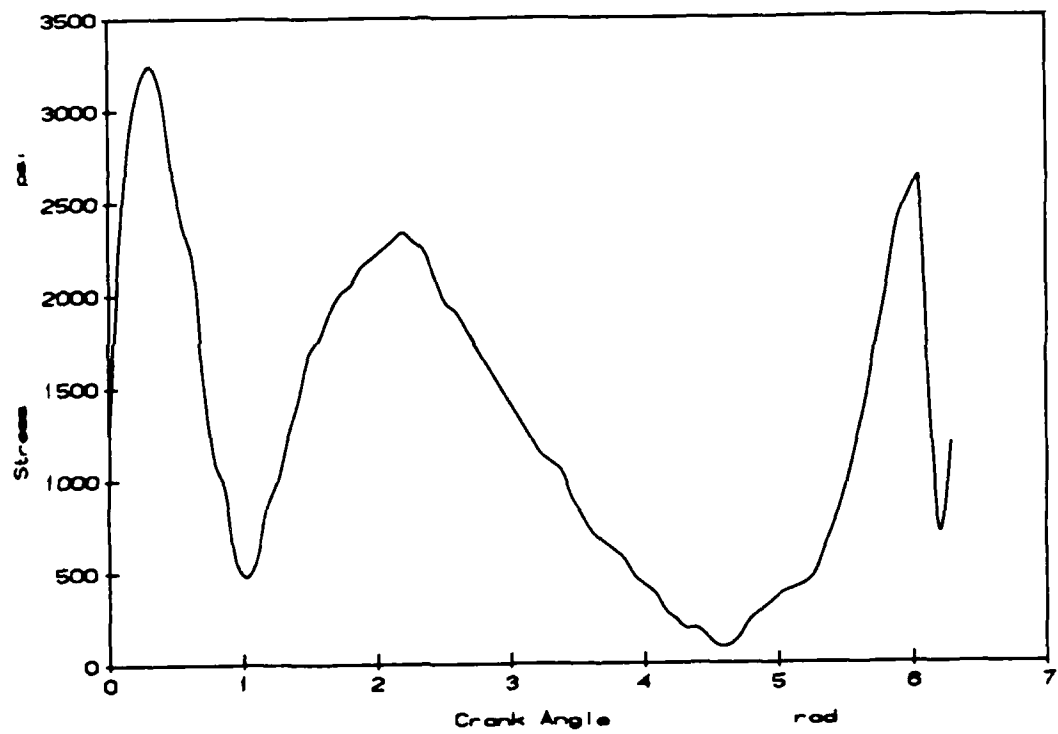


Figure 20 Maximum Stress of the element $2.|\sigma_2|$ $\omega = 150$. rad/sec.

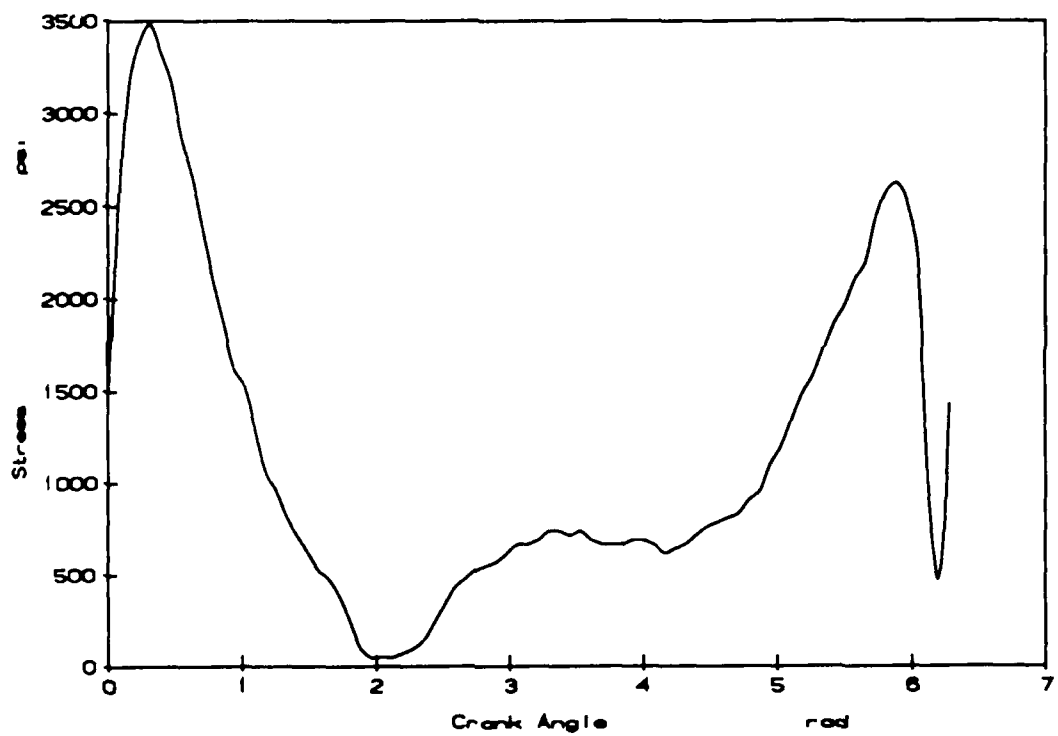


Figure 21 Maximum Stress of the element 3. $|\sigma_3|$ $\omega = 150$. rad/sec.

END

DATE

FILMED

5-88

DTIC